

**Green synthesis and characterization of silver nanoparticles (AgNPs)
from *Bulbine frutescens* leaf extract and their antimicrobial effects.**

Shakeela Lucas

Student number: 3340226



**UNIVERSITY *of the*
WESTERN CAPE**

**A Thesis submitted in partial fulfilment of the requirements for the degree -
Magister Scientiae in Biotechnology in the Department of Biotechnology at the
University of the Western Cape, Bellville, South Africa.**

Supervisor: Prof. Abram Madiehe

Co-supervisor: Prof. Mervin Meyer

August 2019

Keywords

Nanoparticles

Nanotechnology

Green synthesis

Bulbine frutescens

Antimicrobial resistance

Antimicrobial activity

Silver nanoparticles



Abstract

Thesis title: Green synthesis and characterization of silver nanoparticles (AgNPs) from *Bulbine frutescens* leaf extract and their antimicrobial effects.

S. Lucas

MSc Thesis, Faculty of Natural Science, Department of Biotechnology, University of the Western Cape

Combating antimicrobial resistant infections caused by nosocomial pathogens poses a major public health problem globally. The widespread use of broad-spectrum antibiotics for the treatment of wound infections has led to the appearance of multidrug-resistant (MDR) microbes which further exacerbates the growth of microbes amongst patients. It may result in prolonged debility of the patient and an increase in healthcare costs due to prolonged hospital stays and expensive treatment regimens to avoid patient-patient transmission. Therefore, it is imperative that alternative sources of treatment to antimicrobial use in wound infections needs to be developed in order to inhibit or kill resistant microbes and to provide point of care medical treatment to the less fortunate at an affordable cost.

The green synthesis of silver nanoparticles (AgNPs) is a cost-effective strategy for wound healing and has been employed in this thesis. Plants are able to reduce inorganic metals to form nanoparticles (NP) without the production of toxic by-products, are an eco-friendly and are a green alternative to conventional methods for mining nanomaterials. Green synthesized NPs are biocompatible and potentially safe for human therapeutic use. *Bulbine frutescens* leaf extract is stocked with valuable metabolites that are mainly employed as a vulnerary to treat a host of skin infections, colds and even arthritis.

AgNPs were synthesised in direct sunlight with method of synthesis adapted from Vivek and colleagues. The AgNPs produced have been confirmed with UV-Vis spectra analysis. Using the principle of Dynamic Light Scattering (DLS), the hydrodynamic size, Polydispersity Index (PdI) and Zeta Potential (ZP) of the NPs were examined. The core-diameter and the morphology of the NPs were determined using High-resolution Transmission Electron Microscopy (HR-TEM). The Total Phenolic Content (TPC) and Fourier-transform Infrared Spectroscopy (FTIR) spectra of

both the extract and AgNPs were investigated. The antimicrobial activity of the extract and AgNPs were investigated using agar well diffusion technique.

Total Phenolic Content (TPC) analysis combined with the DLS data confirmed the antimicrobial effects observed with AgNPs. The TPC analysis confirmed that an ionic charge on the pH 10 AgNPs enhanced the activity of polyphenols; thus influencing the amount of phenols present within the AgNPs, providing a greater antimicrobial effect. Neutral pH AgNPs had 49.65 ± 0.02125 TPC content in comparison to 243.003 ± 0.01175 for pH 10 AgNPs. The ZP decreased during the purification process which aided in the agar well-diffusion studies as the more negative the ZP, the more potent the AgNPs were against bacterial cell walls. Both AgNPs had a negative ZP of -22.3 mV for neutral pH and -25.4 mV for pH 10. The hydrodynamic size increased with centrifugation steps from 89.02 d.nm – 180.4 d.nm for neutral pH, and 101.2 d.nm – 279.7 d.nm for pH10 AgNPs. FTIR analysis confirmed that the presence of flavonoids, amine groups, polyphenols and proteins are responsible for reducing the AgNO₃ to form AgNPs. The FTIR spectra obtained showed similarities between the extracts and AgNPs with some variation in the peak shifts positions which clearly indicated that the residual plant material is responsible for the capping agents of the AgNPs. The HR-TEM analysis confirmed that the AgNP suspensions within this study are comprised of an array of different shapes which include oval, spherical, triangular, irregular and even rod shaped particles. Based on the HR-TEM images it was clear that pH 10 AgNPs is comprised of more circular shaped particles than neutral pH AgNPs. The core diameter of each particle was between 0.9 nm and 2 nm respectively.

The TPC analysis confirms the antimicrobial activity displayed by the AgNPs in that pH 10 AgNPs have a greater activity than neutral pH AgNPs due to the presence of more phenols which has been stabilised through the applied ionic charge. *Bulbine frutescens* leaf extract has shown no antimicrobial activity, however, the AgNPs has shown promising antimicrobial activity against all the microbes within this study which include: *Methicillin resistant Staphylococcus aureus (MRSA)*, *Staphylococcus aureus*, *Staphylococcus epidermidis*, *Staphylococcus pyogenes*, *Escherichia coli*, *Klebsiella pneumonia*, *Pseudomonas aeruginosa*, *Fusarium culmorum*, *Fusarium oxysporum*, *Fusarium proliferatum* and *Fusarium verticilloides*. Both AgNPs displayed the highest activity against *S. aureus* and *F. oxysporum*, and the lowest activity against *E. coli* and *F.*

culmorum. The difference within the antimicrobial effects of the AgNPs on the different microbes can potentially be attributed to the nature of the microbial cell membranes.

August 2019



Declaration

I declare that this thesis "***Green synthesis and characterization of silver nanoparticles (AgNPs) from *Bulbine frutescens* leaf extract and their antimicrobial effects***" is a presentation of my original research work and it has not been submitted for any degree or examination in any other university. Wherever contributions of others are involved, every effort is made to indicate this clearly, with due reference to the literature and acknowledgement of collaborative research and discussions. The work was done under the guidance of Professor Abram Madiehe, at the University of the Western Cape, South Africa.



Shakeela Lucas 

Date: 26th August 2019

Acknowledgements

- I would firstly like to thank the Almighty. All of this would not have been possible without the grace of the Almighty; for it is he who has given us the power to seek knowledge from the cradle to the grave.
- My sincere gratitude is expressed to Prof Abram Madiehe for his invaluable contribution and guidance to the success of my Masters degree in the Department of Biotechnology. I thank you for going above and beyond to provide me with the necessary tools to progress within my project.
- Thank you to the National Research Foundation (NRF) and DST-MINTEK Nanotechnology Innovation Centre (NIC) for financial support.
- I would also like to extend my gratitude and thanks to Prof Mervin Meyer and Prof Martin Onani for their guidance and interest in my success.
- I thank Dr. Ashwil Klein for providing me with the fungal strains, reagents and technical expertise for the antifungal studies.
- I thank Mr Yunus Kippie for his assistance with analyzing the FTIR spectra of my extracts and AgNPs.
- I would like to extend my gratitude to Mrs Eloise Braaf, Mrs Francis Starkey and all the other staff members at the University of the Western Cape for their contribution towards my success.
- To all my colleagues in the Nanobiotechnology Research Group and the NIC lab who have assisted me, I thank you for your patience and time spent in helping me.
- I would like to express my heartfelt thanks to my family for their continuous and unparalleled love, help and support.
- I would like to thank Abdul-Qadir Sampson for his support and motivation when things were tough. Thank you for all the sacrifices you have made and ensuring that I get to and from university safe at night when I was working late.
- I thank all my friends, especially Lee-Ann Niekerk, Bilqees Salie and Taahirah Boltman for your guidance and constant motivation.

Table of contents

Keywords.....	i
Abstract.....	ii
Declaration.....	v
Acknowledgements.....	vi
Table of contents	vii
List of Abbreviations	x
List of figures.....	xii
List of tables	xv
Chapter 1: Literature review.....	1
1.1. Introduction	1
1.2. Aim, objectives and hypothesis.....	3
1.3. What are antibacterial compounds?	4
1.3.1. Microbial resistance to antimicrobial drugs.....	4
1.3.2. Bacterial cell wall and sensitivity to antimicrobial agents.....	4
1.3.3. Classes of antibiotics and their sites of action on bacteria	6
1.3.4. Mechanisms of resistance of microbes against antimicrobial drugs.....	8
1.4. <i>Fusarium</i> fungal species.....	10
1.4.1. Susceptibility to various antimicrobial compounds.....	10
1.5. Current management of antimicrobial resistance in wound infections.....	11
1.5.1. Antimicrobial potential of herbal medicines	11
1.5.2. Polyphenols.....	13
1.5.3. <i>Bulbine frutescens</i>	14
1.5.4. Antimicrobial activity of <i>B. frutescens</i> plant extract in previous literature.....	15

1.6. Nanotechnology and nanoscience.....	17
1.6.1. What is nanoscience and nanotechnology?	17
1.5.2. Classification of NPs	18
1.5.3. Green nanotechnology	20
1.6. Silver.....	21
1.6.1. Biosynthesis of AgNPs.....	22
1.6.2. The role of plant biomolecules in the green synthesis of AgNPs	23
1.6.3. Mechanism involved in the green synthesis of AgNPs	25
1.6.4. Factors affecting the synthesis of AgNPs.....	27
1.6.5. NPs against antimicrobial resistance	28
1.6.6. Application of AgNPs.....	31
1.6.6.1. <i>In vitro</i> studies using AgNPs.....	32
1.6.6.2. <i>In vivo</i> studies using AgNPs.....	33
1.6.6.3. Antibacterial effects of biogenic AgNPs.....	34
Chapter 2: Materials and Methodology	39
2.1. List of equipment, chemicals and reagents	39
2.2. Preparation of <i>B. frutescens</i> plant extract.....	41
2.3. Synthesis of AgNPs in the dark and sunlight	42
2.4. Determination of the Total Phenolic Content (TPC).....	42
2.5. Determination of Hydrodynamic Size, Polydispersity Index and the Zeta Potential measurements	43
2.6. Large scale synthesis of AgNPs	44
2.7. Characterization of extract and AgNPs.....	44
2.7.1. HR-TEM analysis.....	44
2.7.2. Fourier-transformed Infrared (FTIR) spectroscopy	44
2.8. Determination of antibacterial activity using agar well-diffusion assay	45

2.9. Broth microdilution method for determining the minimum inhibitory concentration (MIC)	48
Chapter 3: Results and Discussion	50
3.1. The effects of different parameters on the green synthesis of AgNPs in the dark	50
3.1.1. Effect of time and reducing agent concentration	50
3.1.2. The effect of stirring on AgNP synthesis	50
3.1.3. The effect of time on AgNP synthesis using sunlight	55
3.1.4. The effect of temperature on AgNP synthesis	78
3.1.5. The effect of AgNO ₃ and extract concentration on the size distribution and uniformity of AgNPs	79
3.1.6. Hydrodynamic size, PDI and Zeta potential measurements of optimum AgNO ₃ concentrations with various extract concentrations	94
3.1.7. The effect of pH on AgNP synthesis	100
3.2. Preparation of extract and TPC analysis	101
3.3. FTIR analysis	105
3.4. HR-TEM analysis of AgNPs	111
3.5. Antimicrobial activity of AgNPs	114
Antimicrobial analysis of <i>B. frutescens</i> leaf extract	128
Chapter 4: Conclusion	130
4.1. Limitations of the study	131
4.2. Future prospects	131
References	133
Appendix	148

List of Abbreviations

Ag	Silver
Ag ⁺	Silver ion
Ag ⁰	Silver atom
AgCl	Silver chloride
AgNO ₃	Silver nitrate
AgNPs	Silver nanoparticles
ATCC	American Type Culture Collection
ATR	Attenuated Total Reflectance
CC-NPs	Chitosan-containing nanoparticles
CuO	Copper oxide
DLS	Dynamic light scattering
FC	Folin-Ciocalteu
FTIR	Fourier transform infrared
GAE	Gallic Acid Equivalents
hMSCs	Human mesenchymal stem cells
HR-TEM	High-Resolution Transmission Electron Microscopy
IR	Infrared
MIC	Minimum Inhibitory Concentration
MC-NPs	Metal-containing nanoparticles
MDR	Multidrug-resistant
MHB	Mueller Hinton Broth
MRSA	Methicillin resistant <i>Staphylococcus aureus</i>
NA	Nutrient Agar
NiO	Nickel oxide
NO NPs	Nitric oxide-releasing nanoparticles

NPs	Nanoparticles
PAA-MNP	Polyacrylic acid-coated iron oxide (magnetite)
PD	Particle Diameter
PdI	Polydispersity index
PG	Peptidoglycan
rhEGF	Human epidermal growth factor
ROS	Reactive Oxygen Species
SPR	Surface Plasmon Resonance
TEM	Transmission Electron Microscopy
TPC	Total Phenolic Content
UV	Ultraviolet light
UV-Vis	Ultraviolet-visible spectroscopy
WHO	World Health Organization
ZP	Zeta Potential
ZnO	Zinc oxide
XDR	Extensively drug-resistant



List of figures

Figure 1.1: Classes of antibiotics/ antimicrobial agents and their mode of action against bacteria.....	7
Figure 1.2: Examples of the different mechanism of antibiotic resistance.....	9
Figure 1.3: Photographic image of the <i>Bulbine frutescens</i> plant.....	15
Figure 1.4: Schematic representation of the chiral phenylanthraquinones knipholone (1) and isoknipholone (2) found within the <i>B. frutescens</i> plant species.....	16
Figure 1.5: Different types of nanoparticles.....	19
Figure 1.6: Advantages of green nanotechnology.....	21
Figure 1.7: Different approaches for synthesis of metallic NPs.....	23
Figure 1.8: The different parts of plant used in green synthesis of NPs.....	24
Figure 1.9: A hypothetical mechanism involved in the reduction of silver ions to form AgNPs using green synthesis.....	26
Figure 1.10: NPs and their ions (e.g. Ag ⁺ , Zn ²⁺) producing free radicals, resulting in the induction of oxidative stress.....	29
Figure 2.1: Cross-section of <i>B. frutescens</i> showing gel sap of the leaves.....	41
Figure 3.1: UV-Vis spectra of neutral pH (7.11) AgNPs synthesized with 1mM AgNO ₃ at various <i>B. frutescens</i> leaf extract concentrations over a period of 9 hours at 100 °C in the dark.....	52
Figure 3.2: UV-Vis spectra of pH 10 AgNPs synthesized with 1 mM AgNO ₃ at various <i>B. frutescens</i> leaf extract concentrations over a period of 9 hours at 100 °C in the dark.....	53
Figure 3.3: Effect of time on AgNP formation at various <i>B. frutescens</i> leaf extract concentrations over a period of 9 hours at 100 °C in the dark.....	54
Figure 3.4: Visible colour change of reaction mixture after 60 minutes of synthesis in direct sunlight.....	56
Figure 3.5: Effect of time on AgNP formation at various <i>B. frutescens</i> leaf extract concentrations over a period of 6 hours in direct sunlight at various extract and AgNO ₃ concentrations.....	58
Figure 3.6: Effect of time on AgNP formation at various <i>B. frutescens</i> leaf extract concentrations over a period of 6 hours in direct sunlight at various extract and AgNO ₃ concentrations.....	59
Figure 3.7: Effect of time on AgNP formation at various <i>B. frutescens</i> leaf extract concentrations over a period of 6 hours in direct sunlight at various extract and AgNO ₃ concentrations.....	60

Figure 3.8: UV-Vis spectra of neutral pH (7.11) AgNPs synthesized with 0.5 mM AgNO ₃ at various <i>B. frutescens</i> leaf extract concentrations over a period of 6 hours in direct sunlight.....	62
Figure 3.9: UV-Vis spectra of pH 10 AgNPs synthesized with 0.5 mM AgNO ₃ at various <i>B. frutescens</i> leaf extract concentrations over a period of 6 hours in direct sunlight.....	63
Figure 3.10: UV-Vis spectra of neutral pH AgNPs synthesized with 1 mM AgNO ₃ at various <i>B. frutescens</i> leaf extract concentrations over a period of 6 hours in direct sunlight.....	65
Figure 3.11: UV-Vis spectra of pH 10 AgNPs synthesized with 1 mM AgNO ₃ at various <i>B. frutescens</i> leaf extract concentrations over a period of 6 hours in direct sunlight.....	66
Figure 3.12: UV-Vis spectra of neutral pH AgNPs synthesized with 2 mM AgNO ₃ at various <i>B. frutescens</i> leaf extract concentrations over a period of 6 hours in direct sunlight.....	68
Figure 3.13: UV-Vis spectra of pH 10 AgNPs synthesized with 2 mM AgNO ₃ at various <i>B. frutescens</i> leaf extract concentrations over a period of 6 hours in direct sunlight.....	69
Figure 3.14: UV-Vis spectra of neutral pH (7.11) AgNPs synthesized with 3 mM AgNO ₃ at various <i>B. frutescens</i> leaf extract concentrations over a period of 6 hours in direct sunlight.....	71
Figure 3.15: UV-Vis spectra of pH 10 AgNPs synthesized with 3 mM AgNO ₃ at various <i>B. frutescens</i> leaf extract concentrations over a period of 6 hours in direct sunlight.....	72
Figure 3.16: UV-Vis spectra of neutral pH (7.11) AgNPs synthesized with 4 mM AgNO ₃ at various <i>B. frutescens</i> leaf extract concentrations over a period of 6 hours in direct sunlight.....	74
Figure 3.17: UV-Vis spectra of pH 10 AgNPs synthesized with 4 mM AgNO ₃ at various <i>B. frutescens</i> leaf extract concentrations over a period of 6 hours in direct sunlight.....	75
Figure 3.18: UV-Vis spectra of pH 10 AgNPs synthesized with 5 mM AgNO ₃ and 50 mg/ml <i>B. frutescens</i> leaf extract concentration after 45 minutes of synthesis in direct sunlight.....	76
Figure 3.19: UV-Vis spectra of optimum neutral pH (7.11) <i>B. frutescens</i> leaf extract concentrations for various AgNO ₃ concentration in direct sunlight.....	81
Figure 3.20: UV-Vis spectra of optimum pH 10 <i>B. frutescens</i> leaf extract concentrations for various AgNO ₃ concentration in direct sunlight.....	83
Figure 3.21: Time course of AgNP synthesis using optimum conditions.....	96
Figure 3.22: UV-Vis spectra of the pellets and supernatants of neutral pH (7.11) and pH 10 AgNPs after each centrifugation step.....	98
Figure 3.23: Gallic acid calibration curve for <i>B. frutescens</i> extract.....	103

Figure 3.24: Gallic acid calibration curve for neutral pH and pH 10 AgNPs synthesized from <i>B. frutescens</i> leaf extract.....	104
Figure 3.25.1: FTIR spectra of freeze dried extract (A), neutral pH (7.11) extract (B) and neutral pH AgNPs (C).....	106
Figure 3.25.2: FTIR spectra of freeze dried extract (A) pH 10 extract (B) and pH 10 AgNPs (C).....	108
Figure 3.26 A: The morphology and average core diameter of neutral pH (7.11) and pH 10 AgNPs.....	112
Figure 3.26 B: HR-TEM images showing the Crystalline nature lattice fringes of AgNPs.....	113
Figure 3.26 C: HR-TEM images showing the SAED pattern of AgNPs.....	113
Figure 3.27: Comparative analysis of 0.1 mg/ml ampicillin, 0.6 mg/ml, 0.3 mg/ml, 0.15 mg/ml, 0.075 mg/ml, 0.0375 mg/ml neutral pH AgNPs to 7 human pathogenic bacteria after 24 hours of incubation at 37 °C.....	120
Figure 3.28: Comparative analysis of 0.1 mg/ml ampicillin, 0.47 mg/ml, 0.24 mg/ml, 0.12 mg/ml, 0.06 mg/ml, 0.03 mg/ml pH 10 AgNPs to 7 human pathogenic bacteria after 24 hours of incubation at 37 °C.....	121
Figure 3.29: Comparative analysis of the antifungal effects of 0.1 g/l carbendazim, 99% ethanol, 0.6 mg/ml, 0.3 mg/ml, 0.15 mg/ml, 0.075 mg/ml, 0.0375 mg/ml pH 10 AgNPs to 4 <i>Fusarium</i> fungal strains after 5 days of incubation at 25 °C.....	126
Figure 3.30: Comparative analysis of the antifungal effects of 0.1 g/l carbendazim, 99% ethanol, 0.47 mg/ml, 0.24 mg/ml, 0.12 mg/ml, 0.06 mg/ml, 0.03 mg/ml pH 10 AgNPs to 4 <i>Fusarium</i> fungal strains after 5 days of incubation at 25 °C.....	128

List of tables

Table 1.1: Various bacterial targets of antibacterial drugs.....	6
Table 1.2: Applications of eco-friendly NPs in antibacterial therapy.....	35
Table 2.1: Details of microorganisms within this study.....	47
Table 2.2: Sample concentrations for antimicrobial activity analysis.....	48
Table 3.1: Optimum synthesis conditions and DLS analysis for neutral pH and pH 10 AgNPs for various extract concentrations with 0.5 mM AgNO ₃	85
Table 3.2: Optimum synthesis conditions and DLS analysis for neutral pH and pH 10 AgNPs for various extract concentrations with 1 mM AgNO ₃	87
Table 3.3: Optimum synthesis conditions and DLS analysis for neutral pH and pH 10 AgNPs for various extract concentrations with 2 mM AgNO ₃	89
Table 3.4: Optimum synthesis conditions and DLS analysis for neutral pH and pH 10 AgNPs for various extract concentrations with 3 mM AgNO ₃	91
Table 3.5: Optimum synthesis conditions and DLS analysis for neutral pH and pH 10 AgNPs for various extract concentrations with 4 mM AgNO ₃	93
Table 3.6: DLS analysis of the optimum conditions for various AgNO ₃ concentrations showing the average time for synthesis, optimum plant extract concentration, λ_{max} , particle size (PD) and polydispersity index (Pdl) values in direct sunlight.....	95
Table 3.7: DLS and ZP analysis of neutral pH (7.11) and pH 10 AgNPs after each centrifugation step.....	99
Table 3.8: Total phenolic content of various <i>B. frutescens</i> extract concentrations expressed as the amount of gallic acid per dried weight of extract.....	103
Table 3.9: Total phenolic content of neutral pH and pH 10 <i>B. frutescens</i> AgNP concentrations expressed as the amount of gallic acid per dried weight of AgNP.....	104
Table 3.10: The antimicrobial effects of green synthesized <i>B. frutescens</i> AgNPs against seven human pathogenic bacteria.....	118
Table 3.11: The antifungal effects of green synthesized <i>B. frutescens</i> AgNPs against four <i>Fusarium</i> fungal strains.....	124

Chapter 1: Literature review

1.1. Introduction

Antimicrobial resistance of microbes to commonly available antibiotics poses a major public health problem globally (Laxminarayan *et al.*, 2016). A report compiled by the UK Department of Health estimated that by 2050 ten million deaths attributed to antimicrobial resistance will occur annually worldwide (Murray *et al.*, 2012). This global burden is disproportionately concentrated in Sub-Saharan Africa (WHO, 2014).

Appropriate treatment of infections is hampered due to lack of basic health services in rural areas and the prohibitive cost of diagnostic tests to identify pathogens and their antimicrobial susceptibility patterns (WHO, 2014). Widespread use of broad-spectrum antibiotics for the treatment of wound infections has led to the appearance of multidrug-resistant (MDR) microbes which further exacerbates the growth of microbes amongst patients (Petti *et al.*, 2006). Approximately 27-82% of people in Africa live in rural areas where hospitals and conventional health services are limited or non-existent making traditional medicine their main option for treatment. It has been reported to have a fast healing time and offers the convenience of returning to their normal lifestyle (Petti *et al.*, 2006). This arose due to conventional methods failing to meet the expectations of patients and also the prejudice involved with regards to the management outcomes of wound conditions such as chronic ulcers, side effects of drugs and the high cost of conventional therapy (Zaidi *et al.*, 2005).

Plants have been used as a source of medicinal compounds against antimicrobial resistance for centuries. According to the World Health Organization (WHO), plant extracts or their respective active constituents are used as folk medicine in traditional therapies of which 80% is used to make antibiotics or drugs to combat infections or disease (WHO, 2015; Tora *et al.*, 2017). Medicinal plants have immunomodulatory and antioxidant properties resulting in adverse antimicrobial activities. The use of plant extracts and phytochemicals with known and unknown antimicrobial properties have shown to be effective in therapeutic treatments (Builders *et al.*, 2015).

Advances made through nanotechnology have changed the way diseases are diagnosed, treated and even prevented. Currently, researchers have drawn their attention to using metallic nanoparticles due to their ease of synthesis and modifications can be easily applied to functionalize nanoparticles (Ngiam *et al.*, 2011). Silver nanoparticles (AgNPs) are said to be the most widely commercialised nanomaterials and have extensively been applied in different industries. It has been incorporated in wound healing for its antimicrobial properties (Shekhawat and Arya, 2008). AgNPs have also been applied in medicinal products such as contraceptive devices, bone prostheses, surgical instruments and dental alloys (Eckhardt *et al.*, 2013). This study focuses on the green synthesis of AgNPs from *Bulbine frutescens* leaf gel sap extract.

The gel sap of *B. frutescens* is used by traditional healers to treat skin ailments such as wounds, rashes, cracked lips, burns, ringworms and even herpes. It has also been used internally for the treatment of coughs, colds, and arthritis (Hutchings *et al.*, 1996). *B. frutescens* gel sap promotes wound healing by increasing cell proliferation and collagen deposition. *B. frutescens* gel sap is known to increase hydration by leaving a layer of fatty vesicles of glycoprotein on the skin surface which exhibits potent antibacterial properties (Pather *et al.*, 2011).

Considering the effective antimicrobial properties of AgNPs and the enormous interest in their application as coatings for medical devices and in wound therapy, of the green synthesis of AgNPs and its application in wound healing is the better alternative (Shekhawat and Arya, 2008).

1.2. Aim, objectives and hypothesis

Aim

To synthesize AgNPs using *Bulbine frutescens* gel sap extract and investigate their antimicrobial effects.

Objectives

- To synthesize AgNPs from leaf extract of *B. frutescens* using green chemistry.
- To characterize the synthesized AgNPs.
- To investigate the antimicrobial activity of the AgNPs against selected sensitive and resistant pathogenic microbes.

Alternate Hypothesis

Bulbine frutescens is capable of forming AgNPs that have antimicrobial activity.

Null hypothesis

Bulbine frutescens is not capable of forming AgNPs that have antimicrobial activity.

Primary Research questions

- Does the aqueous leaf extract of *B. frutescens* effectively reduce silver ions to Ag⁰?
- Are the green synthesized AgNPs capable of inhibiting the growth of various microbes?

1.3. What are antibacterial compounds?

Antibacterial / antibiotic drugs are the most commonly used and abused antimicrobial agents worldwide to manage bacterial infections, to kill or inhibit the growth of bacteria (Barbosa *et al.*, 2014; Hajipour *et al.*, 2012). The antibacterial agents and semi-synthetic compounds which are currently available on the market are β -lactams (like penicillin), carbapenems and cephalosporins. Amino glycosides, which are pure natural products, and sulphonamides, which are purely synthetic antibiotics, are also readily available on the market. Antibacterial agents are vital in the fight against infectious diseases (Hajipour *et al.*, 2012).

Currently there are numerous antibacterial agents used in clinical research for the treatment of bacterial infections (Barbosa *et al.*, 2014). However, due to the broad use and abuse of the compounds, antibacterial resistance has become a common and widespread global problem. Resistance is commonly a result of evolutionary processes which take place during antibiotic therapy resulting in inheritable resistance (Hajipour *et al.*, 2012).

1.3.1. Microbial resistance to antimicrobial drugs

Multidrug resistant microorganisms pose a major threat on the public health system globally (Rai *et al.*, 2009). Resistant microorganisms such as fungi, bacteria, parasites and viruses are unresponsive to drugs used against them such as antifungals, antibiotics, antivirals and antimalarials. Drugs, which are currently being used to treat infectious diseases, have become ineffective allowing for the microbial population to thrive (WHO, 2015). The increase in drug resistant infections has led to an increase in the mortality rate, morbidity and cost due to prolonged hospitalization and treatment regimens (Lara *et al.*, 2010). Annually, 100 000 tonnes of antibiotics are produced (Nikaido, 2009).

1.3.2. Bacterial cell wall and sensitivity to antimicrobial agents

For over a century, microbial infections such as bacterial, fungal, viral and parasitic infections have been treated using antimicrobial agents which are either synthetic or semi-synthetic. These antimicrobial agents are able to kill (microbicidal) or prevent the growth (microbistatic) of microorganisms (Acar *et al.*, 2015). However, a large number of microorganisms have developed the ability to survive under these conditions and are able to adapt and evolve over

time resulting in resistance against every available therapeutic antimicrobial on the market (Acar *et al.*, 2015).

Bacteria can be classified as Gram-positive or Gram-negative organisms through the ability to retain the Gram stain (Wiegel, 1981). Gram-positive bacteria consist of a 20 – 50 nm thick layer of peptidoglycan (PG). They are attached to teichoic acids that are distinct to the Gram-positive cell wall (Barnett *et al.*, 2004; Scott *et al.*, 2006). The cell walls of Gram-negative bacteria are more complex structurally and chemically. Gram-negative bacteria consist of a thin PG layer and an outer membrane which covers the surface membrane. The outer membrane of Gram-negative bacteria is responsible for the resistance to hydrophobic compounds which are comprised of lipopolysaccharides. Lipopolysaccharides augment the negative charge of the cell membranes and are crucial for the structural integrity and viability of the bacteria (Hajipour *et al.*, 2012). The cell wall and membranes are important defensive barriers for bacterial resistance to the external environment. The cell wall helps maintain the bacterium's natural shape. The components of the cell membrane provide different pathways of adsorption of Gram-positive and Gram-negative bacteria (Delcour *et al.*, 2009; Ghai I and Ghai S, 2017; Pages *et al.*, 2008; Stavenger *et al.*, 2014; Vergalli *et al.*, 2017; Winterhalter *et al.*, 2015). The cell wall plays an integral role in the tolerance or susceptibility of bacteria to antibacterial therapeutic agents (Hajipour *et al.*, 2012).

The bacterial cell wall is surrounded by an exoskeleton-like structure which is composed of PG sacculus (Liow *et al.*, 2011). This structure is made up of glycan strands cross-linked by short peptides which generate a covalent mesh that helps in maintaining the shape of the bacteria and prevents their lysis due to the high internal osmotic pressure (Liow *et al.*, 2011). There are two main mechanisms which bacteria employs against antimicrobial therapies (i) enzymatic barrier which primarily destroys the antimicrobial compound, and (ii) membrane barrier which limits the intracellular access of antimicrobial compounds ultimately leading to the failure of the antimicrobial therapy (Ghai *et al.*, 2017).

1.3.3. Classes of antibiotics and their sites of action on bacteria

Different antibacterial drugs are known to target various parts of the bacteria to inhibit or disrupt its functioning. Table 1.1 below shows the different antibacterial drugs which target various parts of the bacteria. These targets include the cell wall and cell membranes, ribosomes, nucleic acids, bacterial cellular metabolism and bacterial cellular enzymes (Barbosa *et al.*, 2014). As demonstrated in the table 1.1 and figure 1.1 below, there are various mechanisms by which these agents are able to inhibit bacterial multiplication and growth or destroy bacteria by (i) inhibition of cell wall synthesis and disruption of the cell membrane function, (ii) inhibition of protein synthesis (50S and 30S), inhibition of nucleic acid synthesis for both (iii) DNA and (iv) RNA, and (v) functioning as anti-metabolites (Barbosa *et al.*, 2014).

Table 1.1: Various bacterial targets of antibacterial drugs (Barbosa *et al.*, 2014).

	Bacterial target	Antimicrobial drugs
(i)	Cell wall synthesis and inhibitors	β -Lactams β -Lactamase inhibitors Glycopeptides Polypeptides Pyridine-4-carbohydrazide Tetracyclines
(ii)	Protein synthesis	Aminoglycosides Furanes Ketolides Lincosamides Macrolides Oxazolidinones Streptogramins
(iii)	DNA synthesis	Coumarins Naphthyridines Quinolones 2-Pyridones
(iv)	RNA synthesis	Rifamycins
(v)	Intermediary metabolism	Sulfonamides

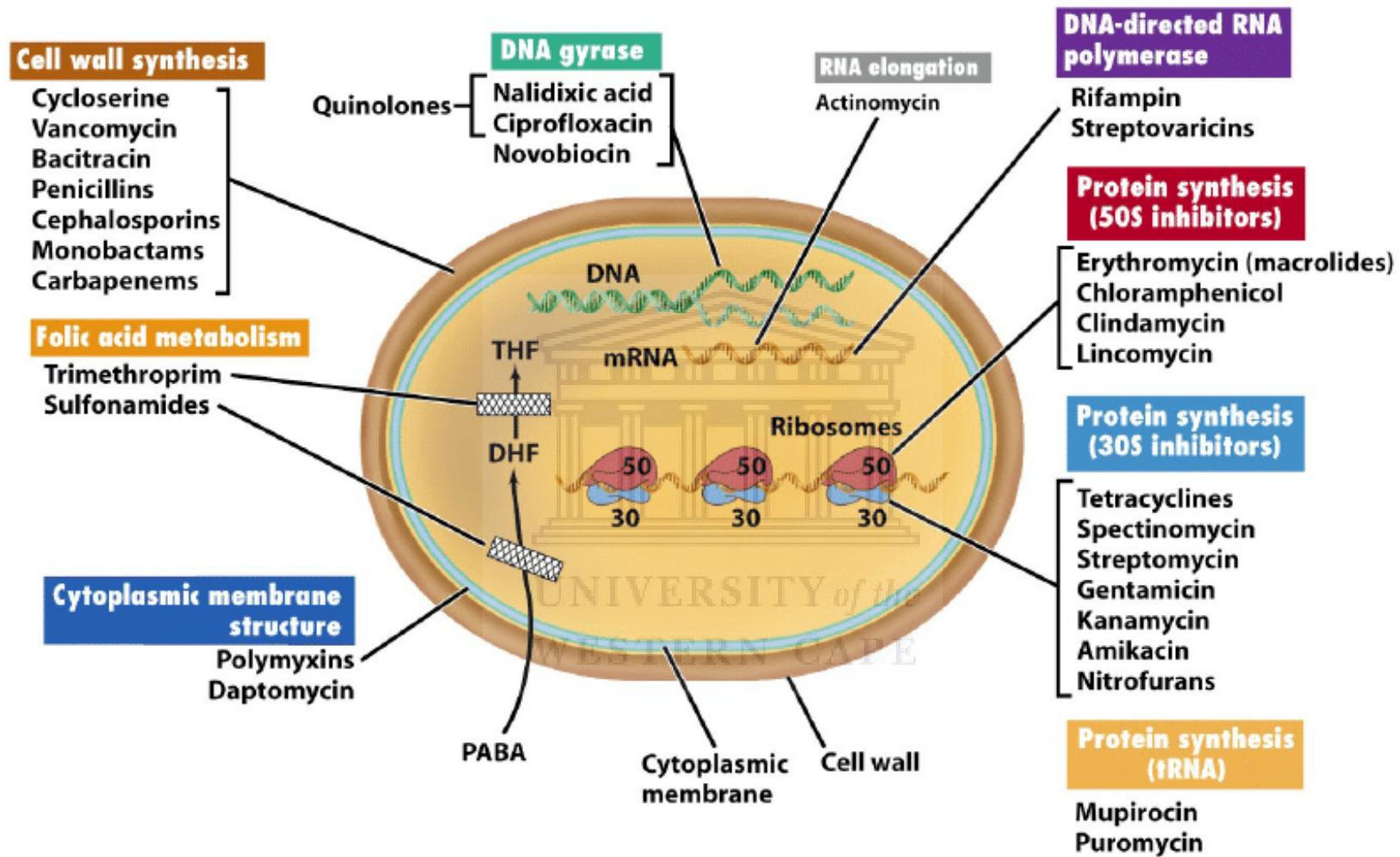


Figure 1.1: Classes of antibiotics/ antimicrobial agents and their mode of action against bacteria (Labnotesweek4, 2013).

Antibacterial agents have a selective structural and metabolic advantage in bacteria cells and mammalian cells in that they cause selective toxicity to the bacteria organisms without damaging the host cells. The current drug-resistant bacteria include: multidrug resistant *Mycobacterium tuberculosis*, *Enterobacter cloacae*, *Escherichia coli*, *Acinetobacter baumannii*, *Haemophilus influenza*, *Pseudomonas aeruginosa*, *Klebsiella pneumoniae*, penicillin-resistant *Neisseria gonorrhoeae* (PPNG), *Shigella flexneri*, *Salmonella enterica*, *Vibrio cholera*, penicillin-resistant *Streptococcus pneumoniae*, macrolide-resistant *Streptococcus pyogenes*, and vancomycin-resistant *Enterococcus* (Pelgrift and Friedman, 2013). *Staphylococcus aureus* is resistant to methicillin, sulphonamide, vancomycin and penicillin (Pelgrift and Friedman, 2013).

1.3.4. Mechanisms of resistance of microbes against antimicrobial drugs

The acquired resistant genes enable the bacteria to develop various resistance mechanisms to avoid the antibiotics that they were exposed to. Figure 1.2 below illustrates the various mechanisms of antibiotic resistance.

As depicted in the illustration, the first mechanism of antibiotic resistance can be achieved by the presence of an enzyme that inactivates – alters the antibiotic. Second mechanism is the metabolic evasion of the targeted pathway or the development of an alternative pathway in which the antibiotic is inhibited by the enzyme. The third mechanism entails the mutation of the antimicrobial target resulting in a decrease in the binding of the antimicrobial agent or the sequestering process of the drugs via protein (50S and 30S) binding. The fourth mechanism encompasses posttranslational or posttranscriptional modifications of the antimicrobial target resulting in the reduction of the binding of antimicrobial target or modifications of the targets. The fifth mechanism involves the decrease in antimicrobial uptake due to modified cell wall proteins. The sixth mechanism of antimicrobial resistance results in the active draining of drugs out of the microbe. The seventh mechanism entails the overproduction of the antimicrobial agents target by the microbes (Barbosa *et al.*, 2014).

Examples of mechanisms of antibiotic resistance

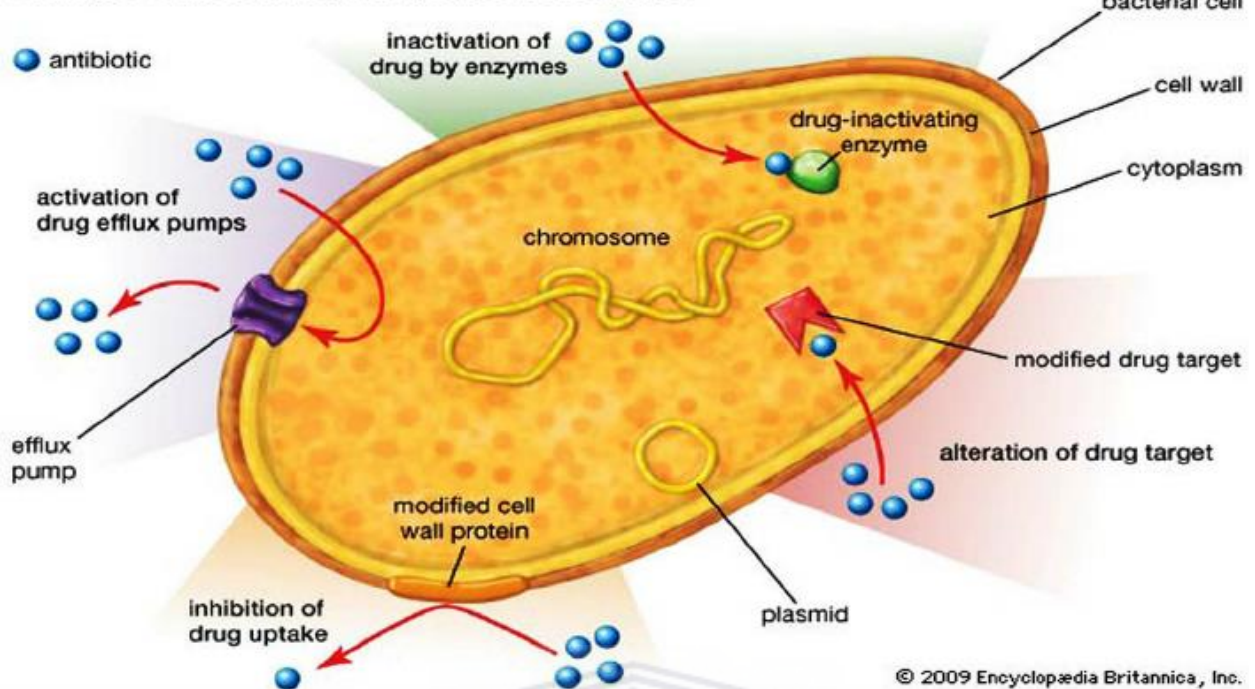


Figure 1.2: Examples of the different mechanism of antibiotic resistance (Encyclopaedia- Britannica, 2009).

Poor patient compliance or the use of time-dependent antibiotics with a long shelf-life is one of many causes of drug resistance (Barbosa *et al.*, 2014). The development of resistance to an antimicrobial agent is dependent on the duration of exposure. Microbistatic drugs are unlike microbicide drugs in that they inhibit the growth of microbes and do not kill all microbes, thus allowing some microbial cells to survive and therefore develop resistance due to overexposure to the antimicrobial agent or drug (Levy and Marshall, 2004). The mismanagement of dose amount and missed schedules doses further increases the selective pressure in favour of drug resistance due to microbial cells not completely being eradicated by the drug (Singer *et al.*, 2016). Due to poor patient compliance, drugs which are developed to treat infections have a short dosage interval resulting in an increase in dosage number for microbial eradication (Levy and Marshall, 2004). However, even when there is good patient compliance, selective pressure in favour of antimicrobial resistance still occurs due to the events that unfold within individual dosing intervals (Barbosa *et al.*, 2014).

1.4. *Fusarium* fungal species

The *Fusarium* species is globally distributed in soil, plants, water and manmade habitats. It is responsible for plant diseases and can be a serious opportunistic human pathogen which affects immunocompromised patients (Kredics *et al.*, 2015; Nucci and Anaisse, 2007). The infections caused by *Fusarium* species are mainly through airborne transmission, skin breakdown due to trauma, burns or insertion of vascular catheters (Nucci and Anaisse, 2007; Raad *et al.*, 2002). Infections in humans can possibly manifest as a fever that does not respond to antimicrobial therapy. It may also cause localised infections, such as onychomycosis, keratitis and other skin infections (Chang *et al.*, 2006; Godoy *et al.*, 2004; Morales-Cardona *et al.*, 2014; Takenaka, 2016; Zaias *et al.*, 2014). In paediatric cancer patients, *Candida* species remain the most important cause of invasive fungal diseases (IFD) followed by invasive infections by *Aspergillus spp.* and other fungi (Castagnola *et al.*, 2005, 2006; Hale *et al.*, 2010). The epidemiology of fungal infections varies markedly according to the geographic region. In Brazil, *Fusarium* species pose a major threat to cancer patients (Nucci *et al.*, 2013). The *Fusarium* species are among the most resistant fungi and systemic and conventional antifungal agents fail to treat those infected with this species of fungi (Guarro & Fusariosis, 2013).

1.4.1. Susceptibility to various antimicrobial compounds

The *Fusarium* species are resistant to azole, echinocandins and polyenes antifungals (Nucci *et al.*, 2014). This poses a major challenge on the agricultural and medicinal sector to find alternative means to inhibit the growth of the *Fusarium* species. Currently on the market, voriconazole is used to treat immunocompromised individuals and has increased the survival rate significantly. Amphotericin B deoxycholate gives relatively poor survival results in comparison to voriconazole. Voriconazole is statistically associated with 60% survival rate, whereas amphotericin B deoxycholate is associated with 28% survival rate (Nucci *et al.*, 2014). Although these antifungal drugs offer more choices for treatment against *Fusarium* species, the most suitable candidate to treat antifungal infections has still not been found (Nucci *et al.*, 2014).

1.5. Current management of antimicrobial resistance in wound infections

For many centuries numerous natural remedies have been used for the treatment of various types of wounds which aim to increase blood clotting, absorb wound exudates, and hasten healing. It is crucial that a moist environment is provided at the wound site for the migration of various cells to facilitate wound contraction.

Selecting an ideal wound dressing is dependent on the wound type, size, amount of exudates and the risk of infection (Shao *et al.*, 2017; Zhang *et al.*, 2014). Currently on the market, hydrogels foam or film, ointment, antibacterial creams and/or antibacterial agents in combination with polymers are being used widely in clinical conditions (Hussain *et al.*, 2018).

In recent years bioactive agents have been incorporated to common antibacterial wound dressing agents (Hussain *et al.*, 2018). Bioactive agents include natural and synthetic polymers, skin substitutes, electrospun micro and nanofibers, foams, films, hydrocolloids, sponges, membranes and even hydrogels. The use of bioactive compounds in wound dressings is significantly more effective in the medicinal treatment for non-healing chronic wounds (Hussain *et al.*, 2018). Bioactive compounds are released via the hydrolysate activity of wound enzymes present in exudates or wound fluid (Boateng *et al.*, 2015). Hydrates, swelling and diffusion are used to release the bioactive compounds from the dressings to the site of injury (Dias *et al.*, 2011). Research has shown that the bioactive agents in the dressings are found to be less effective due to the rapid absorption of compounds by wound exudates (Das *et al.*, 2016). The search of a perfect wound dressing material continues to be a challenge in the field of tissue-engineering.

1.5.1. Antimicrobial potential of herbal medicines

Since the beginning of time, human beings have relied on nature to provide basic needs such as medicine and food (Gurib, 2006). The higher order plants such as conifers and flowering plants are the main source of food for animals and people. These plants are found in abundance across the world and provide inherent and distinct biological and chemical properties beneficial to all species (De Wet *et al.*, 2005; Fennel *et al.*, 2004). In recent years there has been tremendous development in the organic synthesis of medicine, however, statistics obtained

from the World Health Organization has shown that 80% of the world's population still rely on traditional medicine for treatment of various ailments (WHO, 2015).

South Africa is world renowned for its plant biodiversity. Higher order plants have been used for centuries as herbal medicine by traditional healers and indigenous people of Southern Africa which has shaped the socio-cultural heritage of Southern Africa (Thring & Weitz, 2006). There are approximately over 30000 species of higher order plants in South Africa and 3000 of these plants have been used medicinally (Van Wyk *et al.*, 2008). Indigenous people of South Africa believe that extracts from these plants obtained naturally are relatively less toxic and have fewer side effects than the synthetic drugs produced. The use of these plants has played a fundamental role in the daily lives of these people to treat and prevent ailments (Van Wyk *et al.*, 2008). Mainly in rural areas, traditional healers are the health care providers which the community consults (WHO, 2001).

The iconic Southern African medicinal plants are Cape aloes (*Aloe ferox*), devil's claw (*Harpagophytum procumbens*) and buchu (*Agathosma betulina*) (McGaw *et al.*, 2000). These plants have led to growing interest for their extensive medicinal properties and have thus enabled indigenous medicine to come to the forefront of medical research as a better alternative to synthetically produced drugs (McGaw *et al.*, 2000).

Most of the herbal materials which have shown to promote wound healing are known to contain biochemical substances such as amino acids, vitamins, hydrocolloids, fats and some inorganic substances which include mineral salts. The mechanism of wound healing and the benefits of herbal materials have been tracked down to their antioxidant activity (Yates *et al.*, 2012). The antioxidant potential of herbs has been linked to their polyphenol and carotenoid content. Carotenoids are structurally related to vitamin A and have been related to various health benefits which include decreasing the risk of certain cancers and eye disease (Mayer, 2012). Polyphenols are antioxidant compounds such as flavonoids which have been shown to reduce the risk of developing type-2 diabetes. Flavonoids in addition to their antioxidant action also impart protection against ultra-violet light and have metal chelating properties (Marcato *et*

al. 2015). Flavonoids are naturally occurring plant pigments and has been shown to significantly reduce the risk of cardiovascular and lung disease.

1.5.2. Polyphenols

Polyphenols are commonly found in the botanical organs of medicinal herbs, fruits and vegetables. They are found within the fruits, seeds, leaves, and flowers. Polyphenols key responsibility is to maintain the colour, flavour and healing abilities of many plants (Pandey *et al.*, 2009). They can inhibit the oxidation of other molecules. They can potentially terminate any chain reaction due to the free radicals produced within the oxidative processes. In many biological systems, such oxidative reactions often result in cell damage and other harmful processes such as abnormal platelet aggregation, which is a precursor to inflammatory responses. Flavonoids are the largest family of polyphenols; however, not all flavonoids are classified as polyphenols. There are different flavonoids found within plants such as anthocyanins, flavanones, flavonols, flavones and isoflavones.

Polyphenols has been shown to act as wound healing agents (Aslam *et al.*, 2018). Polyphenols block the action of harmful enzymes that cause tissue damage due to ultraviolet radiation, wound ulceration and cell mutations (Aslam *et al.*, 2018). Polyphenols are able to protect tissue cells and body fluids from free radicals generated within the oxidative process. Some polyphenols are able to slow down the growth of certain virulent viruses and microbes such as *S. aureus* and *E. coli*. The antimicrobial and anti-inflammatory properties of polyphenols prevent swelling and itching of wounds by releasing allergic mediators such as serotonin and histamine (Ambiga *et al.*, 2007).

1.5.3. *Bulbine frutescens*

Bulbine frutescens is an indigenous Southern African plant, and is commonly found in the Cape where it is grown as a garden plant (Van Wyk & Gericke, 2000). It is commonly known as snake flower, cat's tail, burn jelly plant, intelezi, ibuchu and geelkatstert (Van Wyk & Gericke, 2000). *B. frutescens* belongs to the *Asphodelaceae* family. The leaf is filled with a clear gel which is similar in appearance and consistency to the *Aloe vera* gel (Van Wyk & Gericke, 2000). There are over fifty species of *Bulbine* species part of the *Asphodelaceae* family, which has extensively been used by traditional healers for the treatment of bruises, burns, stings, rashes, eczema, external sores and other skin related ailments (Van Wyk and Gericke, 2000). *B. asphodeloides* (wilderkopiva), *B. alooides* (rooistorm), *B. natalensis* (rooiwortel), *B. latifolia* and *B. narcissifolia* (geelslangkop) have been used for the treatment of these skin related ailments (Van Wyk & Gericke, 2000). The gel of *B. frutescens* is used for the treatment of cracked lips, ringworms, wounds and herpes (Hutchings *et al.*, 1996). *B. frutescens* is mainly employed as a vulnerary due to its track record of displaying antimicrobial properties. It has also been used internally for the treatment of coughs, colds, arthritis and insanity.

B. frutescens is an aloe succulent plant with a rosette of long, fleshy, yellow-green leaves. The long flower stems bear elongated clusters of yellow-orange or yellow flowers with fluffy stamens. This study focuses on *B. frutescens* plant species with yellow flowers. Figure 1.3 depicts a photographic image of *B. frutescens*. The stems and roots are comprised of knipholone-type anthraquinones and have been employed in topical applications due to the presence of glycoproteins (Bringmann *et al.*, 2008). *B. frutescens* thrives in environments where there is lots of sunlight and requires a small amount of water to grow. It is resistant to drought, heat and frost and can be grown anywhere including a pot on the balcony or even a windowsill. It can grow in any type of soil. *B. frutescens* propagates best in spring. It only requires any piece of stem to grow. It can be watered only once a week and attracts bees all year round (Dyson, 1998; Joffe, 1993).

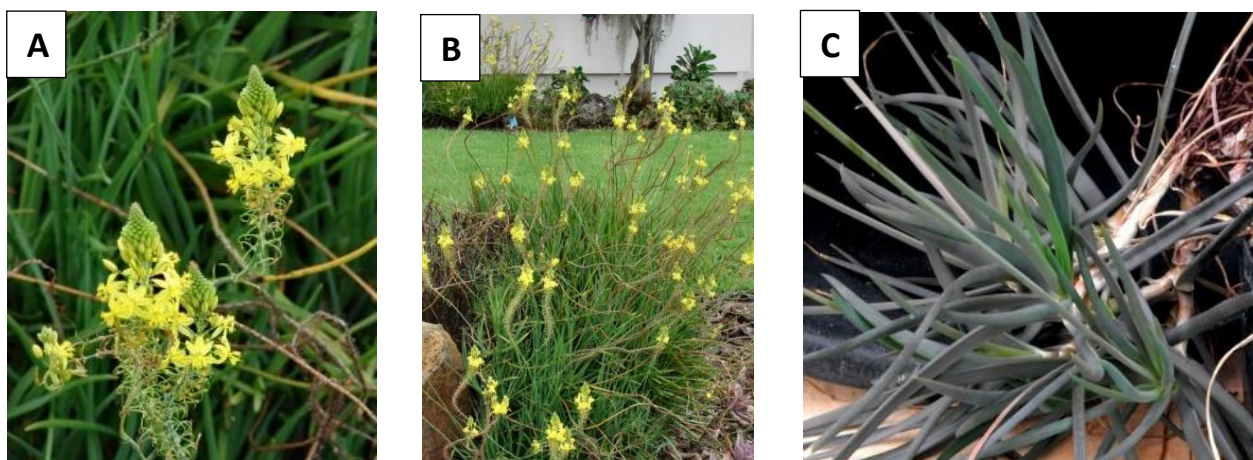


Figure 1.3: Photographic image of the *Bulbine frutescens* plant (Forest Starr & Kim Starr, 2009). **A:** Clusters of yellow flowers. **B:** Rosette of long, fleshy, yellow green flowers. **C:** Leaves of *B. frutescens* plant.

1.5.4. Antimicrobial activity of *B. frutescens* plant extract in previous literature

The antimicrobial activity of *B. frutescens* has been extensively investigated by Coopassamy and colleagues (Coopoosamy *et al.*, 2010). The findings of this study showed that *B. frutescens* acetone and ethyl extracts are able to inhibit the activity of Gram-positive bacteria such as *Bacillus subtilis*, *Micrococcus kristinae* and *S. aureus* (Coopoosamy *et al.*, 2010).

Previous phytochemical analysis has resulted in the isolation and characterization of the axially chiral phenylanthraquinones knipholone (**1**) from the polar fractions of *B. frutescens* plant. This is illustrated in figure 1.4 which also shows the isolation and characterization of 4'-O-demethylknipholone, gaboroquinones A and B, 4'-O-demethylknipholone-4'- β -D-glucopyranoside, and isoknipholone (**2**) (Mutanyatta *et al.*, 2005). The polar fraction of the *B. frutescens* plant contains 6'-O-sulfated phenylanthraquinones making this species a rich source of novel bioactive compounds (Mutanyatta *et al.*, 2005).

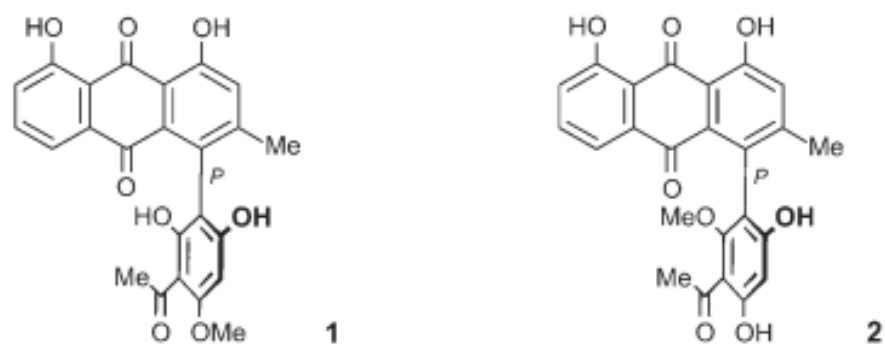


Figure 1.4: Schematic representation of the chiral phenylanthraquinones knipholone (1) and isoknipholone (2) found within the *B. frutescens* plant species (Pather *et al.*, 2011).

Widgerow and Chait used the leaves gel to promote wound healing by increasing cell proliferation and collagen deposition (Widgerow and Chait, 2000). They included the gel of the leaf in a microporous tape. The *B. frutescens* increased the hydration by leaving a layer of fatty vesicles of glycoprotein on the skin surface which exhibited antibacterial properties (Widgerow and Chait, 2000). Pather and colleagues further established that the leaf gels stimulates collagen deposition and possibly increases fibroplasia (Pather *et al.*, 2011).

1.6. Nanotechnology and nanoscience

Nanotechnology offers various new strategies for regenerative medicine. In recent years, the molecular engineering of various self-assembling biocompatible NPs were developed as an active area of nanoresearch (Chakraborty *et al.*, 2011). Metal nanoparticles (NPs) like silver, gold and zinc exhibit excellent properties such as low in vivo toxicity, and bacteriostatic and bactericidal activities (Eustis *et al.*, 2006; Rai *et al.*, 2009).

The physicist, Richard P. Feynman described the concept of nanotechnology in 1959 as, “There’s plenty of room at the bottom”. Nanomaterials provide a much greater sensitivity and permeability allowing more unique interactions than larger particles. The merging of biotechnology and nanotechnology seem logical considering the fact that biological samples can interact with nanostructures on a nanometer scale (Jeevanadam *et al.*, 2018). Interactions with similarly sized biological materials possess the ability to traverse these materials and thus allow for the discovery of novel and intriguing biological innovations (Jeevanadam *et al.*, 2018).

1.6.1. What is nanoscience and nanotechnology?

Nanoscience can be described as the production and structural manipulation of materials between 1-100 nm ranges, thus producing nanomaterials which display novel properties (Jeevanandam *et al.* 2018). These nanomaterials can be manipulated for a variety of applications called nanotechnology (Sujitha *et al.*, 2013).

Materials at nanoscale possess remarkable properties which have led to great strides in the research field of nanotechnology. Nanoparticles have been applied to a vast array of fields such as healthcare, water remediation, communication technologies, healthcare, transport and energy due to its exceptional novel characteristics at the nanoscale (Rajoriya, 2017; Das *et al.*, 2012).

Nanotechnology is an exciting and powerful discipline of science in the present century. The biosynthesis of NPs is eco-friendly, reliable and an important aspect of green chemistry approach that intersects biotechnology and nanotechnology. NPs have magnetic, electrical and optical properties which are influenced by the size, shape and interaction with stabilizers and surrounding media (Ahn-Tuan *et al.*, 2011).

1.5.2. Classification of NPs

NPs can be classified according to their composition, dimensionality and uniformity. Dimensionality classifies NPs produced according to their morphology and shape. They can either be one-dimensional (1D), two-dimensional (2D) or three-dimensional (3D). They can either be spherical, irregular or tubular shaped and can exist in fused, agglomerated or aggregated forms (Buzea *et al.*, 2007; Novack & Bucheli, 2007). The physiochemical properties in conjunction with the large surface-to-volume ratio make researchers believe that these nanomaterials are hazardous to the environment and biological organisms that live in it (Kruszewski *et al.*, 2011). Despite this, nanomaterials are continuously being developed in various industries.

NPs can be produced naturally or by anthropic sources, such as engineered or unwanted/incidental NPs. Studies conducted in the past has revealed that NPs can be present in nature where they are synthesized by natural processes such as bio-mineralization and bio-degradation (Huang *et al.*, 2007). Under *in vivo* conditions NPs can be synthesized through erosion, forest-fires, friction, volcanic eruptions, marine wave strokes, physical and chemical weathering of rocks, etc (Kersharwani *et al.*, 2014). NPs are generated through regular human activities such as fuel combustion, welding fumes, industrial effluents, automobile exhaust, etc. Engineered NPs are synthesized to serve a specific purpose for the benefit of mankind.

As shown in figure 1.5 below, nanomaterials can be categorized into polymers, carbon-based materials, magnetic-based materials, composites, dendrimers, quantum dots, and lipid NPs. These can be found in various shapes such as tubes, wires, crystals, rods, spheres and even core-shell nanoparticles (Huang *et al.*, 2007; Kersharwani *et al.*, 2014; Liu *et al.*, 2014).

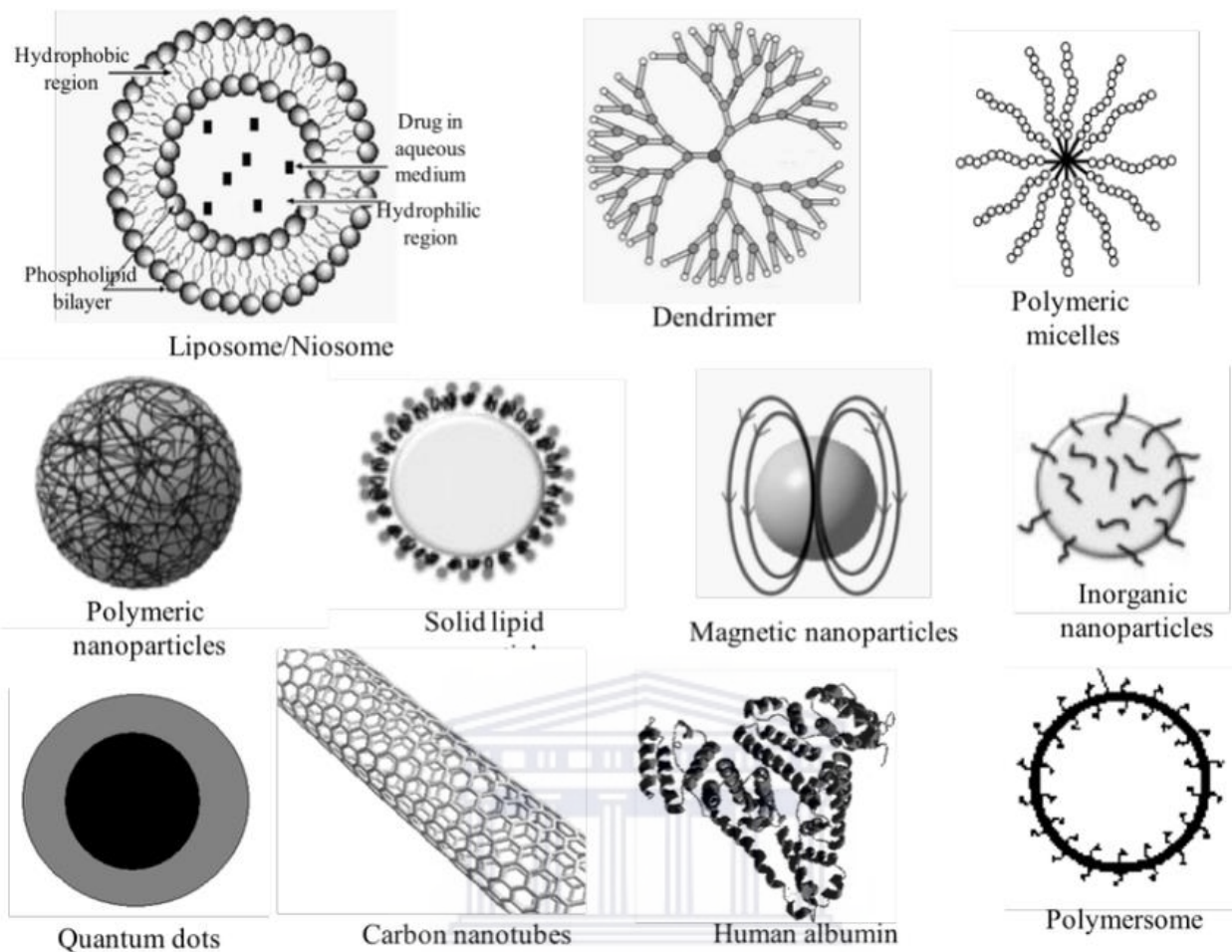


Figure 1.5: Different types of nanoparticles (Berciano-Guerrero *et al.*, 2014).

UNIVERSITY of the
WESTERN CAPE

1.5.3. Green nanotechnology

Traditionally, metallic NPs are synthesized by physical methods such as pulsed laser ablation or ion sputtering and chemical methods such as solvothermal synthesis, hydrothermal, sol-gel methods, and reduction. The chemical method of NP synthesis is expensive, it involves chemicals that can be hazardous when disposed in the environment and it requires stabilizing agents to prevent NPs from aggregating (Akhtar *et al.*, 2013; Mollick *et al.*, 2015). For these reasons, more environmentally friendly approaches for synthesis of metallic NPs have been developed called 'green synthesis'. Microorganisms and plant extracts have recently been used for the synthesis of NPs (Binupriya *et al.*, 2010).

The green synthesis of NPs can be achieved intracellularly and extracellularly (Akhtar *et al.*, 2013). Intracellular synthesis involves the synthesis of NPs using microorganisms. Bacteria and fungi have been reported in previous literature to synthesise NPs by absorbing the metals and using their cellular machinery to convert them into NPs (Mollick *et al.*, 2015). However, the use of microbes to synthesise NPs has its limitations. Microbes are expensive to maintain and they require multi-step processes to be isolated (Akhtar *et al.*, 2013). Synthesizing NPs extracellularly using plants would eliminate these steps, be less time-consuming and more cost-effective (Akhtar *et al.*, 2013).

Plants are known as green factories in the genesis of NPs. The major advantage of using plant extract for the biogenesis of AgNPs is that they are readily available, safe, non-toxic have a wide array of metabolites and can contribute to the reduction of silver ions quicker than microbes. Interest of researchers grew dramatically as plant material used as the reducing agent in synthesis of NPs minimizes the cost, time, waste and etc. This is illustrated in figure 1.6. It provides a sustainable procedure for the development of an eco-friendly and simple method for the fabrication of AgNPs leading to the introduction of a photo-biological approach. Green nanotechnology is also commonly known as the 'photo-biological approach' which makes use of the plants or their extracts of plants as reducing or capping agents in the synthesis if AgNPs (Reddy et al, 2014).

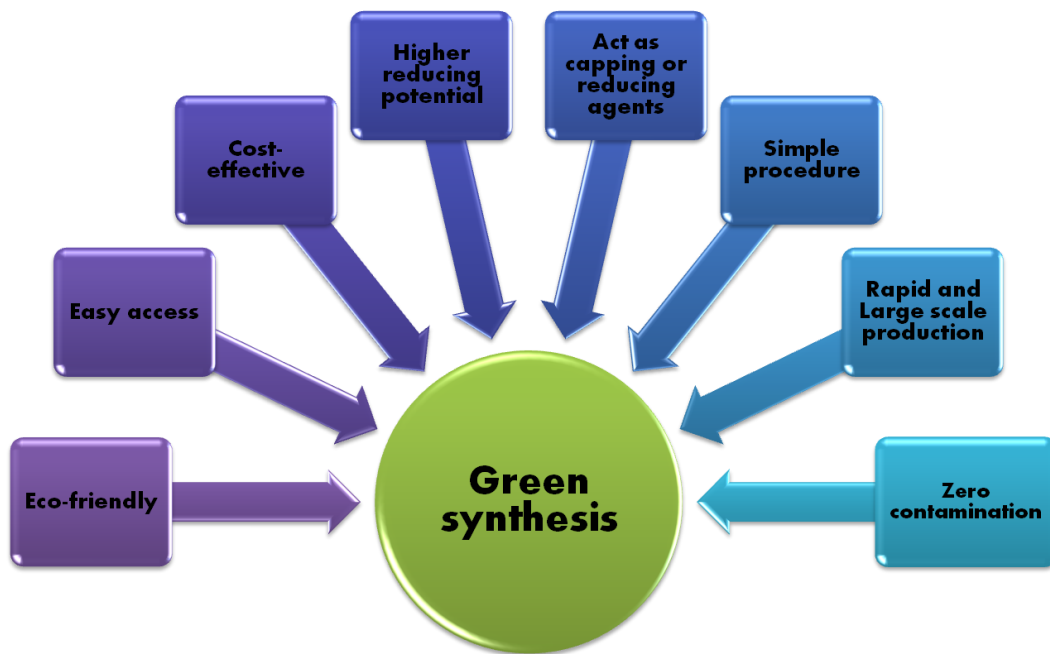


Figure 1.6: Advantages of green nanotechnology.

1.6. Silver

Silver (Ag) is a soft greyish-white lustrous element with atomic weight of 47. It is insoluble in water, whereas its metallic salts, such as AgNO_3 (silver nitrate) and AgCl (silver chloride), are soluble in water. Metallic silver in its finely dispersed form exhibits unique properties normally associated with noble metals such as chemical stability, excellent electrical conductivity, anti-bacteriostatic effects, non-linear optical behaviour and catalytic activity (Henglein, 1989; Mulvaney, 1996).

Silver has been known as an environmental hazard for over 7000 years even though the history of human life has been associated with it. Since the 18th century it has been exploited for its medicinal and antibacterial properties. However, the bioaccumulation properties, toxic effects and persistence of silver within the environment made it imperative for the usage of silver and exposure to be controlled (Jabeen *et al.*, 2013; Li *et al.*, 2009; Luoma, 2008).

1.6.1. Biosynthesis of AgNPs

The fabrication of NPs can occur via biological, physical, chemical, electrochemical, photochemical, sonolytic and radiolytic methods (Zakir, 2006). AgNPs can be synthesized either by top-down (physical) and bottom-up (chemical methods and via green pathway) approaches.

The top down approach involves the breakdown of bulk material into the nanoscale size without changing the elemental composition of the bulk material, while the bottom-up approach deals with fabricating NPs by collecting, consolidating and using individual atoms and molecules to nanosized particles (Bar *et al.* 2009; Mirunalini, 2011; Rosarin & Mirunalini, 2011) . The top-down approach for NP production is mainly used for industrial scale synthesis, and is not favoured by the scientific community. This method of synthesis is difficult, expensive and requires complex instrumentation (Ju-Nam & Lead, 2008; Powers *et al.*, 2006).

The bottom-up approach consists of chemical/physical methods or green synthesis or biological methods (plants or microbes). Chemical and physical methods, such as sol-gel process or chemical vapor deposition, are costly and extremely toxic to the environment. Up-scaling of NPs produced by physical processes are difficult and have a short shelf lifespan. Physical methods require NPs to be capped with capping agents thus contributing to its very low thermal stability. Chemical processes involve multiple purification rounds using explosive solvents, high consumption for processes (sonication and microfluidization) and by-products have harmful effects on the environment.

Plants are known as green factories in the genesis of NPs. The major advantage of using plant extract for the biogenesis of AgNPs is that they are readily available, safe, non-toxic have a wide array of metabolites and can contribute to the reduction of silver ions quicker than microbes (Iravani & Zolfaghari, 2013). NPs synthesised using plants are found to be more polydispersed with different shaped particles due to the presence of phytochemicals such as polyphenols, flavones, organic acids and quinones within the plant extract (Prathna *et al.*, 2010; Kumar *et al.*, 2008). It provides a sustainable procedure for the development of an eco-friendly and simple method for the fabrication of AgNPs.

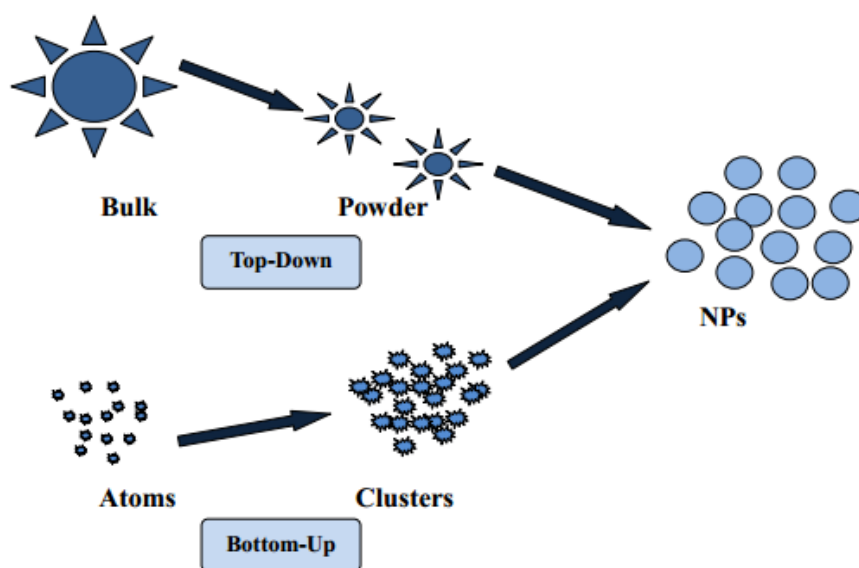


Figure 1.7: Different approaches for synthesis of metallic NPs (Prathna *et al.*, 2010).

1.6.2. The role of plant biomolecules in the green synthesis of AgNPs

Phytosynthesis or phytofabrication or green synthesis involves the reduction of silver ions by the plant biomass into AgNPs. Aqueous extracts are considered more eco-friendly over organic extracts making it the better alternative for green synthesis.

It is known that almost all plants such as herbs, shrubs or trees contain phenols, latex, flavonoids, alcohols and proteins which can produce AgNPs from silver salts. The whole plant or parts of the plant such as the roots, leaves, seeds, bark, fruits, pulp or secretory substances and *in vitro* raised calli have been reported in previous studies for the synthesis of NPs (figure 1.8) (Manjumeena *et al.*, 2014).

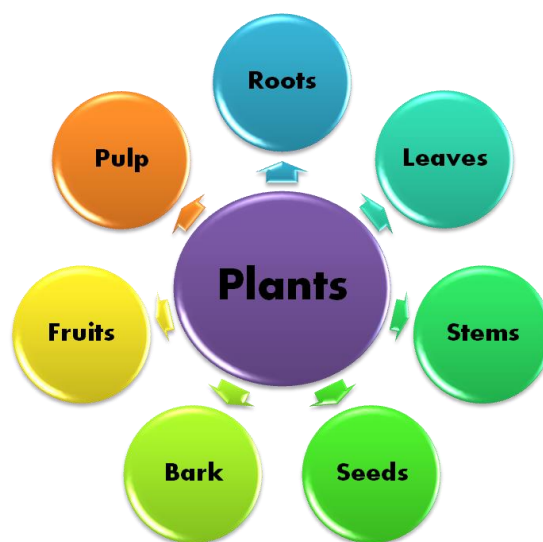


Figure 1.8: The different parts of plant used in green synthesis of NPs.

The nature of the plant extract directly influences the type of NPs synthesized with the source of the plant extract being the most vital factor affecting the morphology and size distribution of the NPs produced (Luoma,2008). This can be attributed to the vast array of biomolecules present within the plant extract (Manjumeena *et al.*, 2014).

Plants contain primary metabolites such as proteins, peptides, amino acids, and reducing sugars which play a critical role in the stabilization and reduction of silver into AgNPs. Park and colleagues have shown that polysaccharides play a role in the synthesis of gold nanoparticles (AuNPs) and beta D-glucose serves as a reducing agent (Pratna *et al.*, 2010). Starch has been reported as a stabilizing agent in the synthesis of AgNPs (Pratna *et al.*, 2010).

AgNPs have been synthesized from *A. vera* due to the presence of natural phytochemicals which act as natural capping and reducing agents (Yebpella *et al.*, 2011). The polyphenol, rosmarinic acid, in *C. aromaticus* has been reported to be responsible for the observed antioxidant activity in AgNPs (Vanaja & Annudurai, 2013). *Dioscorea bulbifera* tuber which has a high amount of flavonoids and phenolic acid derivatives has been reported to synthesise AgNPs (Ghosh *et al.*, 2012).

Phytochemical analysis of *D. bulbifera* tuber extract strongly supports its reducing capability of Ag^+ to Ag^0 . *Pulicaria glutinosa* plant extract is rich in phenolic compounds, which are known to play a vital role in the reduction of silver ions (Kora & Arunachalam, 2012).

1.6.3. Mechanism involved in the green synthesis of AgNPs

Researchers have proposed a preliminary mechanism for the accumulation of NPs after the reduction of metal ions and the reduction process which is mediated by reducing agents or enzymes which are bound to the cell wall (Kesharwani *et al.*, 2014). It has been reported that biosynthetic products or reduced cofactors play an important factor in the reduction of respective salts to form NPs. Plants have a complex network of enzymes and antioxidant metabolites which work around the clock to prevent oxidative damage to cellular components. Although each plant's phytochemical profile varies, the reduction of ions seems to be the major mechanism taking place within the synthesis of NPs. Though the exact mechanism involved in AgNP synthesis may not be fully deciphered, it is believed that the biomolecules involved directly cause the reduction process to occur (Jha *et al.*, 2009).

Figure 1.9 illustrates a hypothetical mechanism for the bioreduction of silver ions using plant extracts to form AgNPs. The core mechanism for the bioreduction of silver ions firstly involves the entrapment of the silver ions on the surface of proteins within the extract by electrostatic interactions. Silver ions are then reduced by the proteins resulting in secondary structures being formed, which contain silver nuclei. The silver nuclei then grow, through the reduction of more silver ions and the aggregation at the nuclei (Li *et al.*, 2007). This mechanism of plant-mediated synthesis can somewhat be associated with the phytoremediation process found within plants (Anderson *et al.*, 1998; Huang *et al.*, 1996).

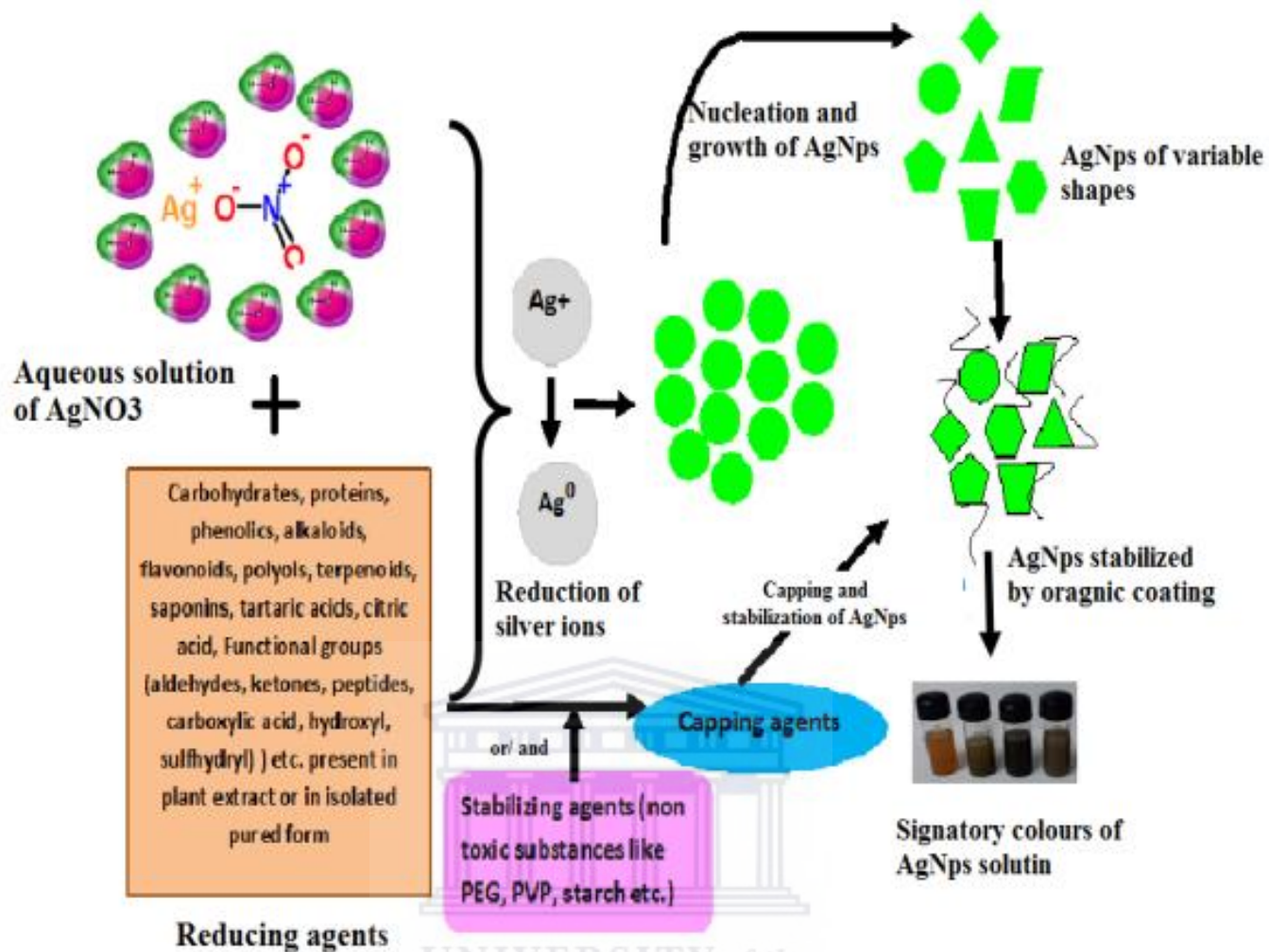


Figure 1.9: A hypothetical mechanism involved in the reduction of silver ions to form AgNPs using green synthesis (Rajoriya, 2017).

1.6.4. Factors affecting the synthesis of AgNPs

Although the plant material provides natural reducing and capping agents, the parameters for the green synthesis of AgNPs are equally responsible for the reducing and capping ability of AgNPs. The shape, size and morphology of NPs produced are directly affected by the reaction conditions such as time, pH, incubation temperature, concentration of extract and AgNO₃, and pH (Chan & Don, 2013).

The rate of synthesis and final conversion to AgNPs has been reported to be faster with a larger quantity of plant extracts and metal ions (Song *et al.*, 2009). The amount of reducing agent present within the reaction affects the stability of the AgNPs. Previous studies have shown that smaller NPs are produced at higher temperatures (Dubey *et al.*, 2010; Song *et al.*, 2008). Heating a reaction mixture to 95 °C using Magnolia leaf extract as the reducing material resulted in 90% formation of AgNPs within a few minutes (Song *et al.*, 2008).

pH has been shown to influence the synthesis of NPs. The net charge on the biomolecules changes from a positive to a negative charge thus creating repulsion between the negatively charged ions within the biomolecules. It has been reported that increasing the pH results in smaller NPs and prevents further nucleation from taking place (Shankar *et al.*, 2004). Acidic pH retards the formation of AgNPs whilst alkaline pH promotes the formation of AgNPs (Sithole, 2015). Sathishkumar and colleagues were able to form spherical and decahedral NPs by gradually increasing the pH of the medium (Sathishkumar *et al.*, 2009). The stability of AgNPs increases with increase in the time of synthesis. Similarly, other factors within the synthesis such as salt concentration and amount of reducing agent present influence the desired morphology of NPs.

1.6.5. NPs against antimicrobial resistance

Metallic NPs have been used in previous studies to exert antimicrobial activities against a range of bacteria and have been effective against numerous infectious diseases including antibiotic resistant ones (Baek & An, 2011; Devi & Joshi, 2012; Sondi & Salopek-Sondi, 2004). Although NPs such as silver (Ag), zinc oxide (ZnO), copper oxide (CuO) and nickel oxide (NiO) have antimicrobial properties, the precise mechanism involved in the toxicity of the NPs against bacteria still needs to be validated (Pelgrift & Friedman, 2013).

NPs can exert their effects by the direct interaction with the bacterial cell wall, inhibition of biofilm formation, generation of Reactive Oxygen Species (ROS) and induction of intracellular effects (Aderibigbe, 2017; Al Matar *et al.*, 2017; Basseghoda *et al.*, 2018; Hemeg, 2017; Katva *et al.*, 2018; Natan and Banin, 2017; Rai *et al.*, 2017; Siddiqi *et al.*, 2018; Singh K. *et al.*, 2014; Slavin *et al.*, 2017; Zaidi *et al.*, 2017).

It is well known that NPs adhere to the bacterial membranes via electrostatic interactions consequently causing the disruption of the integrity of the bacterial membranes (Hajipour *et al.*, 2012). The increase in reactive oxygen species (ROS) production has been closely related to the cytotoxicity of the NPs against bacteria. ROS damage can be achieved against the bacterial membrane, DNA and mitochondria which eventually leads to bacterial death, as illustrated in figure 1.10 below (Baek and An, 2011; Devi & Joshi, 2012; Hajipour *et al.*, 2012; Sondi and Salopek-Sondi, 2004). NPs can generate distinctive ROS such as superoxide or hydroxyl radical.

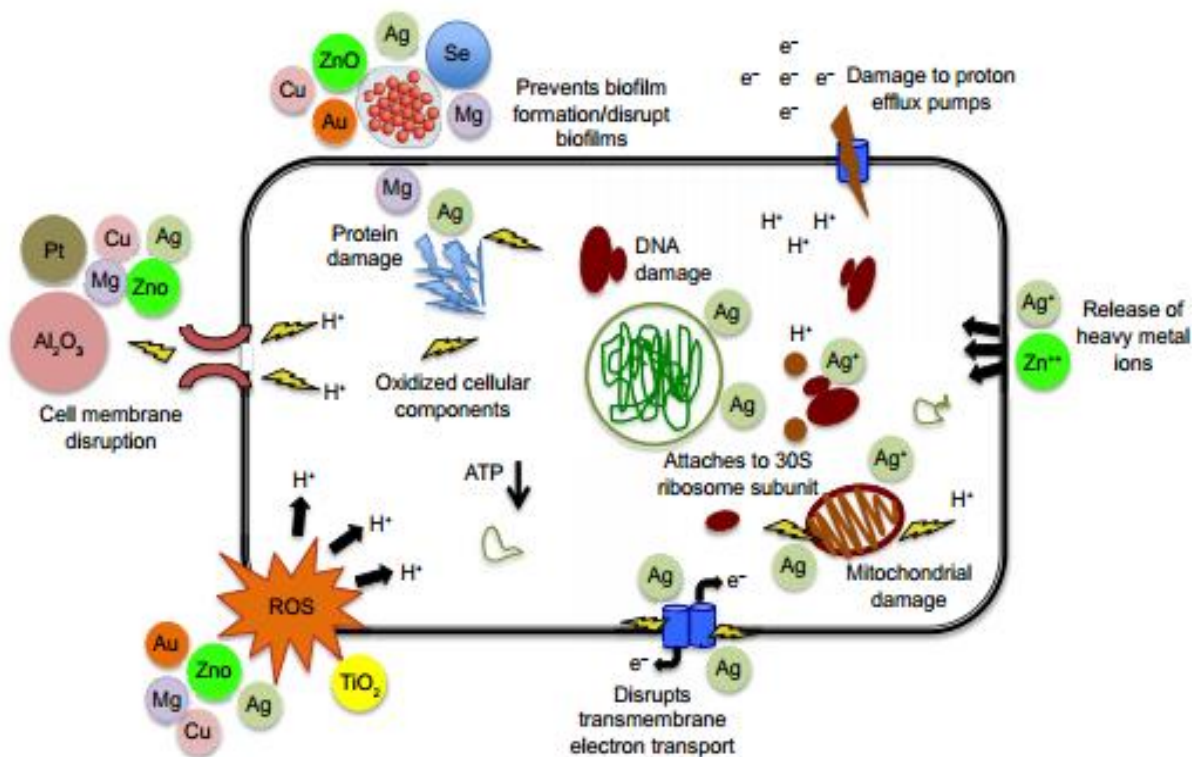


Figure 1.10: NPs and their ions (eg. Ag^+ , Zn^{2+}) producing free radicals, resulting in the induction of oxidative stress. The produced ROS irreversibly damages the bacteria resulting in bacterial death (Hajipour *et al.*, 2012).

Various metallic NPs use a multitude of mechanisms to simultaneously combat microbes. These NPs include nitric oxide-releasing NPs (NO NPs), metal-containing NPs (MC-NPs) and chitosan-containing NPs (CC-NPs). These multiple simultaneous mechanisms of antimicrobial action highly decreases the chance of the development of resistance to these NPs, as multiple simultaneous gene mutations in the same microbial cell would be required for resistance to develop (Hajipour *et al.*, 2012). NPs also possess the ability to target and deliver antimicrobial drugs to the site of infection, thus reducing the dosage amount required to treat the infection and potentially overcoming microbial resistance (Hajipour *et al.*, 2012).

NPs exert their bactericidal activity by being closely associated with R-SH groups. The heavy metal ions of non-essential transition metals with high atomic numbers such as Ag^+ or Hg^{2+} can easily bind to SH groups, such as in cysteine, which can directly disrupt the function of specific enzymes or break S-S bridges necessary to maintain the integrity of folded proteins, causing detrimental effects to the metabolism and physiology of the cell (Mu *et al.*, 2015).

The inhibition of the efflux pumps is another possible mechanism for the bactericidal activity of NPs. Bonaee and colleagues adduced a novel efflux pump inhibitory role of zinc oxide nanoparticles in *E.coli* and *S. aureus* (Bonaee *et al.*, 2010). A 27% and 22% increase in the zone of inhibition for ciprofloxacin in the presence of zinc oxide nanoparticles in *S. aureus* and *E. coli*, respectively (Banoee *et al.*, 2010). A study conducted by Padwal and colleagues using polyacrylic acid-coated iron oxide (magnetite) nanoparticles (PAA-MNP) with rifampicin against *Mycobacterium smegmatis* with emphasis on the efflux inhibitory role of PAA-MNP determined that the function of the efflux pump (Padwal *et al.*, 2015). The function of the efflux pumps can be inhibited by the metallic nanoparticles by blocking the extrusion of antibiotics outside the cells or disrupting the efflux kinetics by terminating the proton gradient. This results in deterioration of the driving force essential for efflux pump activity (Choi *et al.*, 2008; Dibrov *et al.*, 2002; Padwal *et al.*, 2015).

Biofilms provide resistance to bacteria, but this defiance gets intensified if the biofilm produced is produced by drug-resistant bacteria (Christena *et al.*, 2015). NPs can act as anti-biofilm agents by disintegrating the thick biofilm barrier through various modes of action (Ansari *et al.*, 2014; Morones-Ramirez *et al.*, 2013; Roe *et al.*, 2008; Velázquez-Velázquez *et al.*, 2015). This can be achieved by using antibiotics in symbiosis with NPs. A previous study has shown that the symbiotic use of ampicillin and AgNPs greatly enhanced the inhibition in Gram-negative and Gram-positive bacteria by 55 and 70 %, respectively, in contrast with 20 % biofilm inhibition after treatment with AgNPs alone (Gurunathan *et al.*, 2014).

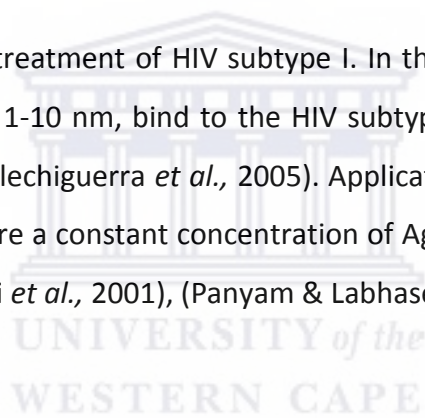
Efflux pumps play an integral role in cell to cell signalling of biomolecules to assist biofilm formation. One mechanism that can potentially be used to combat drug resistance is to employ the efflux pumps to block the quorum-sensing mechanism, hindering biofilm formation (Gurunathan *et al.*, 2014).

1.6.6. Application of AgNPs

Recently, AgNPs have been introduced into the market due to exploit of the novel properties of materials produced by nanoscience and nanobiotechnology. AgNPs are said to be the most widely commercialised nanomaterials and have extensive applications in different industries (Braydich-Stolle *et al.*, 2010).

According to Xiu and his colleagues the release of silver ions are responsible for the antimicrobial activity of AgNPs. Many companies have thus incorporated AgNPs into their products to serve as antimicrobial agents. It has also been incorporated in wound healing and medicinal products such as contraceptive devices, bone prostheses, surgical instruments, wound dressings and dental alloys. It has also been included in appliances such as refrigerators, textiles, washing machines (Kruszewski *et al.*, 2011; Stensberg *et al.*, 2011; Tian *et al.*, 2007).

AgNPs have been used for the treatment of HIV subtype I. In this *in vitro* study, it was shown that AgNPs in the size range of 1-10 nm, bind to the HIV subtype I virus, preventing the virus from binding to the host cells (Elechiguerra *et al.*, 2005). Applications for drug delivery systems and treatment of diseases require a constant concentration of AgNPs in the blood to target the specific cells or organs (Moghimi *et al.*, 2001), (Panyam & Labhasetwar, 2003).



1.6.6.1. *In vitro* studies using AgNPs

The toxicity of AgNPs is influenced by the size, type, zeta potential, dispersion status, agglomeration abilities and interaction with biomolecules. (Asare *et al.*, 2012). A study conducted by AshaRani and colleagues has shown that IMR-90 human lung fibroblast and U251 human glioblastoma cells which were exposed to 6 – 20 nm starch coated AgNPs at concentrations between 25 - 400 µg/ml for 24,48 and 72 hours respectively, has extensive DNA damage, oxidative stress, apoptosis, necrosis and low ATP levels. From the study it was concluded that exposure to AgNPs over an extended period of time resulted in metabolic arrest (AshaRani *et al.*, 2009).

In a separate study, N2A murine neuroblastoma cells were exposed to 25 nm polysaccharide coated and uncoated AgNPs at concentrations between 0.5 – 100 µg/ml for a period of 24 hours. Results from this experiment has shown that there was disruptions in the actin cytoskeleton, a decrease in the cell proliferation rate as well as oxidative stress degradation of mitochondrial integrity which persisted even after the administration of the nerve growth factor (Schrand *et al.*, 2008). In another study conducted by Yen and colleagues uncoated AgNPs (3.08, 5.75 and 24.85 nm) was administered to J774 AI macrophages at concentrations of 1 - 10 µg/ml for 24, 48 and 72 hours respectively. Cytotoxicity was only prevalent in cells which were exposed to smaller AgNPs. One may suggest from these findings that only smaller AgNPs which enter the cells are able to cause damage (Yen *et al.*, 2009).

A study conducted by Greulich and colleagues used polyvinylpyrrolidone-coated AgNPs to treat human mesenchymal stem cells (hMSCs). The AgNPs were 100 nm in size, spherical in structure and was administered between 0.05 - 50 µg/ml for a period of seven days. The treatment regime decreased proliferation and chemotaxis, and increased the release of IL-8 (Greulich *et al.*, 2009). AshaRani and colleagues have conducted an experiment which showed a concentration dependent toxic effect of both polyvinyl acetate and starch-coated AgNPs on human erythrocytes and haemagglutination resulting in swelling of cells, loss in biconcavity and haemolysis (AshaRani *et al.*, 2009).

1.6.6.2. *In vivo* studies using AgNPs

In vivo studies using AgNPs are only limited to non-human organisms (Kruszewski *et al.*, 2011). A study conducted by McAuliffe and colleagues confirmed that NPs introduced into the human body via ingestion, injection or inhalation accumulates in any or all organs of the body via circulatory and lymphatic system distribution (McAuliffe *et al.*, 2007; Panyala *et al.*, 2008). AgNPs possesses the ability to not only traverse blood vessels, but cross biological barriers of the body such as blood-testes barrier or blood-brain barrier (Lankveld *et al.*, 2010; McAuliffe *et al.*, 2007). The physiological functions of the human body are affected by acute and chronic exposure to AgNPs (Lankveld *et al.*, 2010; Sung *et al.*, 2011).

In a separate study conducted by Lee and colleagues, C57BL/6 mice that have several genes linked with motor neuron disorders, neurodegenerative disease and immune cell function in the brain was affected by exposure to AgNPs (Lee *et al.*, 2010). The inhalation and intratracheal exposure to AgNPs between 10 - 100 nm in size resulted in the accumulation of AgNPs in the lungs and blood of the C57BL/6 mice (Lee *et al.*, 2010). Another *in vivo* study conducted by Kim and colleagues involved the oral exposure of male and female Fischer F344 rats to 56 nm AgNPs. This resulted in a dose-dependent increase in alkaline phosphatase and cholesterol levels in the blood, bile-duct hyperplasia, necrosis, fibrosis, pigmentation in liver tissue (Kim *et al.*, 2010). Furthermore, a study conducted with diabetic rats showed that the topical application of recombinant human epidermal growth factor (rhEGF) incorporated poly-(lactic-co-glycolic acid) NPs fast-tracked the wound closure, increased epithelisation, and improved the fibroblast proliferation (Ryu *et al.*, 2009).

1.6.6.3. Antibacterial effects of biogenic AgNPs

Table 1.2 shows a few literature highlights in which the antimicrobial activities of biogenic metallic NPs showed exceptional results.

The functionalization of NPs using antibiotics provides a promising platform to combat bacterial resistance and potentially also reduce the dose and toxicity of the drugs. NPs have the ability to target or even deliver antimicrobial agents to the infected site, mitigating a substantially hazardous effect on normal cells. Synergistic antibacterial efficiency of AgNPs and antibiotics has been observed with *E.coli*, *S. aureus* and *P. aeruginosa* at very low concentrations (Singh *et al.*, 2014). AgNPs is shown to significantly increase the antibacterial effect of several antibiotics including amoxicillin, penicillin G, vancomycin, erythromycin against *E. coli*, *S. aureus*, and MDR bacteria (Singh *et al.*, 2014). The antibiotic-functionalized NPs exhibit the potential to reverse antimicrobial resistance. The combinatorial effect of AgNPs with natural alternative compounds such as cinnamaldehyde and eugenol has also been reported (Singh *et al.*, 2014).



Table 1.2: Applications of eco-friendly NPs in antibacterial therapy. Abbreviations: NPs, nanoparticles; MDR, multidrug resistant; ROS, reactive oxygen species.

Green synthesized NPs	Target bacteria	Antimicrobial effects	References
AgNPs from <i>Phyllanthus amarus</i> extract	MDR <i>Pseudomonas aeruginosa</i>	Membrane damage, release of free ions, inactivation of enzymes by interaction with thiol groups	Singh <i>et al.</i> , 2014
AgNPs from <i>Helicteres isora</i> fruit extract	Extensively drug-resistant (XDR) <i>P. Aeruginosa</i> isolates	Lipid peroxidation, leakage of reducing sugars and proteins, respiratory chain dehydrogenases inactivation, turbulence of membrane permeability	Mapara <i>et al.</i> , 2015
AgNPs from <i>Artemisia cappilaris</i> extract	MRSA	Membrane damage, release of free ions	Jang <i>et al.</i> , 2015
AgNPs from aloe vera extract	<i>Staphylococcus epidermidis</i> , <i>P. aeruginosa</i>	Release of free ions, increase in membrane permeability, ROS production, DNA damage	Tippayawat <i>et al.</i> , 2016
AgNPs from <i>Acalypha indica</i> leaf extracts	<i>Escherichia coli</i> , <i>Vibrio cholerae</i>	Alteration in membrane permeability and respiratory chain	Krishnaraj <i>et al.</i> , 2010
AgNPs from <i>Rhizopus oryzae</i>	<i>E. coli</i> , <i>P. aeruginosa</i>	ROS production, membrane damage, alteration in membrane permeability	Ramalingam <i>et al.</i> , 2016
AgNPs from extracts of <i>Cocos nucifera</i> fluorescence	<i>Vibrio alginolyticus</i> , <i>Klebsiella pneumoniae</i> , <i>P. aeruginosa</i> , <i>Bacillus subtilis</i> , <i>Plesiomonas shigelloides</i>	Interference with the molecular build-up of bacterial cell wall	Mariselvam <i>et al.</i> , 2014

Ag, Zn NPs extracted from <i>Caltropis procera</i> fruits or leaves	<i>V. cholerae, E. coli</i>	Inhibition of adenyl cyclase, restraining biofilm formation	Salem <i>et al.</i> , 2015
Ag, Au, Ag–Au bimetallic NPs extracted from <i>Plumbago zeylanica</i>	<i>E.coli, Acinetobacter baumannii, S. aureus</i>	Biofilm inhibition	Salunke <i>et al.</i> , 2014
Ag, Au and Ag/Au bimetallic NPs using <i>Gloriosa superba</i> leaf extract	<i>S. aureus, Streptococcus pneumoniae, K. pneumoniae, E. coli</i>	Antibiofilm activities	Gopinath <i>et al.</i> , 2016
AgNPs from <i>Rosmarinus officinalis</i> leaf extracts	<i>B. subtilis, E. coli, P. aeruginosa, S. aureus</i>	Membrane damage	Ghaedi <i>et al.</i> , 2015
AgNPs from <i>Ficus benghalensis</i> extract	<i>B. subtilis, E. coli, P. aeruginosa</i>	Membrane damage	Nayak <i>et al.</i> , 2016
AgNPs from <i>Acalypha indica</i> extract	<i>S.aureus, E. coli, P. aeruginosa</i>	Membrane damage	Nayak <i>et al.</i> , 2016
AgNPs from <i>Skimmia laureola</i> leaf extract	<i>B. subtilis, E. coli, S. aureus, P. mirabilis</i>	Increase in membrane permeability, biofilm inhibition	Ahmed <i>et al.</i> , 2015
AgNPs from <i>Delphinium denudatum</i> extract	<i>S.aureus, E. coli, B. cereus, P. aeruginosa</i>	Analgesic activity – mechanism of action not yet determined	Suresh <i>et al.</i> , 2014
AgNPs from <i>Styrax benzoin</i> extract	<i>S.aureus, E.coli</i>	Increase in membrane permeability and loss of cellular components	Du <i>et al.</i> , 2016

AgNPs from <i>Rosa chinensis</i> flower extract	<i>V. alginolyticus</i> , <i>V. Minicus</i> , <i>V. parahaemolyticus</i>	Membrane damage	Meng <i>et al.</i> , 2016
AgNPs from <i>Caesalpinia sappan</i> extract	<i>S. faecalis</i> , <i>E.coli</i> , <i>E. aerogenes</i> , <i>P. aeruginosa</i> , <i>A. niger</i> , <i>C. albican</i>	Novel nanobiotic	Jun <i>et al.</i> , 2015
AgNPs from <i>Coffea arabica</i> seed extract	<i>L. acidophilus</i>	Membrane damage	Dhand <i>et al.</i> , 2016



In conclusion, based on the information provided in the literature review section of this thesis, the aim of this study is to synthesize AgNPs using *Bulbine frutescens* gel sap extract and investigate their antimicrobial effects. This will be achieved by synthesizing AgNPs from leaf extract of *B. frutescens* using green chemistry. Characterizing AgNPs and investigating the antimicrobial activity of the AgNPs against selected sensitive and resistant pathogenic microbes.



Chapter 2: Materials and Methodology

2.1. List of equipment, chemicals and reagents

Equipment	Supplier
Autoclave	Forma Scientific
Benchtop centrifuge	Eppendorf Centrifuge 5417R
Dessicator	Thomas Scientific, South Africa
Field Emission TEM (Tecnai F20)	FEI Company, USA
FT-IR PerkinElmer Spectrum 400	PerkinElmer, Waltham, Massachusetts, U.S
Incubator	Forma Scientific
Lamina flow	Forma Scientific
POLARstar Omega microplate reader	BMG LABTECH, Germany
Thermo mixing heating block	Eppendorff, Hamberg, Germany
Virtis Freeze Mobile 12SL (Freeze-dryer)	United Scientific
Vortex mixer (VX100)	Labnet International, Inc. Woodbridge NJ07095, Whitehead Scientific (Pty) Ltd
Zetasizer Nano-ZS90 instrument	ATA Scientific instruments, Taren Point, Australia
Ecotherm Oven	Labotec

Chemicals/ Reagents	Supplier
Ampicillin	Sigma-Aldrich, Schnelldorf
Carbendazim	Sigma-Aldrich, Schnelldorf
Ethanol	Merck Schuchardt, Germany
Folin-Ciocalteu reagent	Sigma-Aldrich, Schnelldorf
Gallic acid	Sigma-Aldrich, Schnelldorf
Millipore Ultra-purified distilled water (18.2 MΩ cm at 25 °C)	Thermo Scientific™ Oxoid™ , Waltham, Massachusetts
Mueller Hinton Agar (R454082)	Thermo Scientific™ Oxoid™ , Waltham, Massachusetts
Mueller Hinton Broth (CM0405B)	Thermo Scientific™ Oxoid™ , Waltham, Massachusetts
Na ₂ CO ₃	Sigma-Aldrich, Schnelldorf
Nutrient agar	Merck Schuchardt, Germany
Nutrient broth media	Merck Schuchardt, Germany
Peptone Yeast Broth	Merck Schuchardt, Germany
Potato Dextrose Agar	Merck Schuchardt, Germany
Saubaron Dextrose Agar	Merck Schuchardt, Germany

Microbes	Supplier
<i>E. coli</i>	ATCC
<i>F. culmorum</i>	ARC, Pretoria
<i>F. oxysporum</i>	ARC, Pretoria
<i>F. proliferatum</i>	ARC, Pretoria

<i>F. verticilloides</i>	UCT, Cape Town
<i>K. pneumoniae</i>	ARC, Pretoria
MRSA	ATCC
<i>P. aeruginosa</i>	ATCC
<i>S. aureus</i>	ATCC
<i>S. epidermidis</i>	ATCC
<i>S. pyogenes</i>	ATCC

Plastics	Supplier
0.2 µm filter membrane (GVWP)	Merck Schuchardt, Germany
15 ml and 50 ml Conical tubes	SPL LifeSciences, Korea
96-well plates	Olympus
Autoclave tape (3m comply™ steam indicator tape)	3M Science Applied to Life, South Africa
Cotton swabs	Lasec
Disposable capillary cuvette (DTS1070)	Malvern Panalytical, United Kingdom
Disposable cuvette (DTS0012)	Malvern Panalytical, United Kingdom
Glass wool	Thermo Scientific™ Oxoid™ , Waltham, Massachusetts
Parafilm (PM-996)	Bemis, USA
Sterile loops	Lasec, South Africa
Whatman® Grade 1 Qualitative Filter Paper	Merck Schuchardt, Germany

Plant Material	Supplier
<i>Bulbine frutescens</i> plant material	Cape Flats Nature Reserve, UWC

UNIVERSITY of the
WESTERN CAPE

2.2. Preparation of *B. frutescens* plant extract

B. frutescens plants were purchased from Cape Flats Nature Reserve, located at the University of the Western Cape in Bellville, South Africa.

The leaves were picked from the stem of the plant, cleaned with damp paper towel and cut with a surgical blade into fine pieces. Figure 2.1 shows the cross-section of the leaves, and highlights the sap gel. Then, 300 g of leaves were added to 150 ml distilled-deionized water (ddH₂O) (Millipore) and boiled slightly in a microwave until the amount of liquid within the beaker increased. The solid particles were separated from the liquid solution by filtration through glass wool (Thermo Scientific™ Oxoid™, Waltham, Massachusetts). The remaining liquid represented the sap of the leaf in water. The volume of the leaf sap extract plus water was 356 ml. The leaf sap extract was then filtered using Whatman number 1 filter paper (Merck Schuchardt, Germany). The leaf sap extract was then placed in 40 ml volumes in 50 ml Greiner centrifuge tubes, covered with parafilm and stored at – 80 °C overnight. The frozen leaf sap extract was then freeze-dried and stored in desiccators containing activated crystals (Thomas Scientific, South Africa) until use.



Figure 2.1: Cross-section of *B. frutescens* showing gel sap of the leaves.

2.3. Synthesis of AgNPs in the dark and sunlight

The preliminary method of synthesis was adapted from Vivek and colleagues (Vivek *et al.*, 2011). Briefly, 50 mg/ml stock of leaf sap extract was prepared from the freeze-dried material in deionized H₂O as the medium. The original pH was 7.11. Another 50 mg/ml stock was prepared and the pH was adjusted to 10. Serial dilutions were prepared (25, 12.5, 6.25, 3.125, 1.56, 0.78 mg/ml) respectively. Nine hundred µl of 1 mM AgNO₃ was placed in 1.5 ml microcentrifuge tubes and heated for 5 minutes at 100 °C in the mixing heating block (Eppendorf, Hamburg, Germany). Then 100 µl of the various extract concentrations were added into the various tubes and immediately covered with foil to avoid light-induced degradation or synthesis. The reaction mixtures were shaken at 450 rpm for nine hours at 100 °C, and samples were removed every hour during the nine hours, and analyzed by Ultraviolet-visible spectrophotometry (POLARstar Omega microplate reader, BMG Labtech, Germany).

For synthesis of AgNPs using sunlight, 50 mg/ml stock of leaf sap extract was prepared from the freeze-dried material in deionized H₂O as the medium. The original pH was 7.11. Another 50 mg/ml stock was prepared and the pH was adjusted to 10. Serial dilutions were prepared (25, 12.5, 6.25, 3.125 mg/ml) respectively. Nine hundred µl of AgNO₃ (0.5, 1, 2, 3, 4 and 5 mM) was placed in 1.5 ml microcentrifuge tubes and the reaction mixtures were placed in direct sunlight over six hours. Samples were taken every 15 minutes for the first hour and for the remaining 5 hours the reading was taken at two, three and six hours. Based on data obtained by Haiss and colleagues, this was done to determine the optimum conditions of synthesis by fully studying the effect of time, pH, and concentration of extract and AgNO₃ by using various extinction coefficients and the peak absorbance values of AgNPs (Haiss *et al.*, 2007). The Ultraviolet-visible (V-Vis) spectra were collected in a range of 250 - 650 nm at 1 nm increments.

2.4. Determination of the Total Phenolic Content (TPC)

The Folin-Ciocalteu (FC) reagent was used to determine the total phenolic content of *B. frutescens* (Tobwala *et al.*, 2014). Various concentrations of neutral and pH 10 *B. frutescens* freeze-dried leaf extracts and *B. frutescens*-synthesized AgNPs (25 µl) were mixed with 1X FC reagent (125 µl), and allowed to incubate at room temperature for 20 minutes in the dark.

Then 125 µl of 7.5 % Na₂CO₃ was added and allowed to incubate at room temperature for a further 20 minutes in the dark. After the incubation period, the absorbance was measured at 760 nm on a microplate reader (BMG Labtech, Germany) and the gallic acid was used as a standard to establish the calibration curve. The results were recorded as µg of gallic acid equivalents (GAE)/µg of *B. frutescens* dried leaf extract, and µg of gallic acid equivalents (GAE)/µg of *B. frutescens* AgNPs. The equation below was used to calculate the TPC as gallic acid equivalents per dried weight of extract or AgNPs:

$$TPC = \frac{GAE \times \text{volume of extract} \times \text{dilution factor}}{\text{dry weight of sample}}$$

2.5. Determination of Hydrodynamic Size, Polydispersity Index and the Zeta Potential measurements

The *B. frutescens*-synthesized AgNPs at pH 7.11 and 10 which displayed the highest peak absorbance as well as uniformity based on UV-Vis analysis was subjected to centrifugation at 10 000 rpm for 30 minutes to stop the synthesis reaction. The hydrodynamic size and polydispersity index (Pdl) of the AgNPs was then determined in triplicate using the Malvern Zetasizer Nano-ZS90 instrument (ATA Scientific instruments, Taren Point, Australia) by placing a one ml aliquot (comprised of 30 µl AgNPs with 970 µl ddH₂O) into a disposable cuvette (DTS0012). Based on the DLS analysis of the optimum AgNPs and their respective UV-Vis spectra, synthesis conditions of one AgNP was chosen as the optimum for neutral pH and pH 10 respectively. This experiment was replicated > 3 times with the same results produced each time. The optimum conditions stated within this thesis can therefore be considered extremely accurate (p < 0.0001). The zeta potential (ZP) of the selected optimum AgNPs was then determined in triplicate by placing a one ml aliquot into a disposable folded capillary cell (DTS1070). The ZP was measured directly after synthesis, after centrifugation to stop synthesis reaction, and after washing steps. The measured hydrodynamic size, Pdl and ZP results were analysed at 25 °C. The Pdl gives an estimation of the average uniformity of the nanoparticles formed. A Pdl of more than 0.5 is considered polydispersed, and a Pdl of less than 0.5 is considered monodispersed.

2.6. Large scale synthesis of AgNPs

The optimum neutral and pH 10 AgNPs were up-scaled to a volume of 50 ml and washed three times by centrifugation at 10 000 rpm for 30 minutes, 25 °C, soft spin. The AgNPs were then tested for antibacterial and antifungal activities as described below in section 2.8.

2.7. Characterization of extract and AgNPs

The scaled-up *B. frutescens*-synthesized AgNPs were further characterized using High-resolution Transmission Electron Microscopy (HR-TEM), Zeta Potential (ZP) and Fourier-transform Infrared Spectroscopy (FTIR) as described below.

2.7.1. HR-TEM analysis

The HR-TEM micrographs were obtained using the TECNAI F20 TEM microscopic instrument. One drop of AgNPs in liquid suspension was placed on a nickel/copper grid which is supported by a thin film of amorphous carbon. The grid was then dried using xenon light before the analysis of the sample. Within the process of analysing AgNPs produced, electrons are shot through the sample at a high voltage resulting in the interaction between the sample and the electron beam causing a scattering discharge which changes in the electron beam. The interaction between the electrons and the sample causes a difference in contrast between the sample and the background nickel/copper grid. An image is produced which provides information about the morphology of the NPs (Rao and Biswas, 2009). The core diameter of the AgNPs was measured from the HR-TEM images using the Image J software (<https://imagej.net/Welcome>).

2.7.2. Fourier-transformed Infrared (FTIR) spectroscopy

Stocks solutions (50 mg/ml) of neutral and pH 10 extracts were subjected to centrifugation at 10 000 rpm for 30 minutes, 25 °C, soft spin. The supernatant was decanted into a clean tube and the pellet was dried at 65 °C overnight on 0.2 µm filter membrane and then subjected to analysis. The freeze-dried extract was analysed in its powdered form.

The neutral and pH 10 AgNPs were centrifuged at 10 000 rpm for 30 minutes, 25 °C, soft spin to remove unreacted AgNO₃ and extract. The supernatant was carefully decanted into a clean

tube, the pellet collected and resuspended in ddH₂O (Millipore) where it was centrifuged again as described above.

The pellet of AgNPs were then dried at 65 °C overnight on 0.2 µm filter membrane and then subjected to analysis. The spectra of freeze-dried, 50 mg/ml extracts and AgNPs were recorded on an Attenuated Total Reflectance (ATR) sampling tool using the FTIR spectrometer (PerkinElmer Spectrum 400, Waltham, Massachusetts, USA). The spectra were recorded at room temperature using the transmission approach above the wave number range of 4000 – 650 cm⁻¹ at a resolution of 4 cm⁻¹. The respective samples were placed onto the trough crystals. The crystal plates were then pinned with an applied gauge of 65 - 70.

The IR beam was directed onto the optically dense crystal with a high refractive index at a certain angle. In regions of the IR spectrum where the sample absorbs energy, the evanescent wave was attenuated. The attenuated beam thus returned to the crystal, then exited the opposite end of the crystal and was directed to the detector in the IR spectrometer. The detector then recorded the attenuated IR beam as an interferogram signal, which was then used to generate an IR spectrum. The IR spectrum baseline was corrected, smoothed and absorption expansion (Abex) was applied to enhance the detection of the peaks. The apparatus was cleaned with 100 % ethanol and ddH₂O before reading the next sample. The sample peaks were labelled and then superimposed on one graph using the FTIR analysis software.

2.8. Determination of antibacterial activity using agar well-diffusion assay

The antimicrobial activities of *B. frutescens*-synthesized AgNPs and *B. frutescens* leaf extracts were tested by agar well-diffusion method against seven pathogenic bacterial strains and four fungal strains. The bacterial and fungal strains used within this thesis are indicated in Table 2.1. The same AgNP concentrations were used for both antibacterial and antifungal studies as indicated in Table 2.2. The AgNPs used for antimicrobial studies were washed with ddH₂O by centrifuging the AgNPs at soft spin, 25 °C, 10 000 rpm for 30 minutes for the removal of any excess AgNO₃ and extract. AgNPs were resuspended in 100 µl of ddH₂O. The experiment was repeated in triplicate for antibacterial and antifungal studies.

Bacteria were individually plated on NA (Nutrient Agar, Merck Schuchardt) using the quadrant streak technique to isolate individual bacterial colonies. The bacteria were incubated at 37 °C for 24 hours.

Inoculum suspension was prepared for each individual bacterium in MHB (Mueller-Hinton Broth, Sigma Aldrich) and grown at 37 °C in a shaking incubator until a 0.5 MacFarland standard was reached (1×10^8 CFU/ml). The spectrophotometer absorbance (0.08 – 0.1) reading was measured using the plate reader (POLARstar Omega microplate reader, BMG Labtech, Germany). 5×10^5 CFU/ml of each bacterial strain was spread onto NA plates using a sterile cotton swab. Seven wells of 6 mm diameter were created using a gel puncher. Fifty μ l of five different concentrations of AgNPs and extracts, shown in Table 2.2, were added separately to each well. 50 μ l of 0.1 mg/ml Ampicillin stock (which gives 5 μ g ampicillin) and MHB were added to the remaining wells as positive and negative controls, respectively. The agar plates were allowed to dry for approximately 15 minutes at 4 °C. The agar plates were then inverted, to allow for the diffusion of the samples through the agar, and incubated at 37 °C for 16 – 24 hours. Zones of inhibition were measured by using a calliper. Antimicrobial effects of extracts and AgNPs were indicated by the formation of a clear zone around the well/s.

For anti-fungal analysis SDA (Saubaron Dextrose Agar, Merck Schuchardt) and PDA (Peptone Yeast, Merck Schuchardt) plates were prepared and the fungi was sub-cultured and grown at 25 °C for 3 – 5 days. On a clean SDA / PDA plate, six 6 mm diameter wells were created using a gel puncher. A plug of the fungal strain from sub-cultured plate was inserted in the centre of the plate. Fifty μ l of five different concentrations of AgNPs were added to each well. Fifty μ l of five different concentrations of AgNPs were added to each well. Fifty μ l of 0.3 g/l carbendazim anti-fungal compound was added as a positive control. Fifty μ l of 100% ethanol was added as a positive control. The agar plates were allowed to dry for approximately 15 minutes at 4 °C. The agar plates were then inverted and incubated at 25 °C for 3 – 5 days until a zone of clearance was visualised. The results were obtained by measuring the diameter of the zone of inhibition using a calliper.

Table 2.1: Details of microorganisms within this study.

Microorganism	ATCC number	Media plated
<i>Staphylococcus aureus</i>	25923	Nutrient agar
<i>Staphylococcus epidermidis</i>	12.228	Nutrient agar
<i>Staphylococcus pyogenes</i>		Nutrient agar
<i>Escherichia coli</i>	35218	Nutrient agar
<i>Klebsiella pneumonia</i>	13883	Nutrient agar
<i>Methicillin-resistant Staphylococcus aureus (MRSA)</i>	33591	Nutrient agar
<i>Pseudomonas aeruginosa</i>	27853	Nutrient agar
<i>Fusarium culmorum</i>	PPRI 10138	SDA/PDA agar
<i>Fusarium oxysporum</i>	PPRI 19027	SDA/PDA agar
<i>Fusarium proliferatum</i>	MRC 2059	SDA/PDA agar
<i>Fusarium verticilloides</i>	MRC 826	SDA/PDA agar



Table 2.2: Sample concentrations for antimicrobial activity analysis. Abbreviations: [mg/ml] – concentration in mg/ml.

	[Extract] mg/ml	[NP] mg/ml
Neutral pH (7.11)	50	0.6
	25	0.3
	12.5	0.15
	6.25	0.075
	3.125	0.0375
	1.56	0.01875
	0.78	0.09375
pH 10	50	0.47
	25	0.235
	12.5	0.1175
	6.25	0.05875
	3.125	0.029375
	1.56	0.0147
	0.78	0.0074

The concentrations indicated in table 2.2 reflect the concentration of the AgNPs after synthesis and the purification process. The concentrations were not adjusted for antimicrobial analysis.

2.9. Broth microdilution method for determining the minimum inhibitory concentration (MIC)

Bacteria were individually plated on NA (Nutrient Agar, Merck Schuchardt) using the quadrant streak technique to isolate individual bacterial colonies. The bacteria were incubated at 37 °C for 24 hours. Inoculum suspension was prepared for each individual bacterium in MHB (Mueller-Hinton Broth, Sigma Aldrich) and grown at 37 °C in a shaking incubator until a 0.5 MacFarland standard was reached (1×10^8 CFU/ml). The spectrophotometer absorbance (0.08 – 0.1) reading was measured using the plate reader (POLARstar Omega microplate reader, BMG Labtech, Germany). 5×10^5 CFU/ml of each bacterial strain was placed into each well of a 96 well microtiter plate. A two-fold serial dilution of both neutral pH and pH 10 AgNPs were performed with fresh nutrient broth in microcentrifuge tubes prior to transferring into the 96 well microtiter plate. Positive and negative controls were prepared and placed in the 96 well microtiter plates. The plate was then incubated at 37 °C for 24 hours in an ambient air incubator.

The percentage of growth reduction was observed at the 1, 2, 3, 4th, 5th, 6th, 20th, 24th hour mark by the turbidity of the suspension and measuring the absorbance at 450 nm using the plate reader. The turbidity is directly proportional to bacterial growth. Ten µl of Alamar Blue was placed in each well, covered in foil as Alamar Blue is sensitive to light and placed in ambient air incubator. The microtiter plate was incubated for 4 hours and the fluorescence and absorbance was measured every hour using the plate reader as the Alamar Blue reagent reacts differently with different microorganisms. The fluorescence was read at 530-560 nm excitation wavelengths and 590 nm emission wavelength. The absorbance was read at 600 nm and 630 nm reference wavelengths. Growth curves were plotted to observe inhibitory effects of neutral pH and pH 10 AgNPs against various bacterial strains over a period of 24 hours.



Chapter 3: Results and Discussion

Introduction

The present investigation entitled “**Green synthesis of silver nanoparticles (AgNPs) from *Bulbine frutescens* leaf sap extract and investigating their antimicrobial effects**” was conducted to study the green synthesis of AgNPs by reduction of Ag^+ ions using the sap extract of leaves of *B. frutescens* at various reaction conditions. The various outcomes during the course of investigation portrayed in the form of different tables and figures, are described and discussed in this chapter.

3.1. The effects of different parameters on the green synthesis of AgNPs in the dark

3.1.1. Effect of time and reducing agent concentration

During the experiment the colour intensified as the reaction time progressed. The solution changed from colourless to a yellow-orange-brown colour development, indicating the formation of AgNPs. At lower concentrations of extract the reaction mixture took much longer to change from colourless to yellow-orange-brown; whereas in the higher concentrations the reaction mixture colour developed much faster into a yellow-orange-brown. After 1 hour of synthesis silver particle aggregates were found at the bottom of the microcentrifuge tubes.

3.1.2. The effect of stirring on AgNP synthesis

The constant stirring of AgNPs at 450 rpm resulted in the solution forming a more distinct and darker shade of brown and with extended time, flakes of silver were visible within the reaction mixtures. Prolonged stirring increased the probability of collision between particles which ultimately led to aggregation. This can be seen by the shoulder created at lower concentrations of extract (**figure 3.1** and **figure 3.2**). The Surface Plasmon Resonance (SPR) also became wider and started shifting towards longer wavelengths when stirring was extended. Longer stirring time also allows for nucleation to occur over an extended period of time.

The growth processes are occurring at different rates indicating that there is variation for nuclei formed at different reaction times (Noginov *et al.*, 2007). The effect of pH 10 and neutral pH (7.11) showed that the reaction mixtures with neutral pH extract exhibited a lighter and pale yellow colour which later transgressed into a darker brown colour development.

Figure 3.1 and 3.2 indicate the UV-visible spectra of AgNPs synthesized at neutral pH and pH 10 over a period of 9 hours in the dark. From the obtained results, it is evident that AgNPs are synthesized at all extract concentrations. The UV-Vis spectra show the sharp peaks produced within a range of 390 to 430 nm. It is known that AgNPs synthesized at higher temperatures, in this case 100 °C, are smaller in size. A shoulder was also created at 1.56 and 0.78 mg/ml for neutral pH (7.11) AgNPs; and for pH 10 AgNPs a shoulder is created the 8th hour of synthesis for 6.25 mg/ml, indicating that any AgNPs synthesized after the 8th hour is not suitable for application based work. A shoulder is also created at pH 10 AgNPs at an extract concentration of 3.125, 1.56, and 0.78 mg/ml. From the results illustrated in figure 3.1 and 3.2 it is evident that higher concentrations of extract were suitable for synthesis at 100 °C in the dark.

From the time dependent graph in figure 3.3 it is evident that the reducing agent is still not depleted after 9 hours of synthesis because as the time duration increases, the AgNP synthesis also increased and never reached a plateau, which would have indicated depletion of either AgNO₃ or extract. The sediment found at the bottom of the Eppendorf could potentially be due to agglomeration of AgNPs with longer exposure to high temperatures. Based on the UV-Vis spectra and time dependent course graph, it was evident that the optimum extract concentration lies between 12.5 and 6.25 mg/ml for the neutral pH (7.11) extract for synthesizing AgNPs with 1 mM AgNO₃, and 12.5 mg/ml pH 10 extract is suitable for synthesizing AgNPs with 1 mM AgNO₃.

Unfortunately, the results of these experiments could not be replicated due to unknown factors. Various reaction parameters including temperatures at 37, 50, 70 and 80 °C, and mixing heating blocks were investigated. However, no AgNPs were synthesized. It was thus decided that synthesizing AgNPs in sunlight could be an alternative for the progress of this project.

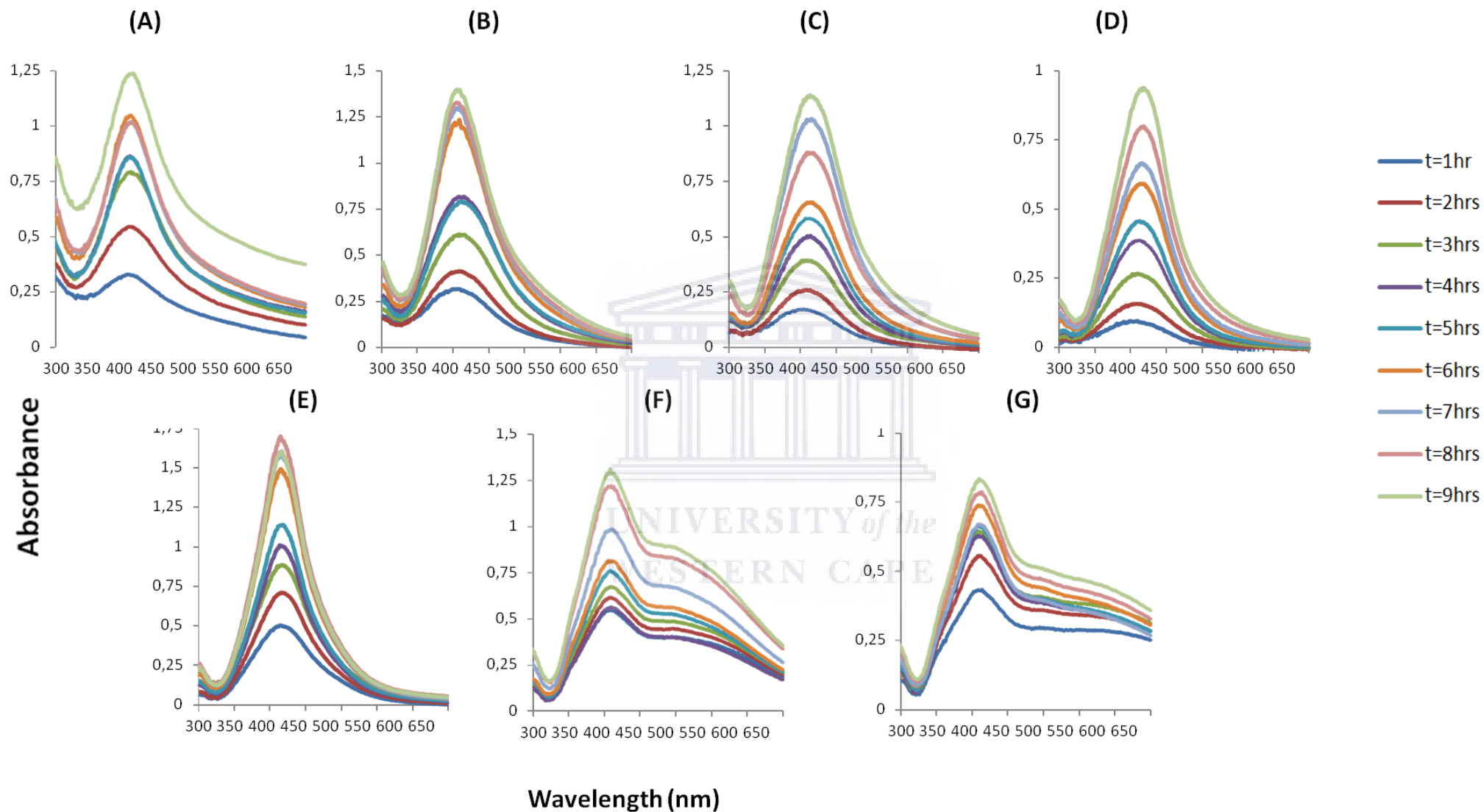


Figure 3.1: UV-Vis spectra of neutral pH (7.11) AgNPs synthesized with 1mM AgNO₃ at various *B. frutescens* leaf extract concentrations over a period of 9 hours at 100 °C in the dark. **(A)** 50 mg/ml **(B)** 25 mg/ml **(C)** 12.5 mg/ml **(D)** 6.25 mg/ml **(E)** 3.125 mg/ml **(F)** 1.56 mg/ml **(G)** 0.78 mg/ml

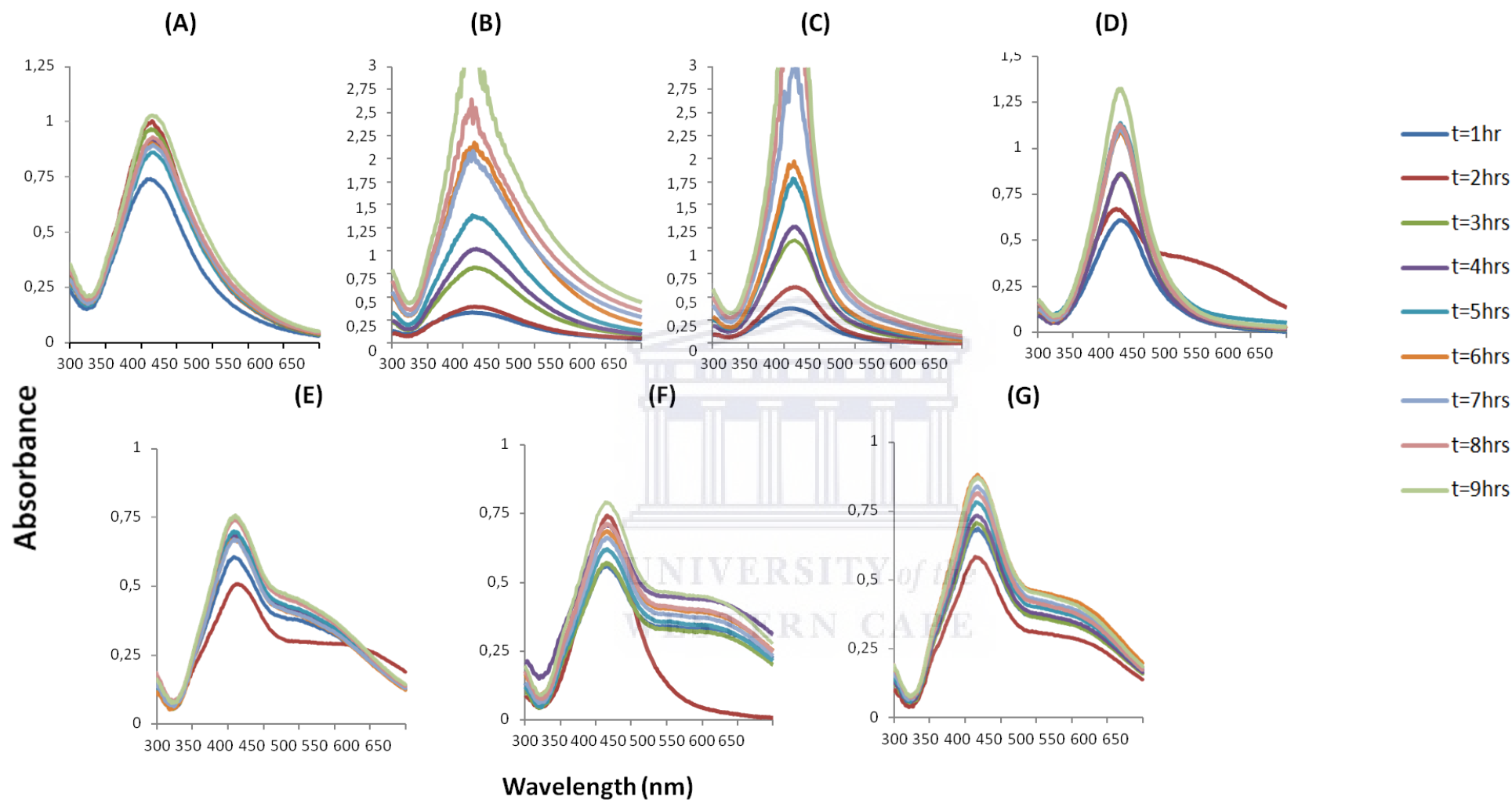


Figure 3.2: UV-Vis spectra of pH 10 AgNPs synthesized with 1 mM AgNO₃ at various *B. frutescens* leaf extract concentrations over a period of 9 hours at 100 °C in the dark. (A) 50 mg/ml (B) 25 mg/ml (C) 12.5 mg/ml (D) 6.25 mg/ml (E) 3.125 mg/ml (F) 1.56 mg/ml (G) 0.78 mg/ml

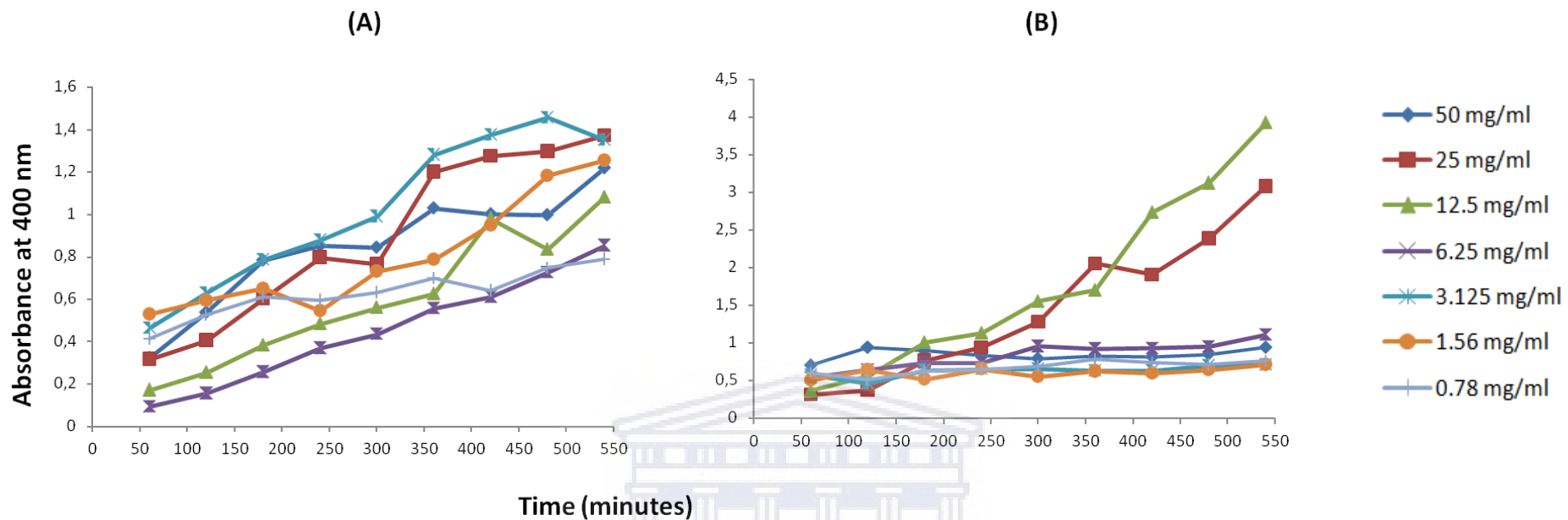


Figure 3.3: Effect of time on AgNP formation at various *B. frutescens* leaf extract concentrations over a period of 9 hours at 100 °C in the dark.

(A) neutral pH (7.11) AgNPs (B) pH 10 AgNPs

3.1.3. The effect of time on AgNP synthesis using sunlight

Figure 3.4 displays the colour change of reaction mixture of synthesis in direct sunlight over a period of 60 minutes. A colour change is immediately visualised after placing the AgNPs in direct sunlight. The colour of the reactions containing higher concentrations of *B. frutescens* extract changed from a pale yellow to dark brown within 15 minutes. The extract control and AgNO₃ control was unaffected by the direct sunlight and displayed no colour change. The colour of the AgNPs intensified as the reaction time increased. After 60 minutes of synthesis, the NP solution turned grey to a milky consistency and the silver aggregates were found at the bottom of the microcentrifuge tube.



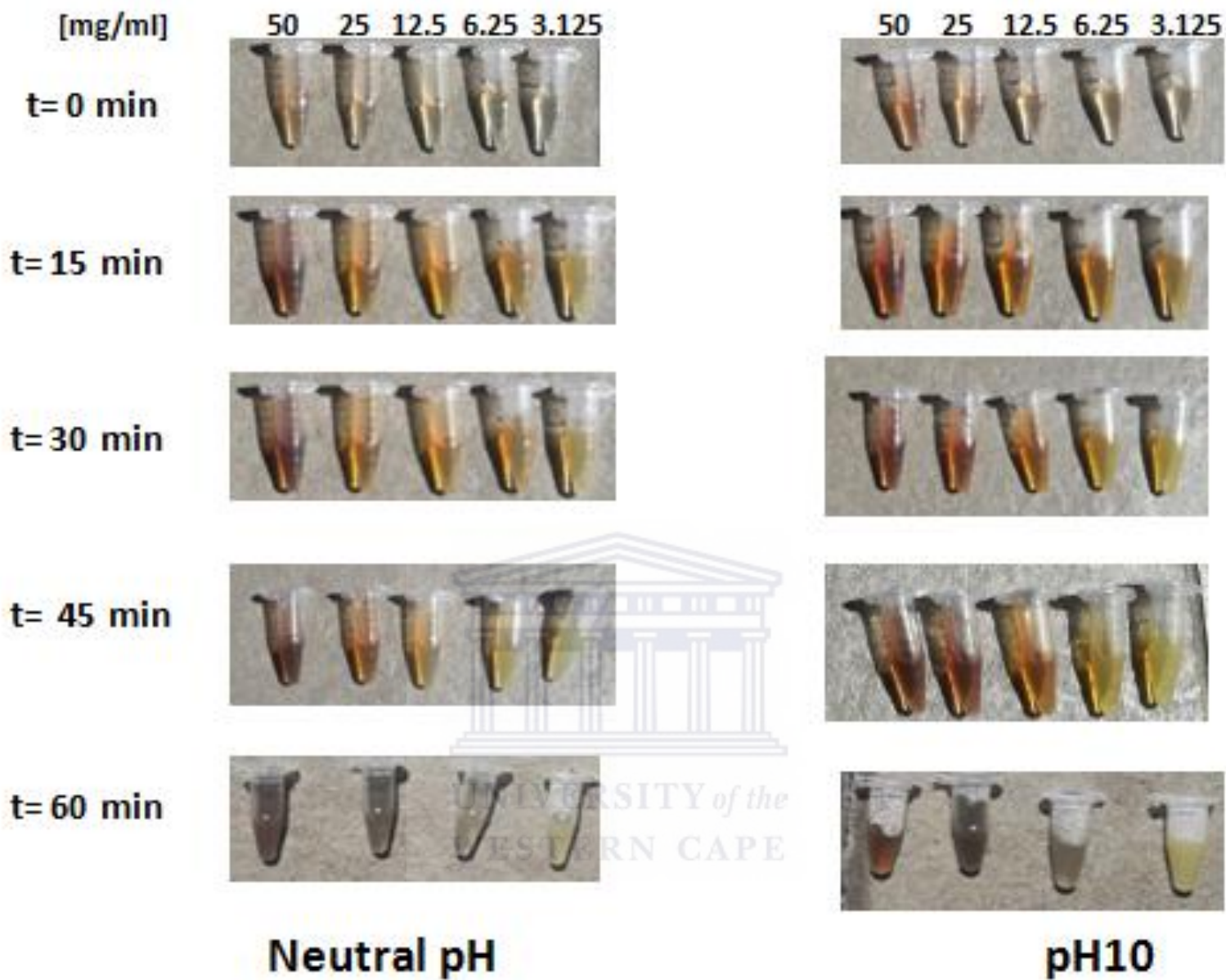


Figure 3.4: Visible colour change of reaction mixture after 60 minutes of synthesis in direct sunlight.

It was observed in the time-dependent course over a six hour period (**figure 3.5 - 3.7**) that the colour of the reaction increased within proportion to the reaction time until +/- 60 minutes after which the absorbance decreased. UV-Vis analysis confirms that there is a correlation between the colour development and the absorbance exhibited by the synthesized AgNPs. As the absorbance increased the colour intensity increased. However, as soon as the reaction colour turns grey to a milky consistency the absorbance decreases. The extract on its own already has a yellowish brown colour. The extract control and AgNO₃ control was unaffected by the direct sunlight and did not show any visible UV-Vis spectra, ruling out the possibility that the SPRs formed at various conditions are due to AgNO₃ or the extract. This colour change intensified to reddish brown colour when Ag⁺ ions were reduced to Ag⁰. This finding is corroborated by Noginov and colleagues as the same result was observed (Noginov *et al.*, 2007).



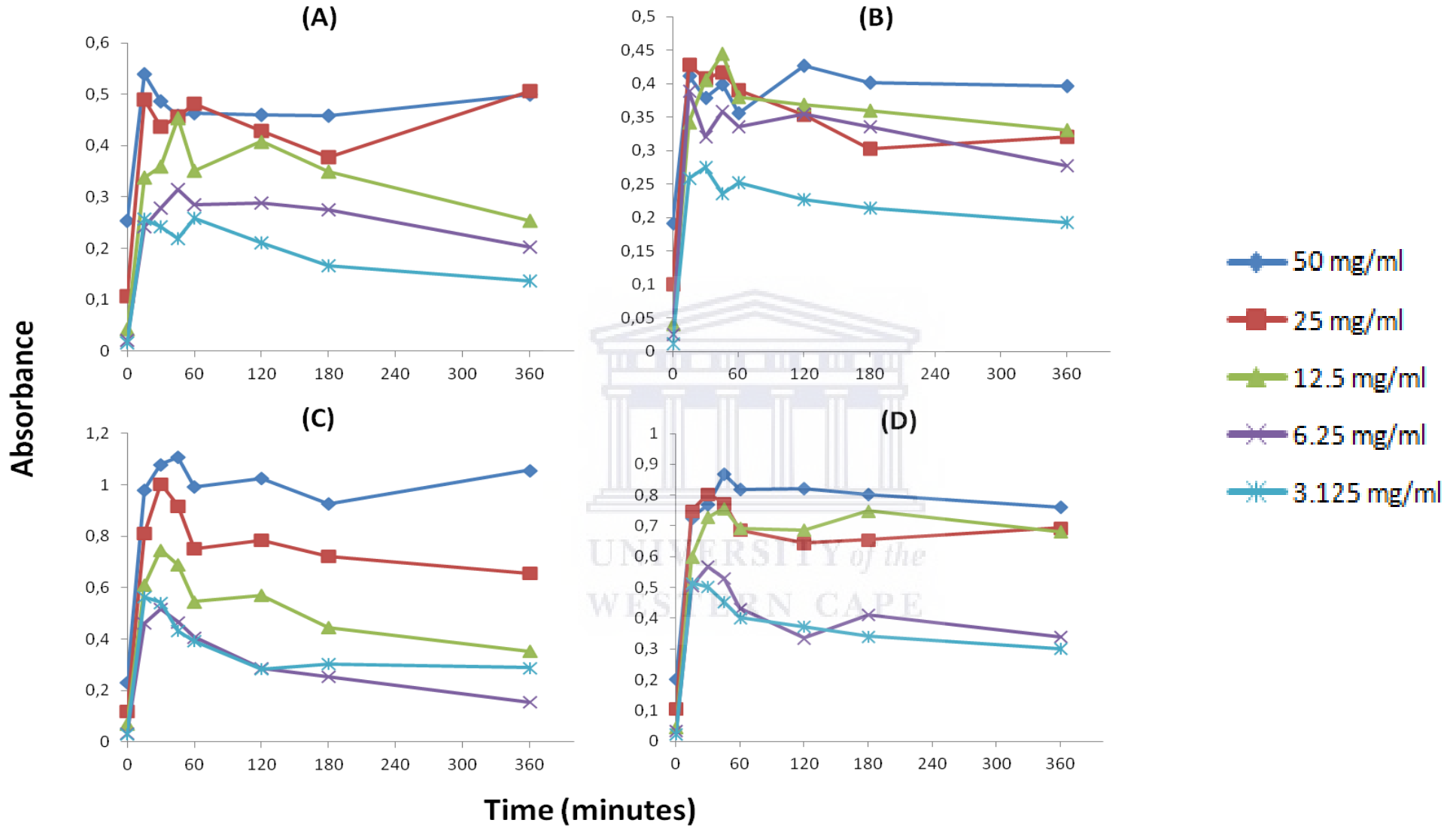


Figure 3.5: Effect of time on AgNP formation at various *B. frutescens* leaf extract concentrations over a period of 6 hours in direct sunlight at various extract and AgNO₃ concentrations. (A) 0.5 mM AgNO₃ neutral pH AgNPs (B) 0.5 mM AgNO₃ pH10 AgNPs (C) 1 mM AgNO₃ neutral pH AgNPs (D) 1 mM AgNO₃ pH10 AgNPs

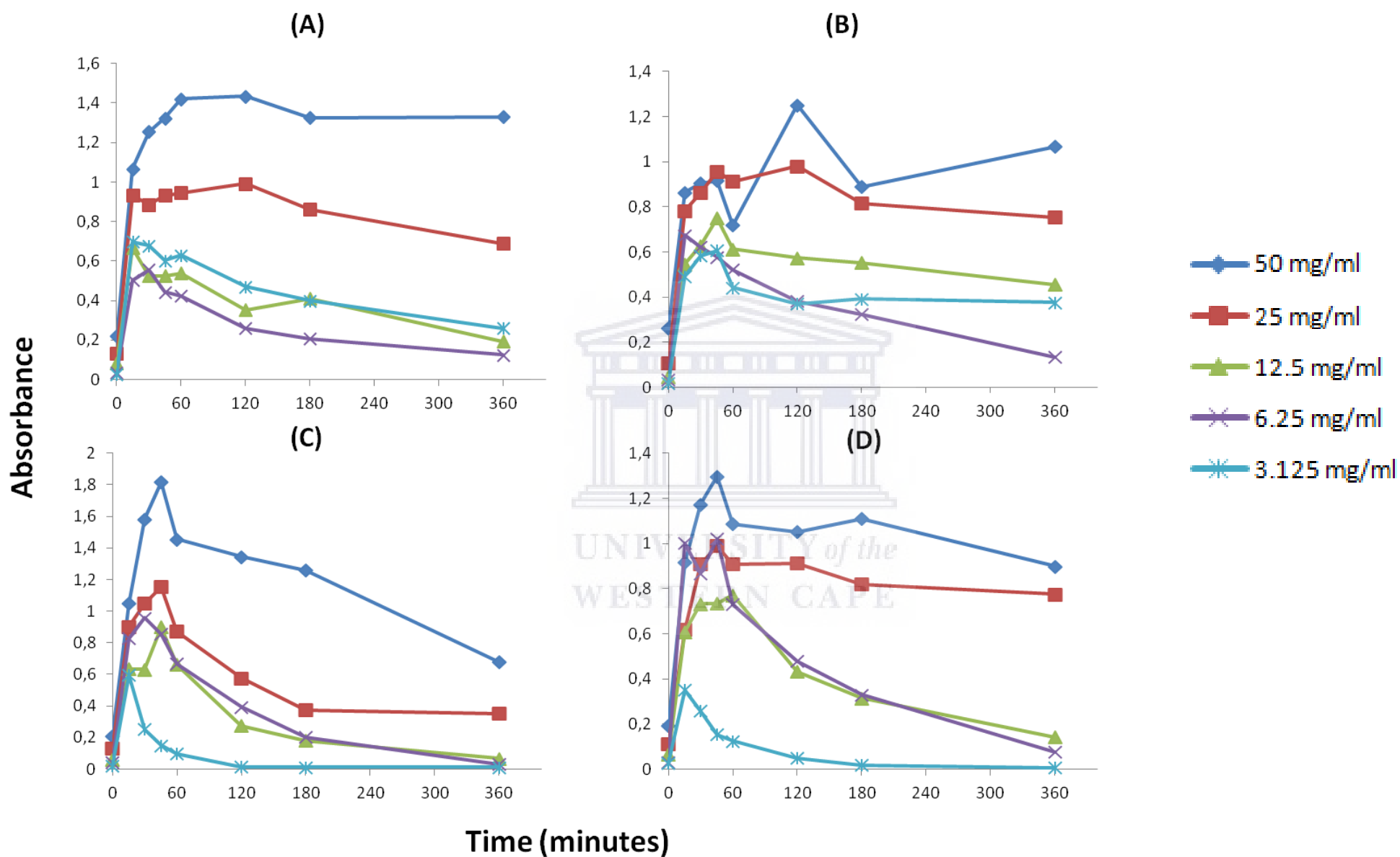


Figure 3.6: Effect of time on AgNP formation at various *B. frutescens* leaf extract concentrations over a period of 6 hours in direct sunlight at various extract and AgNO₃ concentrations. (A) 2 mM AgNO₃ neutral pH AgNPs (B) 2 mM AgNO₃ pH10 AgNPs (C) 3 mM AgNO₃ neutral pH AgNPs (D) 3 mM AgNO₃ pH10 AgNPs

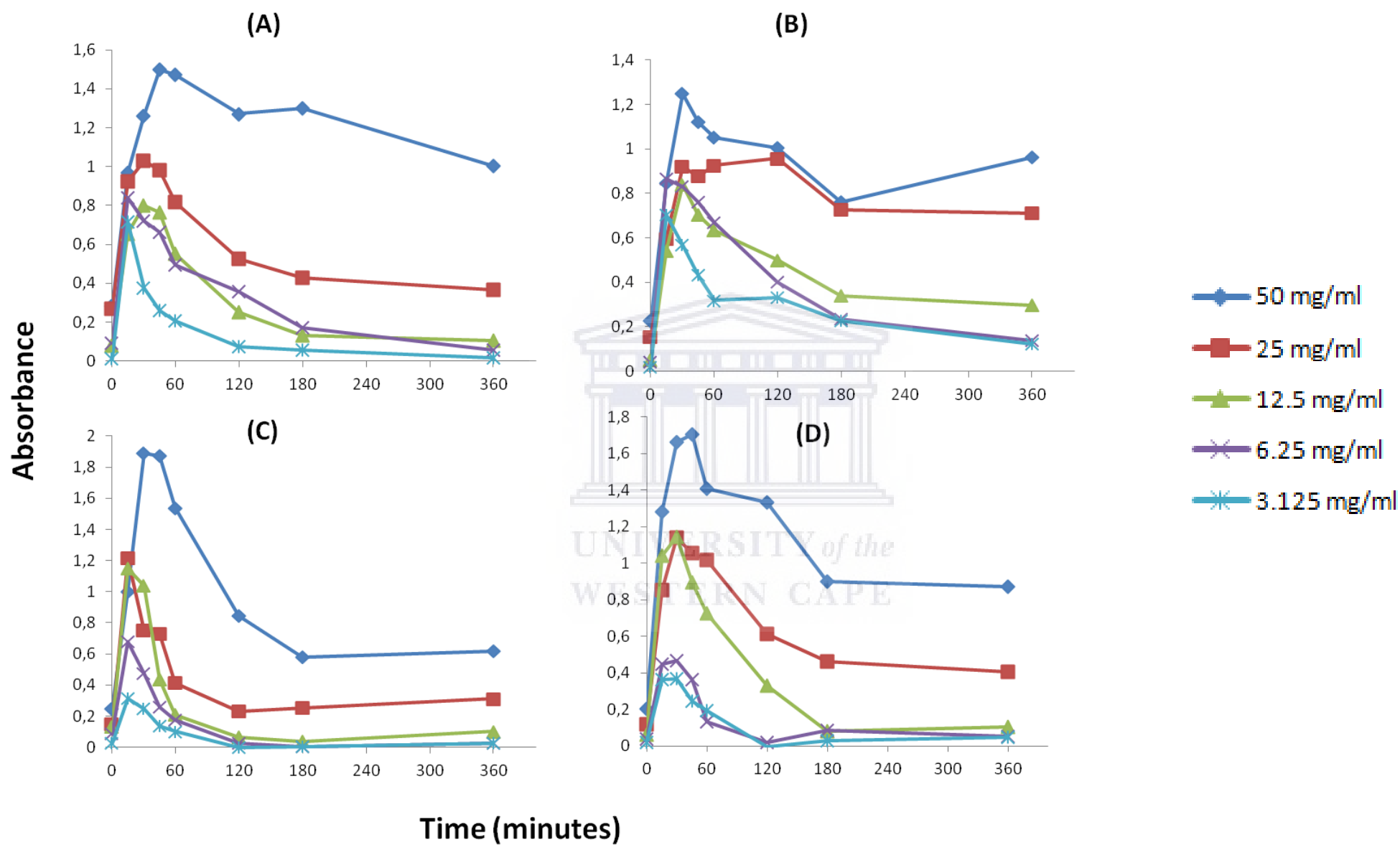


Figure 3.7: Effect of time on AgNP formation at various *B. frutescens* leaf extract concentrations over a period of 6 hours in direct sunlight at various extract and AgNO₃ concentrations. (A) 4 mM AgNO₃ neutral pH AgNPs (B) 4 mM AgNO₃ pH10 AgNPs (C) 5 mM AgNO₃ neutral pH AgNPs (D) 5 mM AgNO₃ pH10 AgNPs

Figure 3.8 and 3.9 represents the UV-Vis spectra of neutral pH (7.11) and pH 10 AgNPs with 0.5 mM AgNO₃ at various *B. frutescens* leaf extract concentrations over a period of 6 hours in direct sunlight. From the results, it is evident that AgNPs are synthesized at all extract concentrations with 0.5 mM AgNO₃ except at 50 mg/ml extract. This can be attributed to the fact that the ratio of plant extract to AgNO₃ is much larger for the reduction process to occur. A shoulder was created in the nucleation phase of synthesis which could possibly be an indication of another peak being formed. Both AgNPs synthesis with 25 mg/ml of extract were complete after 15 minutes. The synthesis of AgNPs using 12.5 and 6.25 mg/ml extract is complete after 45 minutes. And the reaction was complete after 60 minutes for 3.125 mg/ml.



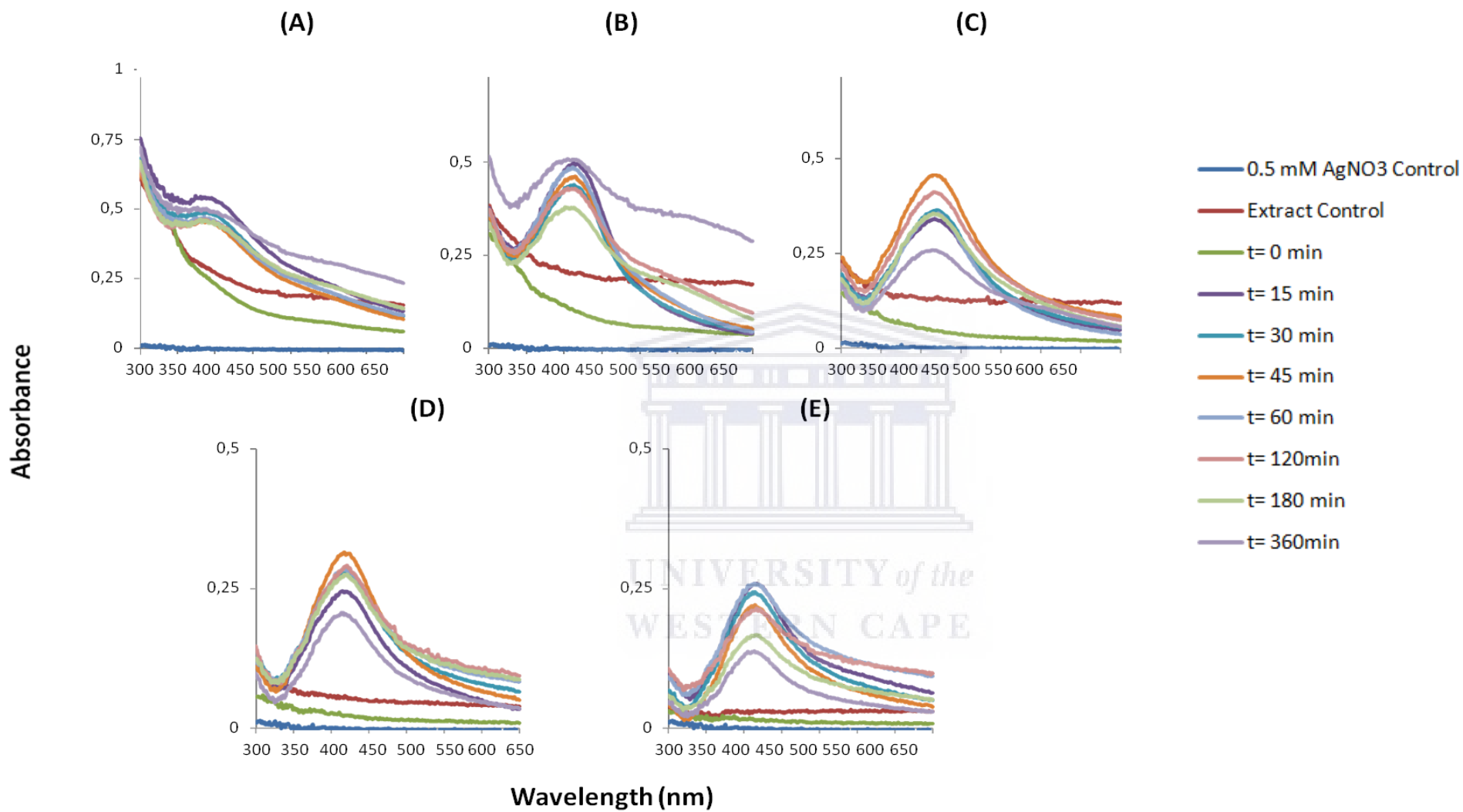


Figure 3.8: UV-Vis spectra of neutral pH (7.11) AgNPs synthesized with 0.5 mM AgNO₃ at various *B. frutescens* leaf extract concentrations over a period of 6 hours in direct sunlight. (A) 50 mg/ml (B) 25 mg/ml (C) 12.5 mg/ml (D) 6.25 mg/ml (E) 3.125 mg/ml

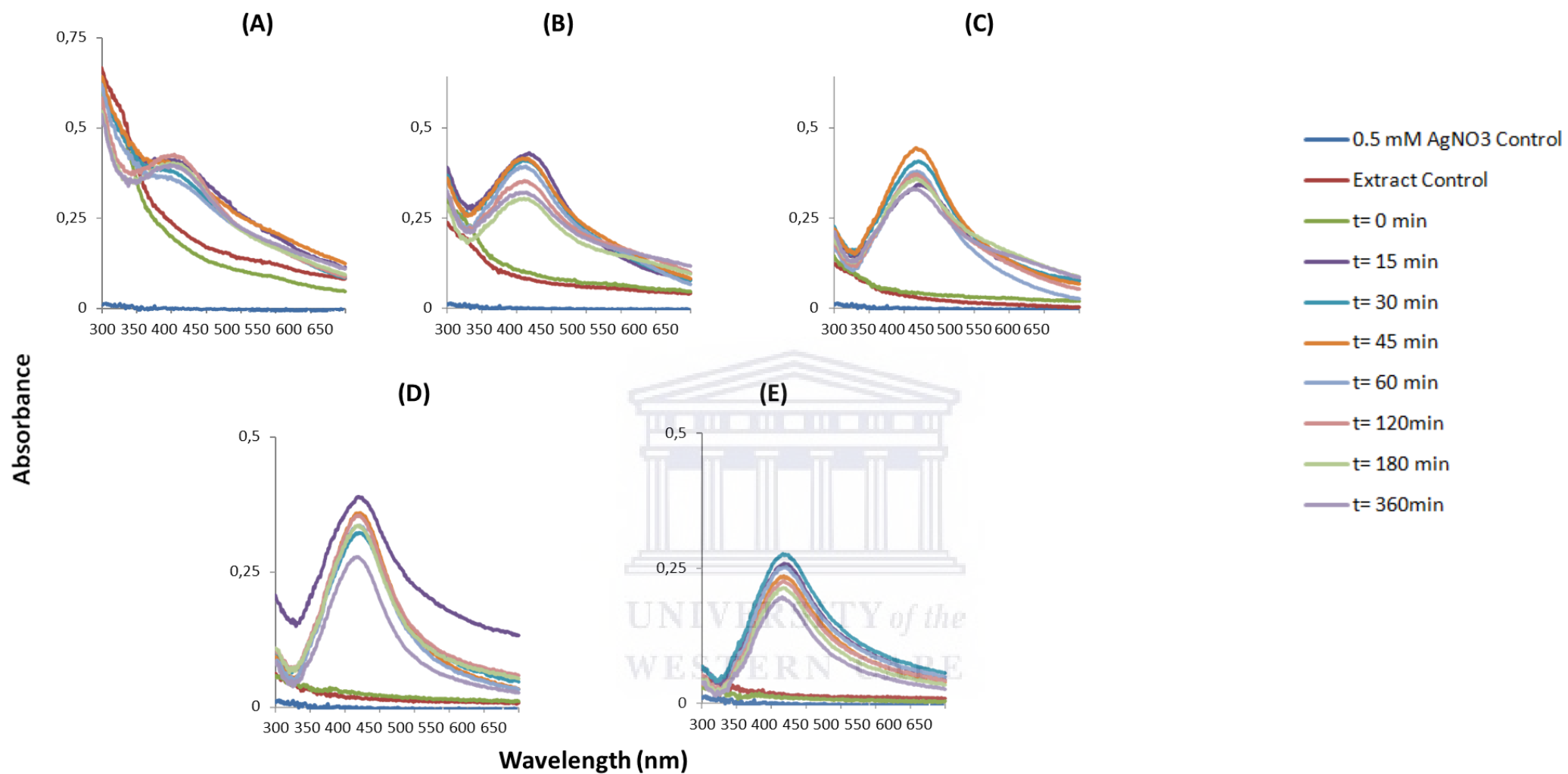


Figure 3.9: UV-Vis spectra of pH 10 AgNPs synthesized with 0.5 mM AgNO₃ at various *B. frutescens* leaf extract concentrations over a period of 6 hours in direct sunlight. (A) 50 mg/ml (B) 25 mg/ml (C) 12.5 mg/ml (D) 6.25 mg/ml (E) 3.125 mg/ml

Figure 3.10 and 3.11 represents the UV-Vis spectra of neutral pH (7.11) and pH 10 AgNPs with 1 mM AgNO₃ at various *B. frutescens* leaf extract concentrations over a period of 6 hours in direct sunlight. AgNPs were formed at all extract concentrations with 1 mM AgNO₃. Neutral pH'd AgNPs at an extract concentration of 3.125 mg/ml produced much smaller and more uniform peaks with a higher absorbance compared to pH 10 AgNPs. The reaction was complete in 45 minutes for 50 mg/ml of extract for both AgNPs. The reaction is complete after 60 minutes for extract concentrations 25, 12.5 and 6.25 mg/ml for neutral pH'd AgNPs. The reaction was complete for pH 10 AgNPs after 45 minutes for 50 and 12.5 mg/ml, 60 minutes for 25 and 6.25 mg/ml. The reaction was complete for both AgNPs at 3.125 mg/ml extract concentration after 15 minutes.



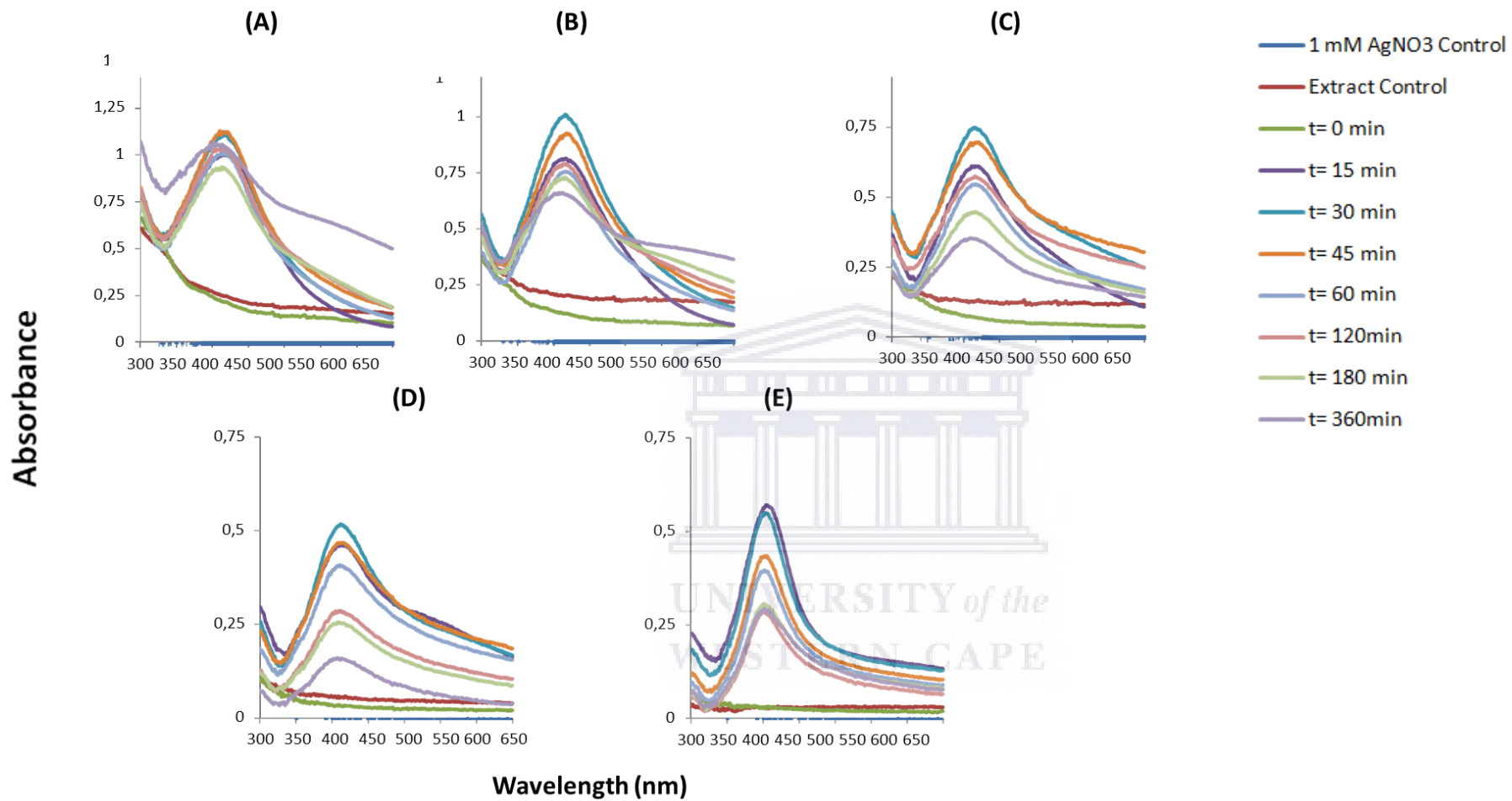


Figure 3.10: UV-Vis spectra of neutral pH AgNPs synthesized with 1 mM AgNO₃ at various *B. frutescens* leaf extract concentrations over a period of 6 hours in direct sunlight. (A) 50 mg/ml (B) 25 mg/ml (C) 12.5 mg/ml (D) 6.25 mg/ml (E) 3.125 mg/ml

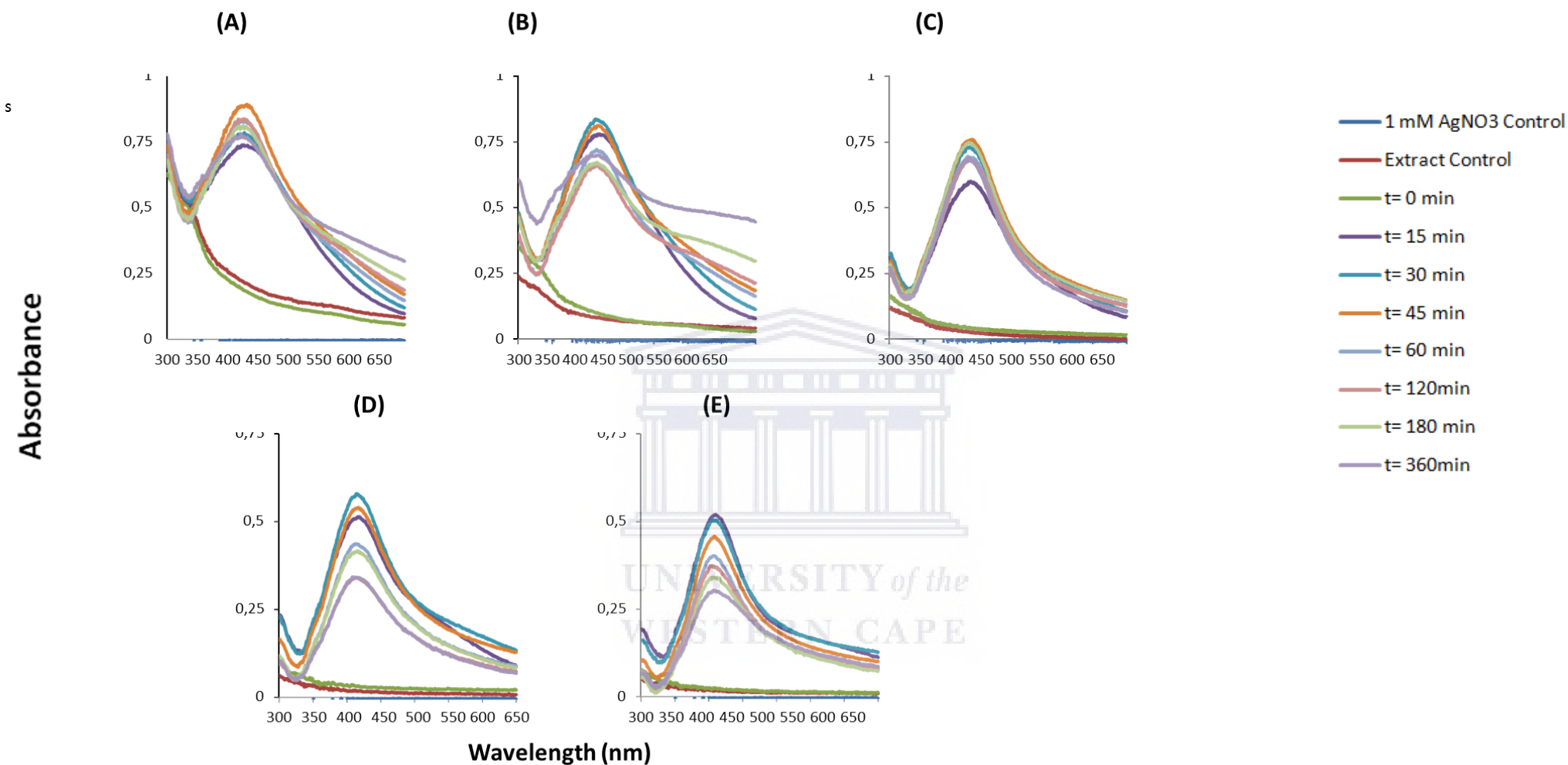


Figure 3.11: UV-Vis spectra of pH 10 AgNPs synthesized with 1 mM AgNO₃ at various *B. frutescens* leaf extract concentrations over a period of 6 hours in direct sunlight. (A) 50 mg/ml (B) 25 mg/ml (C) 12.5 mg/ml (D) 6.25 mg/ml (E) 3.125 mg/ml

Figure 3.12 and 3.13 represents the UV-Vis spectra of neutral pH (7.11) and pH 10 AgNPs with 2 mM AgNO₃ at various *B. frutescens* leaf extract concentrations over a period of 6 hours in direct sunlight. The reaction for neutral pH'd AgNPs is complete for 50 and 25 mg/ml after 120 minutes (2 hours) of synthesis, 15 minutes for 12.5 and 3.125 mg/ml, and 60 minutes for 6.25 mg/ml. The reaction is complete for pH 10 AgNPs after 15 minutes for 50 and 6.25 mg/ml, 120 minutes for 25 mg/ml, and 45 minutes for 12.5 and 3.125 mg/ml.



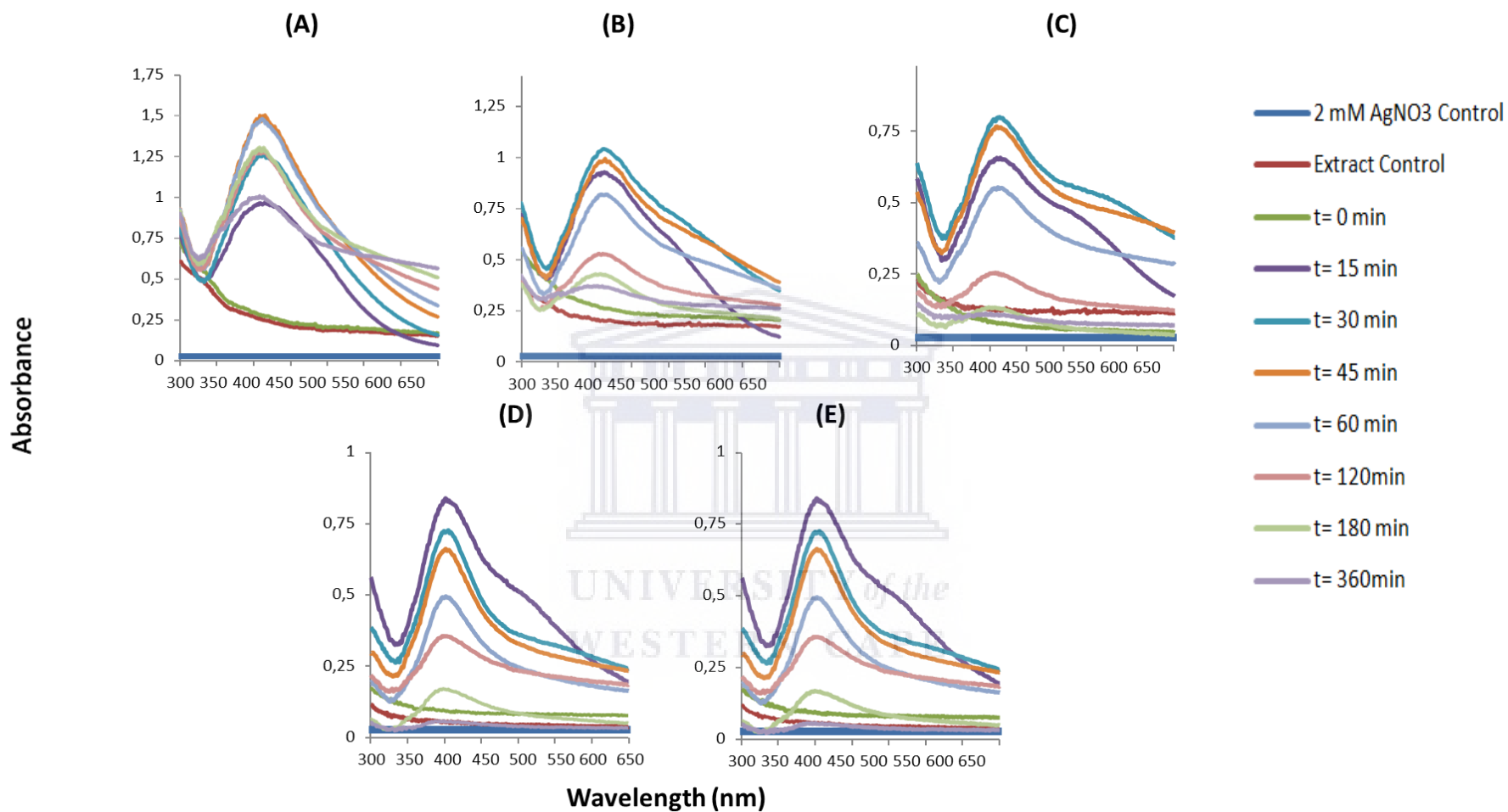


Figure 3.12: UV-Vis spectra of neutral pH AgNPs synthesized with 2 mM AgNO₃ at various *B. frutescens* leaf extract concentrations over a period of 6 hours in direct sunlight. (A) 50 mg/ml (B) 25 mg/ml (C) 12.5 mg/ml (D) 6.25 mg/ml (E) 3.125 mg/ml

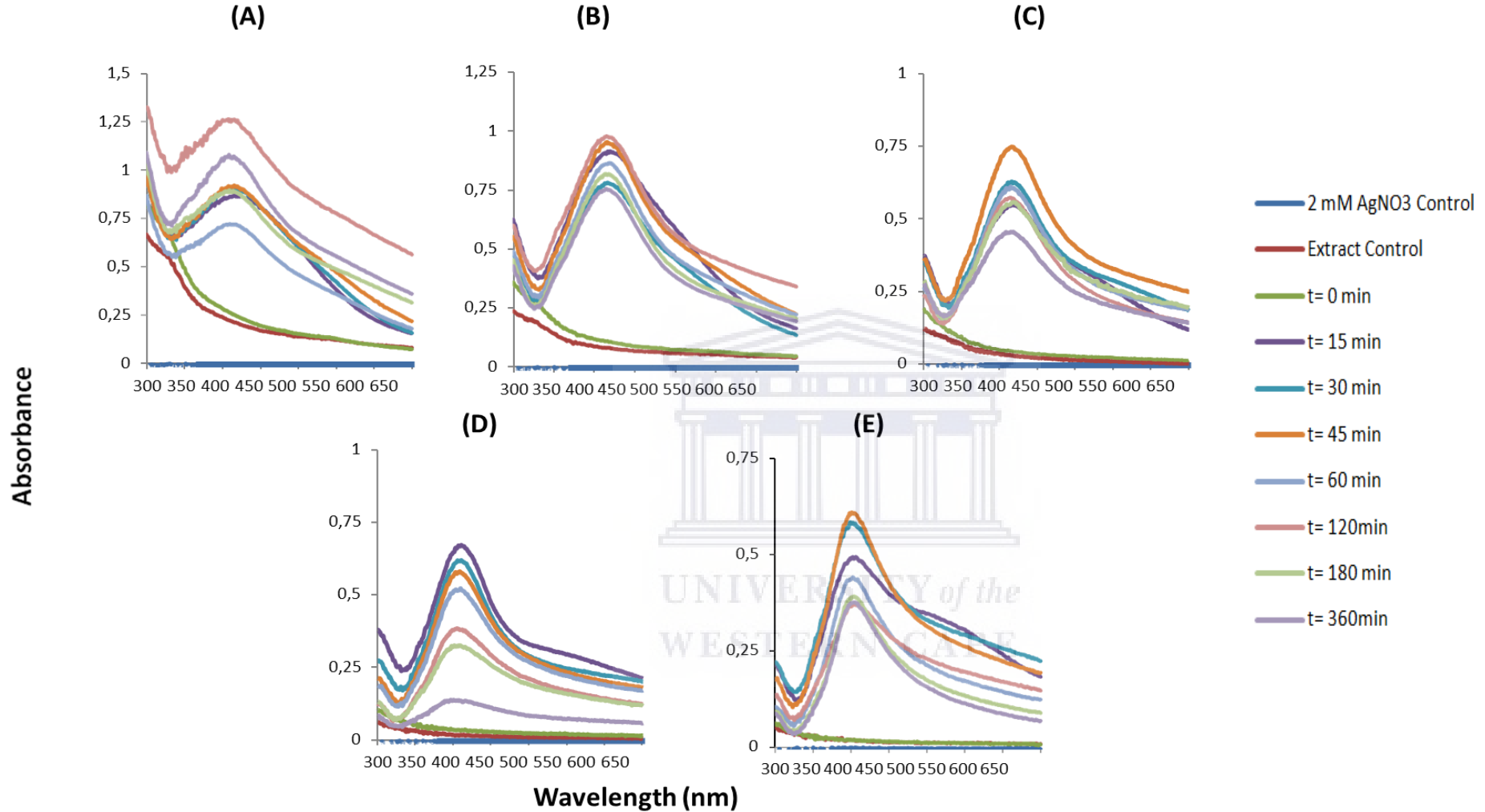


Figure 3.13: UV-Vis spectra of pH 10 AgNPs synthesized with 2 mM AgNO₃ at various *B. frutescens* leaf extract concentrations over a period of 6 hours in direct sunlight. (A) 50 mg/ml (B) 25 mg/ml (C) 12.5 mg/ml (D) 6.25 mg/ml (E) 3.125 mg/ml

Figure 3.14 and 3.15 represents the UV-Vis spectra of neutral pH (7.11) and pH 10 AgNPs with 3 mM AgNO₃ at various *B. frutescens* leaf extract concentrations over a period of 6 hours in direct sunlight. The reaction for neutral pH'd AgNPs is complete for 50, 25 and 12.5 mg/ml after 45 minutes, for 3.125 and 6.25 mg/ml after 60 minutes of synthesis. The reaction is complete for pH 10 AgNPs after 45 minutes of synthesis for 50, 25 and 6.25 mg/ml of extract, 60 minutes for 12.5 mg/ml, and no AgNPs was produced at 3.125 mg/ml extract concentration for pH 10 AgNPs.



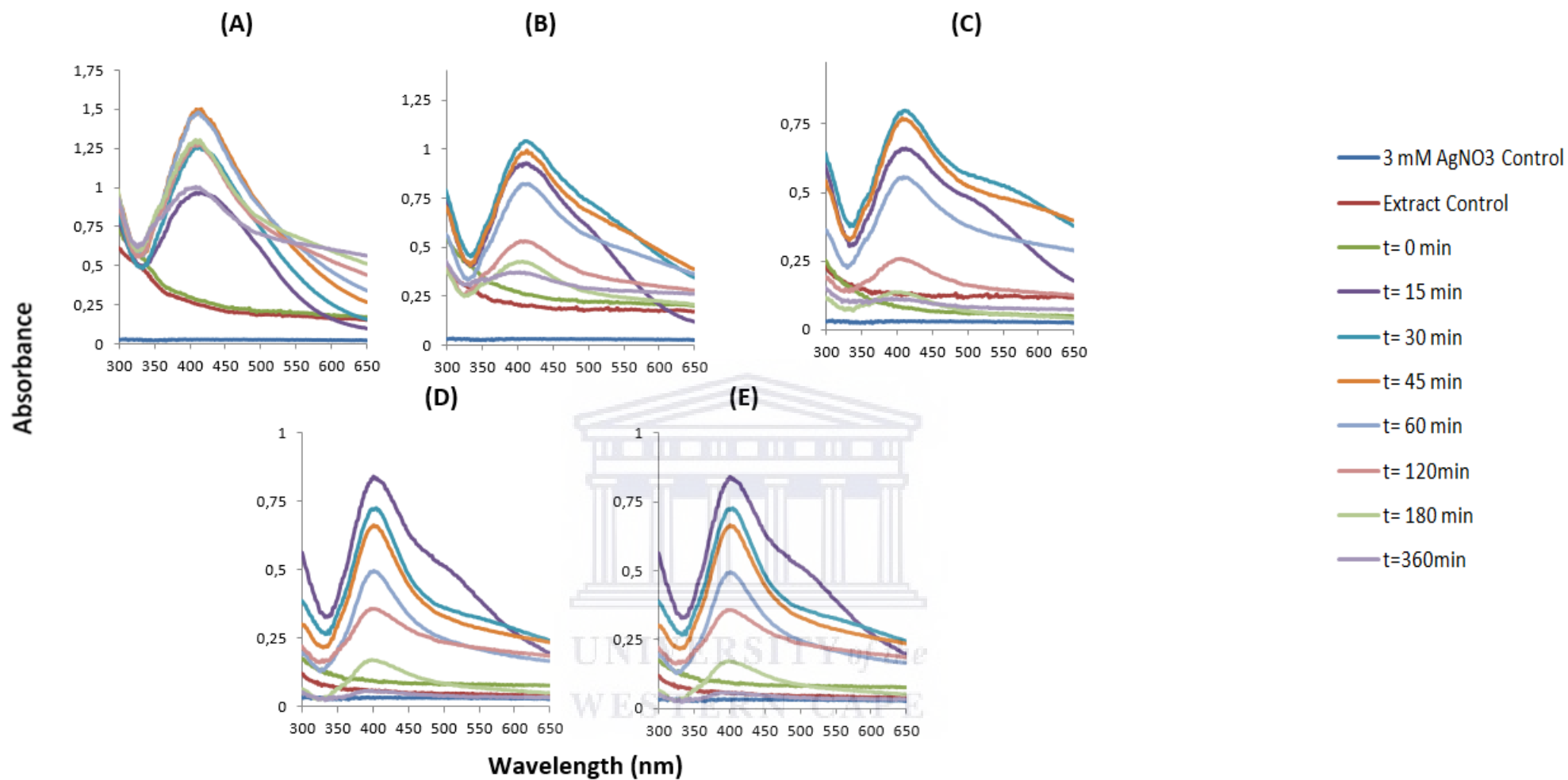


Figure 3.14: UV-Vis spectra of neutral pH (7.11) AgNPs synthesized with 3 mM AgNO₃ at various *B. frutescens* leaf extract concentrations over a period of 6 hours in direct sunlight. (A) 50 mg/ml (B) 25 mg/ml (C) 12.5 mg/ml (D) 6.25 mg/ml (E) 3.125 mg/ml

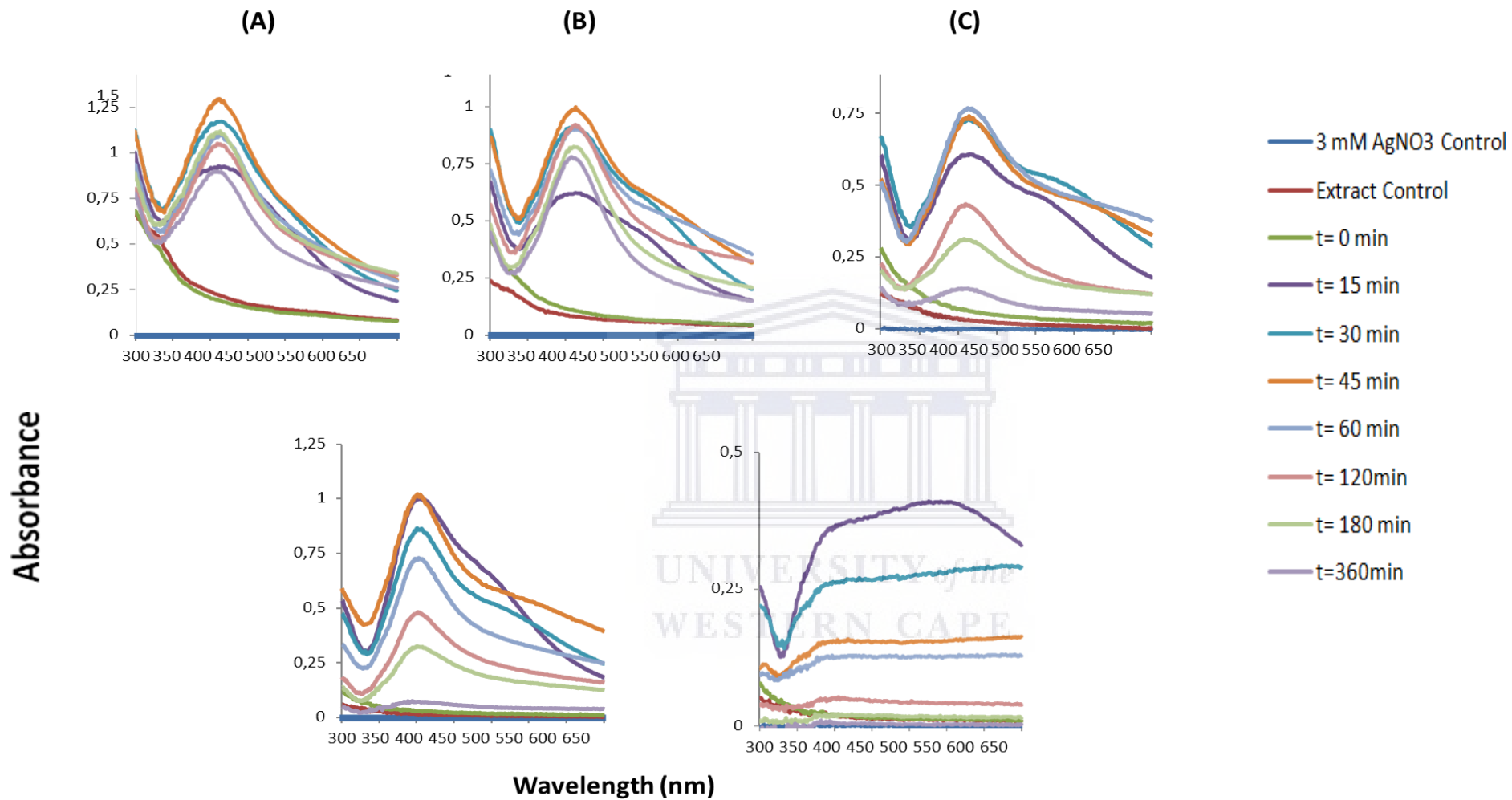


Figure 3.15: UV-Vis spectra of pH 10 AgNPs synthesized with 3 mM AgNO₃ at various *B. frutescens* leaf extract concentrations over a period of 6 hours in direct sunlight. (A) 50 mg/ml (B) 25 mg/ml (C) 12.5 mg/ml (D) 6.25 mg/ml (E) 3.125 mg/ml

Figure 3.16 and 3.17 represents the UV-Vis spectra of neutral pH (7.11) and pH 10 AgNPs with 4 mM AgNO₃ at various *B. frutescens* leaf extract concentrations over a period of 6 hours in direct sunlight. The reaction for neutral pH'd AgNPs is complete for 50 mg/ml after 45 minutes of synthesis, 60 minutes for 25 and 12.5 mg/ml, and 15 minutes for 6.25 and 3,125 mg/ml of synthesis. The reaction is complete for pH 10 AgNPs after 30 minutes of synthesis for 50, 12.5 and 3.125 mg/ml of extract, 120 minutes (2 hours) for 25 mg/ml, and 15 minutes for 6.25 mg/ml. The AgNPs produced at pH 10 3.125 mg/ml are very broad and can therefore be excluded as potential candidates for therapeutic based application work.



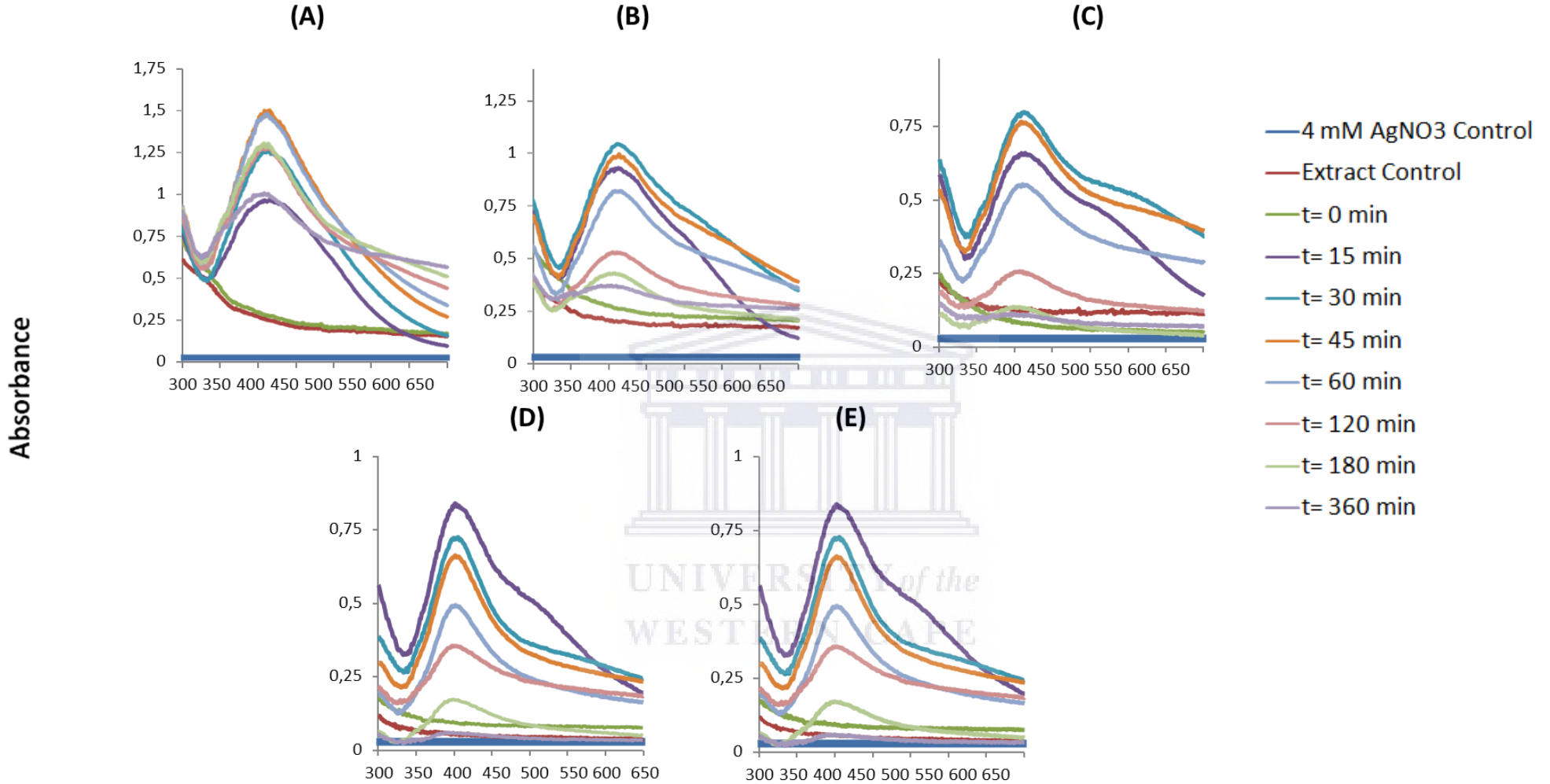


Figure 3.16: UV-Vis spectra of neutral pH (7.11) AgNPs synthesized with 4 mM AgNO₃ at various *B. frutescens* leaf extract concentrations over a period of 6 hours in direct sunlight. (A) 50 mg/ml (B) 25 mg/ml (C) 12.5 mg/ml (D) 6.25 mg/ml (E) 3.125 mg/ml

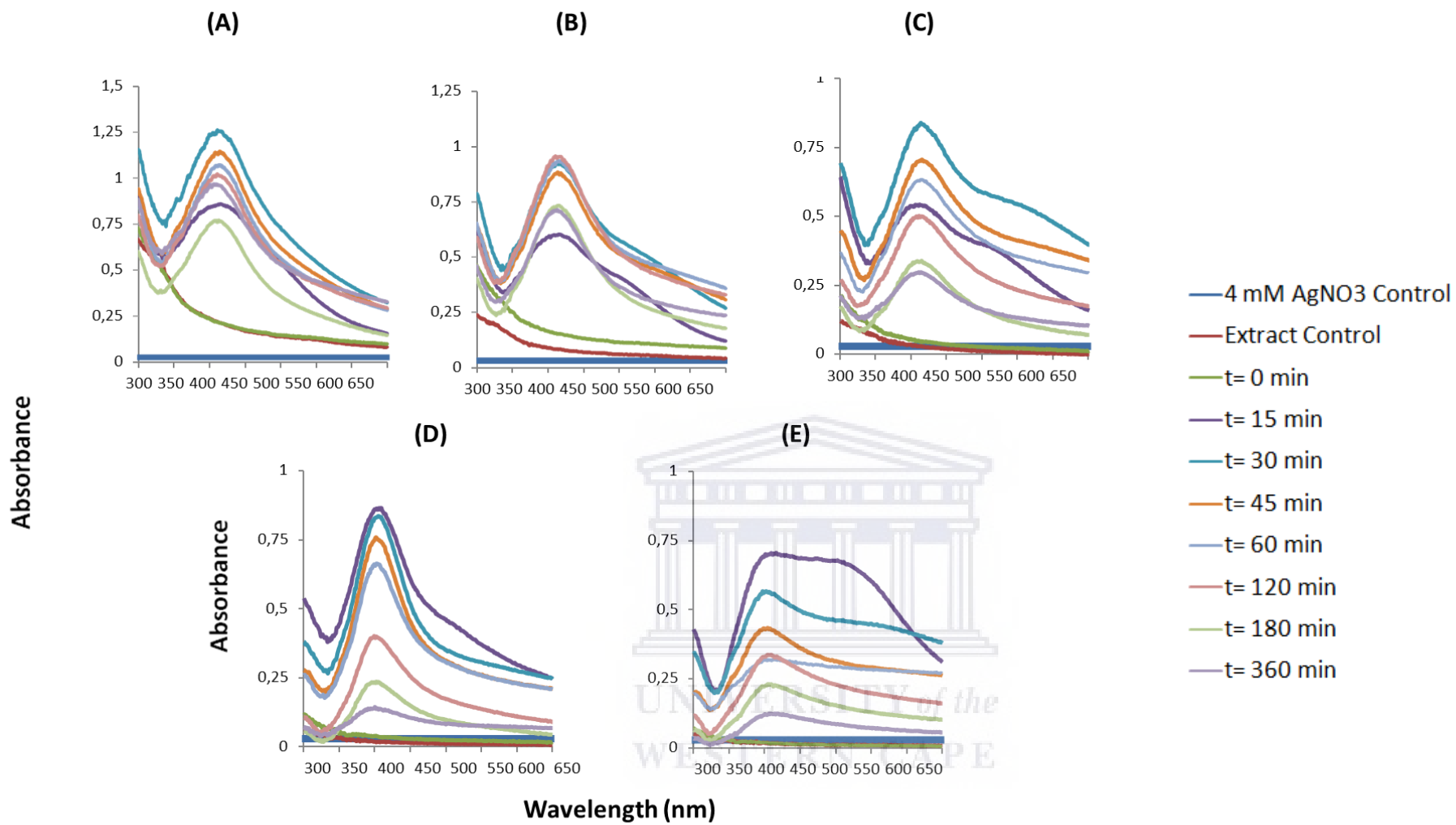


Figure 3.17: UV-Vis spectra of pH 10 AgNPs synthesized with 4 mM AgNO₃ at various *B. frutescens* leaf extract concentrations over a period of 6 hours in direct sunlight. (A) 50 mg/ml (B) 25 mg/ml (C) 12.5 mg/ml (D) 6.25 mg/ml (E) 3.125 mg/ml

Figure 3.18 represents the UV-Vis spectra of pH 10 AgNPs with 5mM AgNO₃ and 50 mg/ml *B. frutescens* extract after 45 minutes of synthesis. AgNPs were only produced at 50 mg/ml extract after 45 minutes of synthesis for pH 10. All other concentrations (25, 12.5, 6.25, and 3.125 mg/ml) of pH 10 extract produced no AgNPs. From the results obtained no AgNPs are produced with neutral pH'd extract (data not shown).

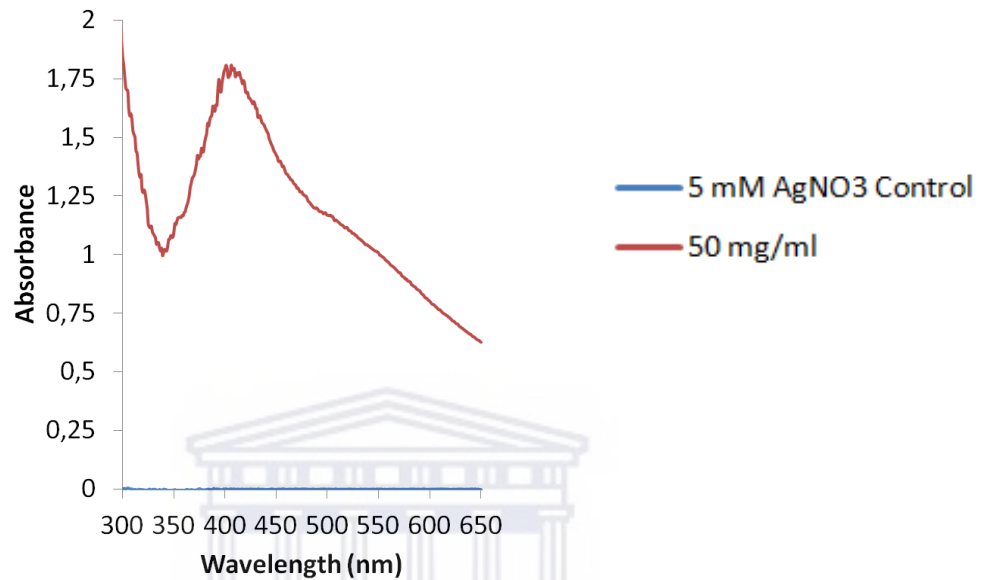


Figure 3.18: UV-Vis spectra of pH 10 AgNPs synthesized with 5 mM AgNO₃ and 50 mg/ml *B. frutescens* leaf extract concentration after 45 minutes of synthesis in direct sunlight.

It is well known that AgNPs possess characteristic absorbance peak between 390 nm to 450 nm (Xu and Kall, 2002). In this study there has been no rise in the peak above this range. There are no peaks that have shifted below this range during the time period of 6 hours which gives a clear indication that the nano solution has no other impurities, organic species or even solvents.

The shift observed within the absorption peak is highly indicative of the size, morphology, quantity and NPs natural growth formation which is further explained using DLS and ZP analysis. The difference in the morphology of the NPs synthesised may be the possible reason for the difference in optical properties presented within the UV-Vis spectra's obtained at the various extract and AgNO₃ concentrations (Xu and Kall, 2002).

The collective oscillation of electrons of the AgNPs produced are in resonance with the light wave bringing to the fore a unique SPR absorption band which is also the origin of the observable colour change over a time period. When a particular wavelength is matched to the size of NPs dipole, oscillation is generated (Henglein, 1993; Link and El-Sayed, 2003). This is in alignment with previous research conducted which shows that in the compensated form of the induced polarization, the electrons in the NPs resonate, introducing a strong absorption (Huang *et al.*, 1996), (Moskovits and Vickova, 2005; Mulvaney, 1996). The SPR broadens over a period of time due to electron surface scattering which can potentially enhance small aggregates (Link and El-Sayed, 2003).

3.1.4. The effect of temperature on AgNP synthesis

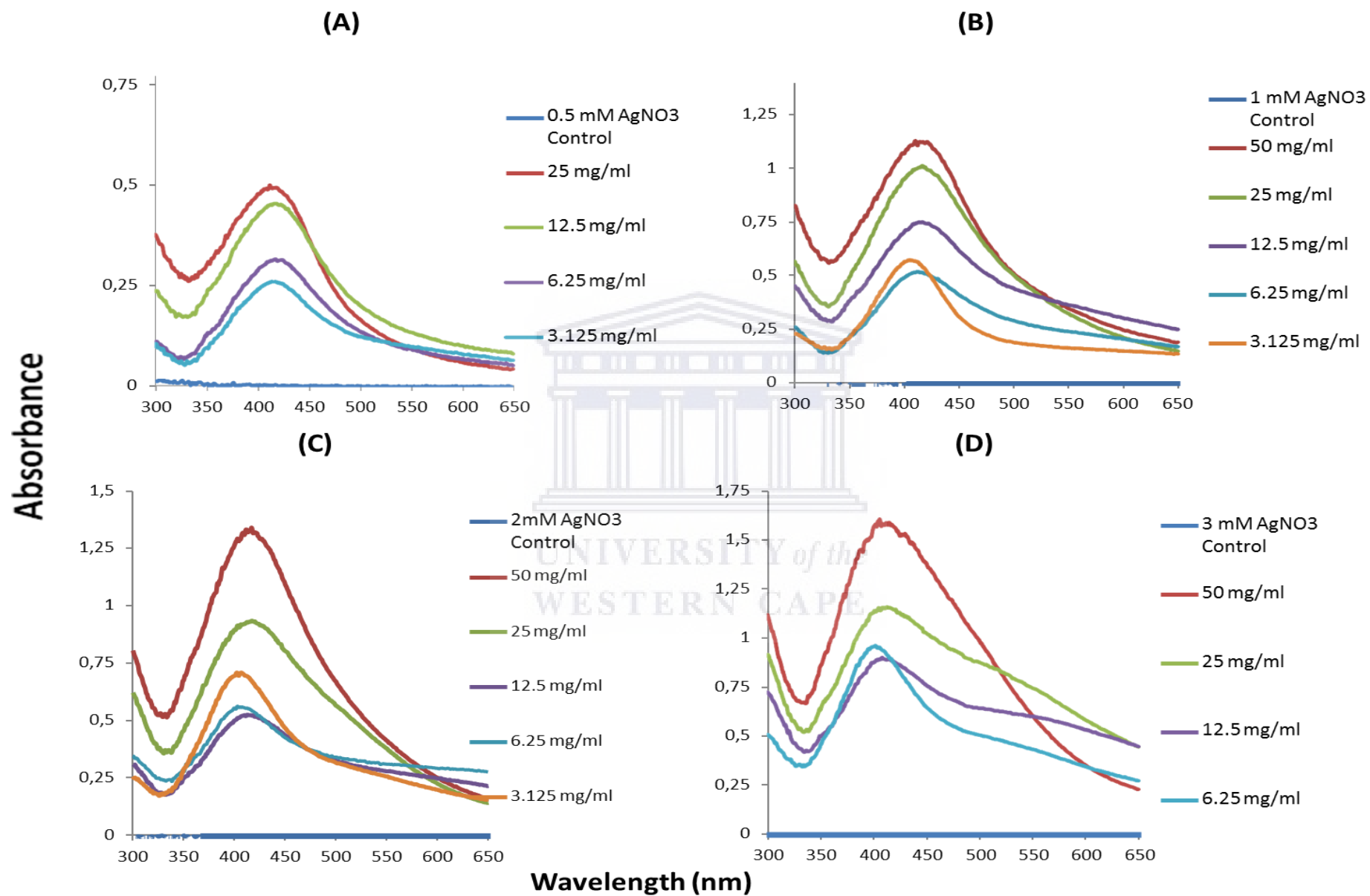
Temperature plays a vital role in the control of the nucleation of the AgNPs fabrication. In this study one can conclude that sunlight produced better AgNPs in comparison to synthesis in the dark at various temperatures on shaking heating blocks in the laboratory. Under controlled settings in the laboratory, the reaction mixture failed to show any visible colour change. These findings were similar to those published in the literature (Rastogi and Arunachalam, 2011; Rajoriya *et al.*, 2016). The characteristic absorbance for AgNPs was recorded at different temperatures (37, 50, 70, 80 and 100 °C) in the dark and no AgNPs were synthesized at any of these temperatures. NPs were only synthesized between 25 – 28 °C in direct sunlight. Temperatures above 28 °C resulted in aggregation and retardation of the secondary reduction process. This could be attributed to the photosensitization of molecules present in the *B. frutescens* extract.

It has been observed that there should be direct sunlight, 0 % cloud cover with a UV-index between 7 and 10, and humidity of above 40 % for the synthesis of AgNPs that fall within the size range of 1- 100 nm, and visible SPR between of 300 – 650 nm and low Pdl. This study has shown that the NP size is dependent on the light exposure. The higher absorption will display a greater reduction resulting in smaller AgNPs whereas less light absorption will result in a lower reduction rate leading to larger size AgNPs.

3.1.5. The effect of AgNO₃ and extract concentration on the size distribution and uniformity of AgNPs

The optimum neutral and pH 10 AgNPs were selected by looking at the UV-Vis spectra of the individual AgNO₃ concentrations with various extract concentrations. The most uniform peaks which fall within a UV-visible range of 390 – 450 nm were chosen. This is illustrated in **figure 3.19** and **3.20**.





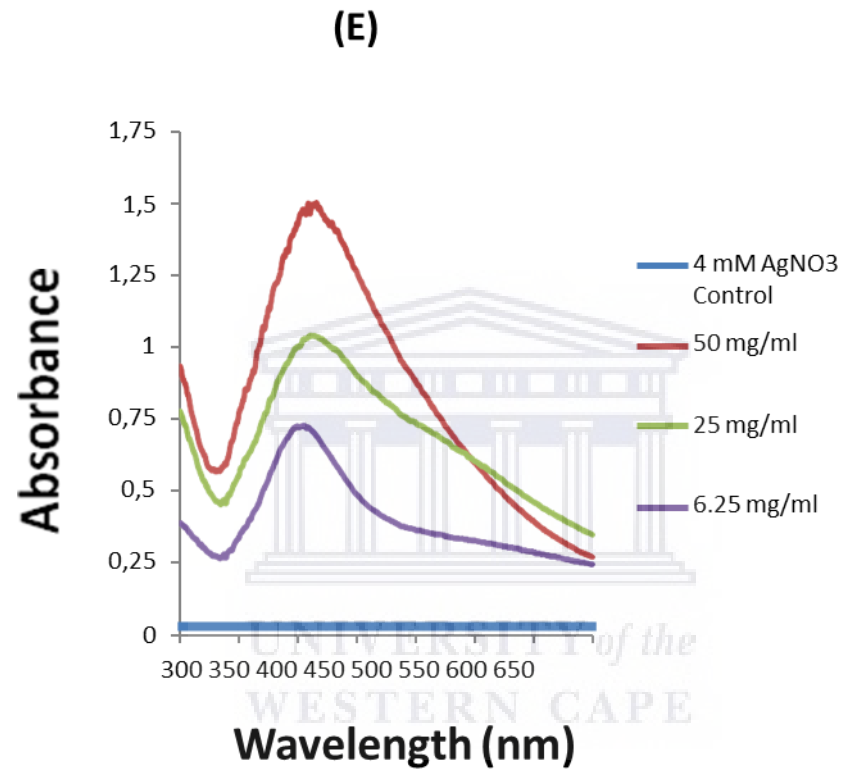
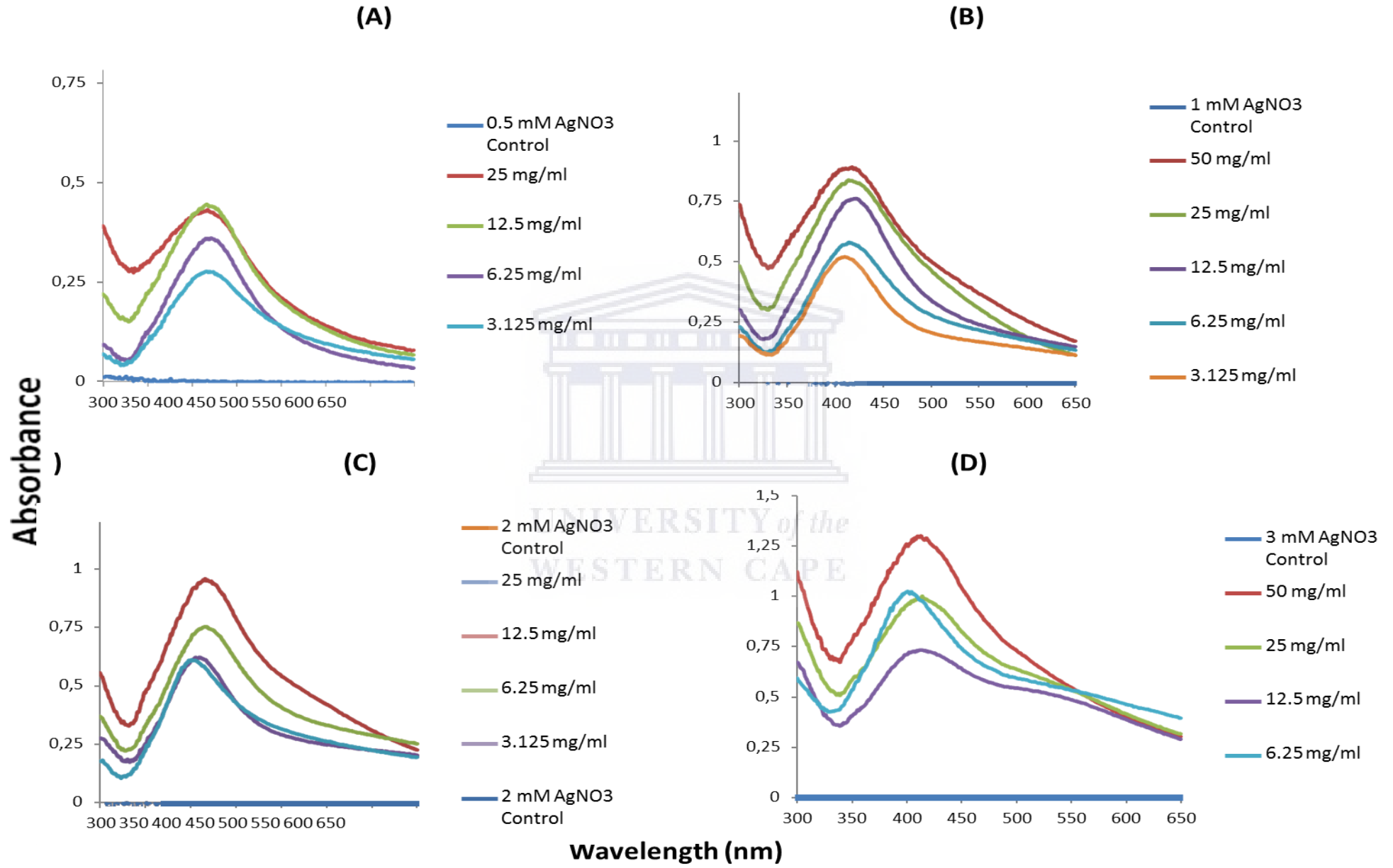


Figure 3.19: UV-Vis spectra of optimum neutral pH (7.11) *B. frutescens* leaf extract concentrations for various AgNO₃ concentration in direct sunlight. (A) 0.5 mM (B) 1 mM (C) 2 mM (D) 3 mM (E) 4 mM



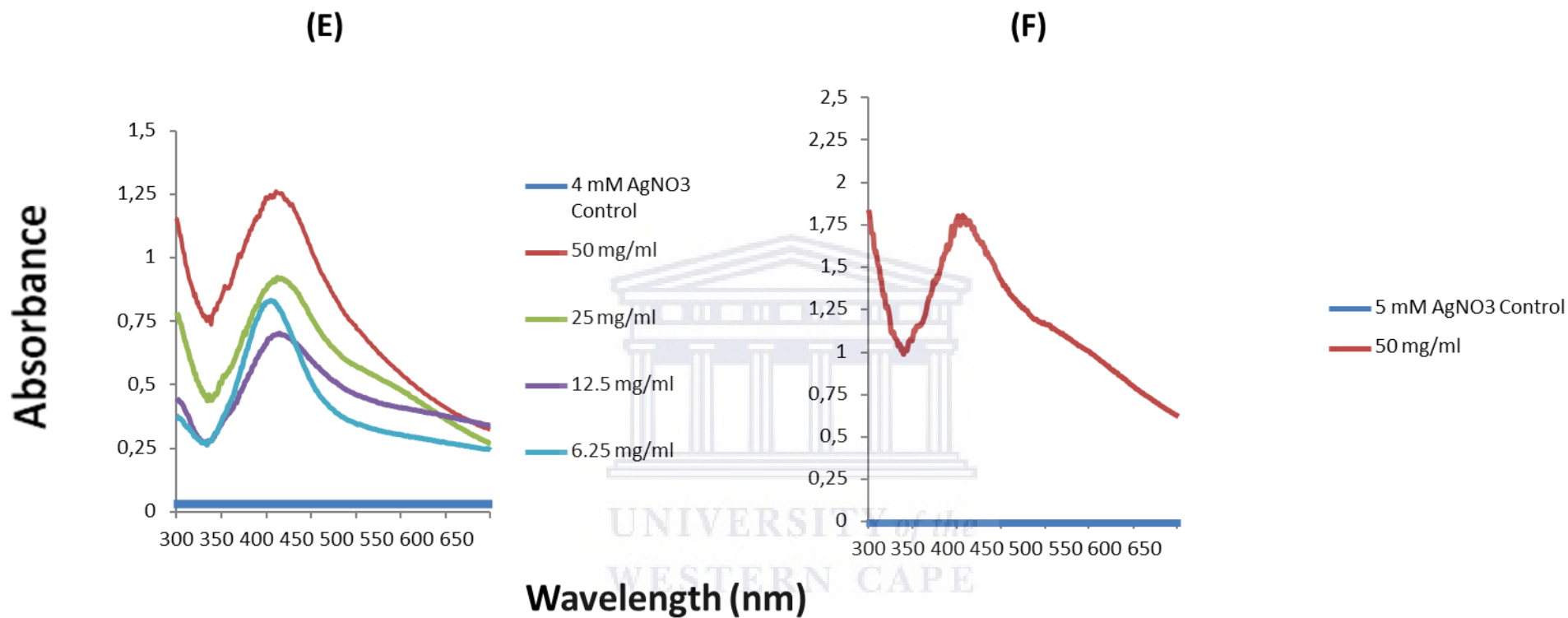


Figure 3.20: UV-Vis spectra of optimum pH 10 *B. frutescens* leaf extract concentrations for various AgNO₃ concentration in direct sunlight.

(A) 0.5 mM (B) 1 mM (C) 2 mM (D) 3 mM (E) 4 mM (F) 5 mM

For neutral pH AgNP at an AgNO_3 concentration of 0.5 mM the optimum extract concentration as illustrated in **table 3.1** is 25 mg/ml which has a λ_{max} of 411 ± 0.494 , hydrodynamic size of 36.10 d.nm and a Pdl of 0.664 indicating that the AgNPs produced are polydispersed. From the results tabulated in table 3.1, it is evident that as the neutral pH extract concentration decreases there is an increase in the hydrodynamic size of the AgNPs from 25 – 6.25 mg/ml and then a decrease in the hydrodynamic size is observed at 3.125 mg/ml extract concentration. For pH 10 extract concentrations as the extract concentration decreases there is an increase in the hydrodynamic size. There are fluctuations with the λ_{max} shifting towards the blue region and then moving towards the red region at lower extract concentrations. The Pdl seems to have a direct relationship with the extract concentration; as extract concentration decreases the Pdl also decreases falling within the acceptable Pdl range of less than 0.5 which is indicative of a monodispersed NP. A similar trend is seen for pH 10 AgNPs where the Pdl decreases as the concentration of extract decreases. The optimum extract concentration for pH 10 AgNPs at 0.5 mM AgNO_3 is 12.5 mg/ml with a λ_{max} of 416 ± 0.444 , hydrodynamic size of 34.22 d.nm and a Pdl of 0.555 indicating that the AgNPs produced are also polydispersed.

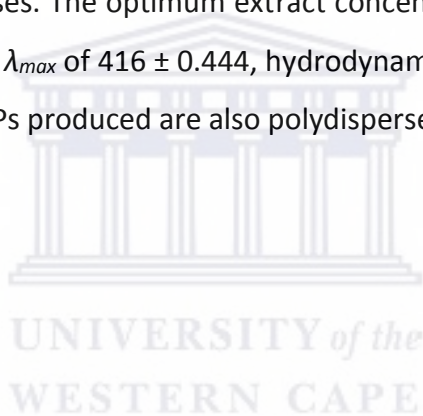


Table 3.1: Optimum synthesis conditions and DLS analysis for neutral pH and pH 10 AgNPs for various extract concentrations with 0.5 mM AgNO₃. Conc. – Concentration of extract, PD – Particle diameter, Pdl – Polydispersity Index, * - no AgNPs are synthesized, **Blue highlighted text** – Optimum extract concentration chosen for 0.5 mM AgNO₃.

Neutral pH (7.11)					pH 10				
Conc. (mg/ml)	Time (min)	λ_{max} (nm)	PD (d.nm)	Pdl	Conc. (mg/ml)	Time (min)	λ_{max} (nm)	PD (d.nm)	Pdl
50	*	*	*	*	50	*	*	*	*
25	15	411±0.494	36.10	0.664	25	15	415±0.428	24.94	0.606
12.5	45	416±0.454	48.01	0.700	12.5	45	416±0.444	34.22	0.555
6.25	45	418±0.315	139.4	0.341	6.25	45	416±0.359	76.58	0.512
3.125	15	415±0.259	75.33	0.340	3.125	30	417±0.277	84.06	0.527

From the results in **figure 3.19** and **3.20** it is evident from the UV-Vis spectra that the optimum concentration of extract for neutral pH'd AgNPs is 25 mg/ml which has a λ_{max} of 414 ± 1.004 , hydrodynamic size of 55.64 d.nm and a Pdl of 0.425 as indicated in **table 3.2** showing that the AgNP produced is monodispersed. The Pdl is directly proportional to the extract concentration. As the extract concentration decreases the Pdl decreases as well. For pH 10 AgNPs the optimum extract concentration is 25 mg/ml at an AgNO_3 concentration of 1 mM. The λ_{max} of 407 ± 0.821 with a hydrodynamic size of 32.88 d.nm and a Pdl of 0.595. The Pdl increases as the extract concentration increases between 50 and 6.25 mg/ml and then decreases at 3.125 mg/ml.



Table 3.2: Optimum synthesis conditions and DLS analysis for neutral pH and pH 10 AgNPs for various extract concentrations with 1 mM AgNO₃. Conc. – Concentration of extract, PD – Particle diameter, Pdl – Polydispersity Index, * - no AgNPs are synthesized, **Blue highlighted text** – Optimum extract concentration chosen for 1 mM AgNO₃

Neutral pH (7.11)					pH 10				
Conc.	Time	λ_{max}	PD	Pdl	Conc.	Time	λ_{max}	PD	Pdl
(mg/ml)	(min)	(nm)	(d.nm)		(mg/ml)	(min)	(nm)	(d.nm)	
50	45	414±1.123	59.57	0.711	50	45	411±0.821	42.08	0.549
25	30	414±1.004	55.64	0.425	25	30	407±0.821	32.88	0.595
12.5	30	414±0.748	59.17	0.438	12.5	45	418±0.758	64.97	0.602
6.25	30	412±0.517	89.87	0.406	6.25	30	416±0.578	89.15	0.603
3.125	15	404±0.571	94.72	0.323	3.125	15	407±0.518	70.19	0.393

From the results in **figure 3.19** and **3.20** it is evident from the UV-Vis spectra that the optimum concentration of extract at an 2 mM AgNO₃ for neutral pH'd AgNPs is 12.5 mg/ml which has a λ_{max} of 413 ± 0.528 , hydrodynamic size of 83.44 d.nm and a Pdl of 0.332 as indicated in **table 3.3** showing that the AgNP produced is monodispersed. There is a fluctuation in the Pdl in correlation with the extract concentration. There is an increase in the Pdl between 50 and 25 mg/ml, followed by a decrease at 12.5 mg/ml, then an increase between 6.25 and 3.125 mg/ml. For pH 10 AgNPs the optimum extract concentration is 25 mg/ml at an AgNO₃ concentration of 2 mM. The λ_{max} of 416 ± 0.957 with a hydrodynamic size of 75.79 d.nm and a Pdl of 0.399. The Pdl increases as the extract concentration increases between 25 and 12.5 mg/ml, then decreases at 6.25 mg/ml, followed by an increase at 3.125 mg/ml.



Table 3.3: Optimum synthesis conditions and DLS analysis for neutral pH and pH 10 AgNPs for various extract concentrations with 2 mM AgNO₃. Conc. – Concentration of extract, PD – Particle diameter, Pdi – Polydispersity Index, * - no AgNPs are synthesized, **Blue highlighted text** – Optimum extract concentration chosen for 2 mM AgNO₃

Neutral pH (7.11)					pH 10				
Conc.	Time	λ_{max}	PD	Pdi	Conc.	Time	λ_{max}	PD	Pdi
(mg/ml)	(min)	(nm)	(d.nm)		(mg/ml)	(min)	(nm)	(d.nm)	
50	45	417±1.342	68.48	0.475	50	*	*	*	*
25	15	417±0.937	88.38	0.351	25	45	416±0.957	75.79	0.399
12.5	45	413±0.528	83.44	0.332	12.5	45	416±0.752	90.94	0.465
6.25	30	404±0.558	120.1	0.395	6.25	30	413±0.614	101.4	0.364
3.125	15	402±0.709	79.20	0.435	3.125	45	398±0.608	44.04	0.634

From the results in **figure 3.19** and **3.20** it is evident from the UV-VIs spectra that the optimum concentration of extract for neutral pH'd AgNPs is 50 mg/ml at 3 mM AgNO₃ which has a λ_{max} of 402 ± 1.581 , hydrodynamic size of 83.75 d.nm and a Pdl of 0.310 as indicated in **table 3.4**. The Pdl is less than 0.5 indicating that the AgNP produced is monodispersed. The optimum pH 10 AgNP extract concentration is 6.25 mg/ml at 3 mM AgNO₃ with a λ_{max} of 401 ± 1.023 , hydrodynamic size of 78.70 d.nm and a Pdl of 0.382.



Table 3.4: Optimum synthesis conditions and DLS analysis for neutral pH and pH 10 AgNPs for various extract concentrations with 3 mM AgNO₃. Conc. – Concentration of extract, PD – Particle diameter, Pdl – Polydispersity Index, * - no AgNPs are synthesized, **Blue highlighted text** – Optimum extract concentration chosen for 3 mM AgNO₃

Neutral pH (7.11)					pH 10				
Conc. (mg/ml)	Time (min)	λ_{max} (nm)	PD (d.nm)	Pdl	Conc. (mg/ml)	Time (min)	λ_{max} (nm)	PD (d.nm)	Pdl
50	30	402±1.581	83.75	0.310	50	45	405±1.28	111.7	0.304
25	45	397±1.123	124.4	0.299	25	45	400±0.953	113.8	0.313
12.5	45	405±0.893	104.0	0.308	12.5	30	395±0.689	114.1	0.341
6.25	30	392±0.924	49.16	0.601	6.25	45	401±1.023	78.70	0.382
3.125	*	*	*	*	3.125	*	*	*	*

From the results in **figure 3.19** and **3.20** it is evident from the UV-Vis spectra that the optimum concentration of extract for neutral pH'd AgNPs is 25 mg/ml at 4 mM AgNO₃ which has a λ_{max} of 405 ± 1.027 , hydrodynamic size of 99.98 d.nm and a Pdl of 0.294 as indicated in **table 3.5**. The Pdl is less than 0.5 indicating that the AgNP produced is monodispersed. The optimum pH 10 AgNP extract concentration is 12.5 mg/ml at 4 mM AgNO₃ with a λ_{max} of 407 ± 0.698 , with a hydrodynamic size of 96.72 d.nm and a Pdl of 0.330 indicating that the AgNP produced is monodispersed.

From the results in **figure 3.19** and **3.20** it is evident from the UV-Vis spectra that no AgNPs were produced at neutral pH with 5 mM AgNO₃, however, only one AgNP was produced at pH 10 of extract with 5 mM AgNO₃. The concentration of pH 10 extract is 50 mg/ml with a λ_{max} of 399 ± 1.784 , with hydrodynamic size of 128.3 d.nm and a Pdl of 0.333 indicating that the AgNP produced is monodispersed although the size distribution is above 100 d.nm.

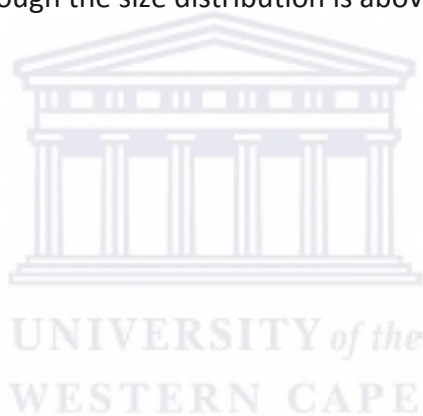


Table 3.5: Optimum synthesis conditions and DLS analysis for neutral pH and pH 10 AgNPs for various extract concentrations with 4 mM AgNO₃. Conc. – Concentration of extract, PD – Particle diameter, Pdl – Polydispersity Index, * - no AgNPs are synthesized, **Blue highlighted text** – Optimum extract concentration chosen for 4 mM AgNO₃

Neutral pH (7.11)					pH 10				
Conc. (mg/ml)	Time (min)	λmax (nm)	PD (d.nm)	Pdl	Conc. (mg/ml)	Time (min)	λmax (nm)	PD (d.nm)	Pdl
50	45	404±1.479	89.04	0.302	50	30	405±1.248	129.8	0.358
25	30	405±1.027	99.98	0.294	25	30	408±0.918	109.7	0.328
12.5	*	*	*	*	12.5	45	407±0.698	96.72	0.330
6.25	30	399±1.784	100.2	0.533	6.25	30	394±0.797	111.6	0.473
3.125	*	*	*	*	3.125	*	*	*	*

3.1.6. Hydrodynamic size, Pdl and Zeta potential measurements of optimum AgNO₃ concentrations with various extract concentrations.

The optimum conditions for synthesis at various AgNO₃ concentrations are represented in **figure 3.21** and **table 3.6** below. This data was constructed to establish the optimum conditions to synthesize AgNPs and pH 10 and neutral pH (7.11).

From the data tabulated in table 3.6 it is evident that for neutral pH AgNPs, as the λ_{max} of the SPR, size, Pdl and ZP that the optimum conditions for synthesis of neutral pH (7.11) AgNPs are 25 mg/ml extract, 1 mM AgNO₃ over a period of 30 minutes in direct sunlight, and for pH 10 AgNPs are 25 mg/ml extract, 2 mM AgNO₃ over a period of 45 minutes. The UV-Vis spectrums for both AgNPs are single, strong and uniformed; they fall within the range of 390 – 450 nm. The hydrodynamic size are below 100 d.nm with a Pdl of lower than 0.5 making it an ideal candidate for application based work; it is believed that the smaller the AgNP the antibacterial activity will be enhanced resulting in greater inhibition or even killing of microbes.

The trend throughout all NPs produced at various AgNO₃ concentrations is that the smallest AgNPs produced with a size distribution of less than 50nm produced a larger Pdl where as AgNPs produced with a larger distribution had a smaller Pdl. It is well documented that AgNPs which fall within 300 to 650 nm have a size distribution of 2 to 100nm. All AgNPs produced were in the range of 390 to 450 nm. It uses light in the visible and adjacent (near-UV and near-infrared (NIR)) ranges where molecules may undergo electronic transitions (Jia *et al.*, 2006). In metallic nanoparticles such as AgNPs, the electrons are able to move freely due to the close proximity of the conduction and valence bands (Nath *et al.*, 2007).

Table 3.6: DLS analysis of the optimum conditions for various AgNO₃ concentrations showing the average time for synthesis, optimum plant extract concentration, λ_{max} , particle size (PD) and polydispersity index (PDI) values in direct sunlight. , Blue highlighted text – Chosen optimum conditions for synthesis

Neutral pH (7.11)					pH 10				
Conc. (mg/ml)	Time (min)	λ_{max} (nm)	PD (d.nm)	PDI	Conc. (mg/ml)	Time (min)	λ_{max} (nm)	PD (d.nm)	PDI
0.5mM 25	15	411±0.494	36.10	0.664	0.5mM 12.5	45	416±0.444	34.22	0.555
1mM 25	30	414±1.004	55.64	0.425	1mM 25	30	407±0.821	32.88	0.595
2mM 12.5	45	413±0.528	83.44	0.332	2mM 25	45	416±0.957	75.79	0.399
3mM 50	30	402±1.581	83.75	0.310	3mM 6.25	45	401±1.023	78.70	0.382
4mM 25	30	405±1.027	99.98	0.294	4mM 12.5	45	407±0.698	96.72	0.330

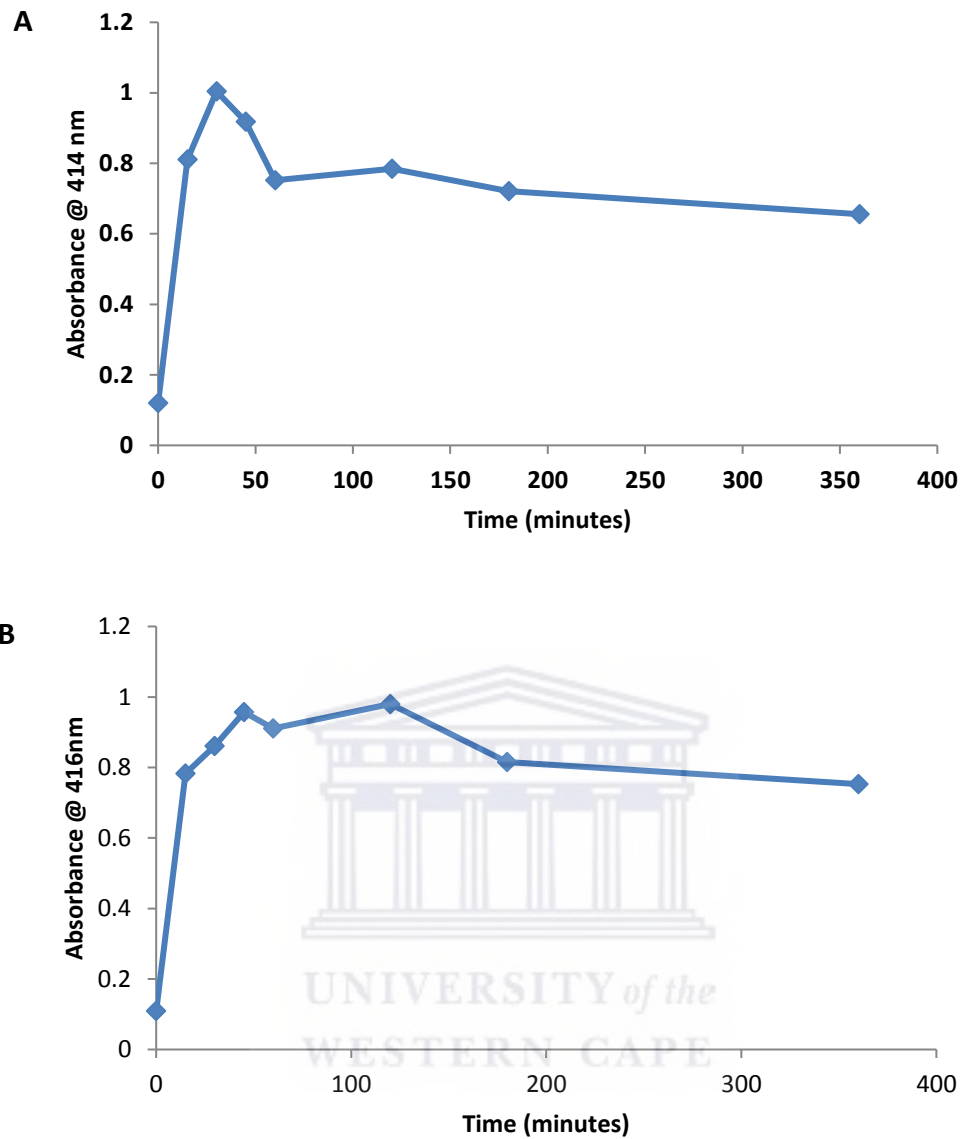


Figure 3.21: Time course of AgNP synthesis using optimum conditions of - A: Neutral pH (7.11), B: pH 10

Large scale synthesis of AgNPs is depicted in **figure 3.22** below. The difference between pellet 2 (500 μ l) and pellet 2 (100 μ l) is the amount of deionized H₂O added after each centrifugation step. One hundred μ l of deionized H₂O was added after the last centrifugation step to give a more concentrated formulation of AgNPs which is evident on the UV-Vis spectra, as the SPR peak is higher than pellet 2 (500 μ l).

From the data obtained in conjunction with the data tabulated in **table 3.7** it is evident that the up-scaling to a larger volume of 50 ml affected the UV-Vis spectra causing the absorbance to shift lower than the small scale synthesis peak. Although there is a shift in the absorbance, the wavelength at which the SPR is reflected remains within the same range. For neutral pH AgNPs the λ_{max} increases as the AgNPs is subjected to centrifugation for purification purposes. The particle size dramatically increases from 89.02 d.nm after synthesis to 133.8 d.nm and 180.4 d.nm respectively after the final washing step. The Pdl remains fairly intact through the purification process indicating that the AgNPs are fairly stable and is monodispersed in uniformity. The ZP also decreases during the purification process. This aids in antimicrobial based application because the more negative the ZP, the more potent the AgNPs are against bacterial cell walls. For pH 10 AgNPs it is evident that as the purification process progresses the λ_{max} increases in proportion to the particle size, Pdl and ZP.

UNIVERSITY of the
WESTERN CAPE

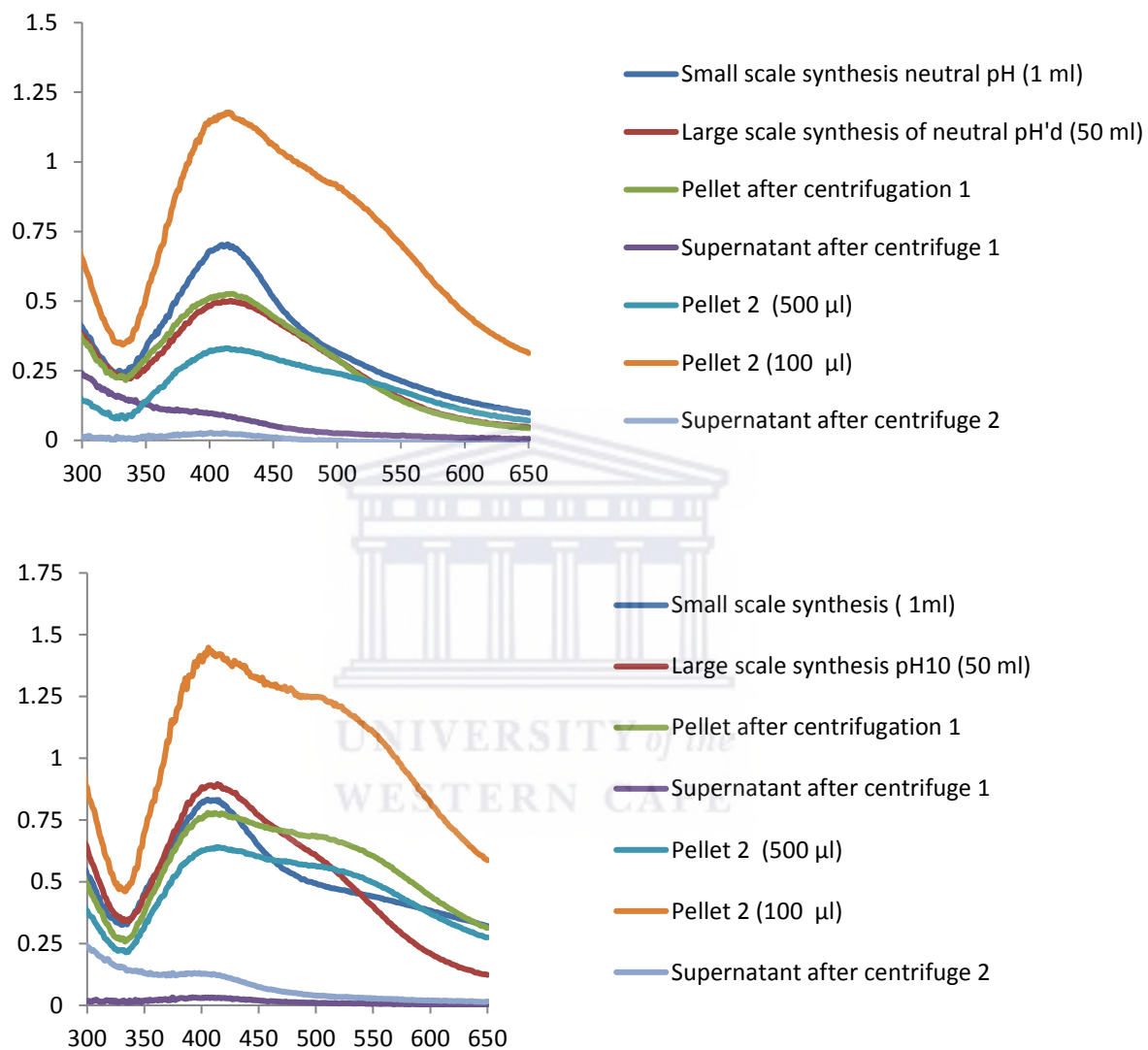
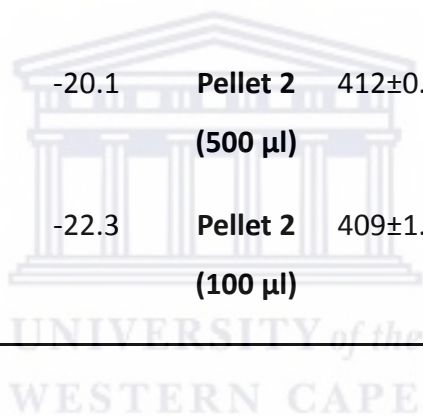


Figure 3.22: UV-Vis spectra of the pellets and supernatants of neutral pH (7.11) and pH 10 AgNPs after each centrifugation step.

Table 3.7: DLS and ZP analysis of neutral pH (7.11) and pH 10 AgNPs after each centrifugation step.

Neutral pH (7.11)					pH 10				
Sample	λ_{max}	PD	Pdi	ZP	Sample	λ_{max}	PD	Pdi	ZP
	(nm)	(d.nm)		(mV)		(nm)	(d.nm)		(mV)
Small scale	410±0.702	55.64	0.425	*	Small scale	405±0.833	32.88	0.595	*
Large scale	410±0.499	89.02	0.236	-18.3	Large scale	408±0.891	101.3	0.274	-20.6
Pellet 1	416±0.526	201.9	0.402	-22.7	Pellet 1	412±0.779	181.1	0.311	-25.1
Pellet 2 (500 µl)	412±0.33	133.8	0.461	-20.1	Pellet 2 (500 µl)	412±0.639	219.5	0.482	-24.8
Pellet 2 (100 µl)	415±1.178	180.4	0.389	-22.3	Pellet 2 (100 µl)	409±1.434	279.7	0.561	-25.4



3.1.7. The effect of pH on AgNP synthesis

From the results tabulated in the optimization studies for large scale synthesis, it has been found that as the pH value increases, the SPR peak shifts to left indicating a decrease in the size of the prepared nanoparticles. Moreover, this shift in the peak is accompanied by a decrease in the width of the peak indicating size uniformity. However, when looking at the two optimised conditions, pH 10 AgNPs are right shifted in comparison to neutral pH AgNPs. When looking at all reactions collectively, no real pattern can be determined.

At neutral pH NPs were produced at all AgNO_3 concentrations, except for 5 mM AgNO_3 . At pH 10 NPs were produced at all AgNO_3 concentrations. The net charge on the biomolecules changes from a positive to negative and it results in an intense repulsion between the negatively charged ions and the biomolecules. The presence of larger NPs and platelets at lower pH's can be attributed to the uncontrolled nucleation and aggregation at lower pH, due to enhanced interaction of negatively charged ions. On the contrary, in acidic pH, increase aggregation outdoes the nucleation process while at alkaline pH greater number of nuclei formation, instead of aggregation, lead to the synthesis of more of NPs with smaller diameter (Shankar *et al.*, 2004). Acidic condition suppresses the formation of AgNPs but the basic condition enhances the formation of AgNPs. This indicates pH plays a very important role controlling size and shape of the AgNPs synthesis.

3.2. Preparation of extract and TPC analysis

The *B. frutescens* extract was prepared as described in section 2.2. From 300 g of leaves that were added to 150 ml ddH₂O and boiled, the weight of the solid particles after glass-wool filtration was 128.93 g, and the freeze-dried sap was 171.01 g. This indicated that the sap constituted almost 60 % of the weight of the leaves.

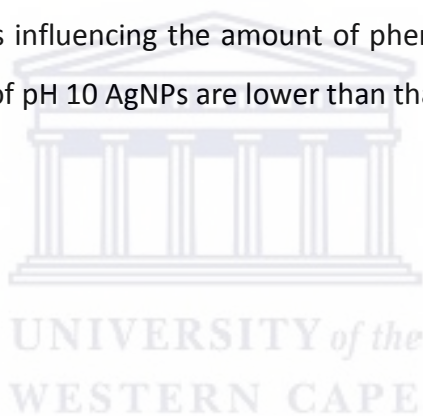
The TPC content of *B. frutescens* leaf sap extract and synthesized AgNPs were determined by spectrophotometry using the FC reagent as described in section 2.3. Polyphenols represent a group of biologically active molecules which are common in plants and are structurally characterized by the presence of one or more phenol units. Polyphenols play very important roles in the prevention of chronic infections or disease due to their antioxidant activities (Silberstein *et al.*, 2016; Queralt *et al.*, 2015). A quantitative estimation of the total phenolic content for both the leaf sap extract and AgNPs are shown in **figure 3.23** and **3.24**; and **table 3.8** and **3.9**. The total phenolic content was measured in terms of gallic acid equivalent (standard equation for extracts: $y = 0.0345x$; standard equation for AgNPs: $y = 0.3333x$).

The results indicate that the AgNPs exhibited elevated levels of TPC content (neutral pH AgNP: 70.34 ± 0.015 , pH 10 AgNP: 243.003 ± 0.01175) compared to both neutral pH and pH 10 extract (235.19 ± 1.25 ; 196.17 ± 1.25). Although the concentrations of the NPs used are different, pH 10 AgNPs still produced a higher TPC level compared to neutral pH AgNPs. Neutral pH extract had a higher TPC level compared to pH 10 extract. The concentration of extract and AgNPs is in direct proportion with the TPC levels. As the extract and AgNPs concentration is decreased the TPC levels also decrease.

Previous research conducted has shown that plants with a higher TPC have a greater antioxidant activity (Zheng *et al.*, 2001; Saleem *et al.*, 2001; Iwalokun *et al.*, 2006; Lopez-Velez *et al.*, 2004). In addition, a study conducted by Cai and colleagues have found that the antioxidant activity is associated with the TPC molecular structure, which directly influences the number and position of the primary hydroxyl group (Cai *et al.*, 2006). This finding is corroborated by studies listed below:

- Subramanian and colleagues demonstrated that the bark of *Shorea roxburghii* contained a high level of total phenolic compounds and that the plant extract can be used as a green reducing agent for synthesis of AgNPs (Subramanian *et al.*, 2013).
- Goordarzi and colleagues study revealed that the order of plants reducing capacity is in alignment with the TPC and antioxidant potential (Goordazi *et al.*, 2014).
- Begum and colleagues established through the kinetic study of AgNPs and AuNPs that the high amount of polyphenols found within tea leaves are responsible for the formation of Ag and Au NPs (Begum *et al.*, 2008).
- Hossain and colleagues researched the TPC in pineapples and discovered that it exhibited high levels of natural antioxidants which could potentially make it an ideal candidate for AgNP synthesis (Hossain *et al.*, 2011).

It can be concluded from the TPC analysis that the ionic charge on the pH 10 AgNPs enhances the activity of polyphenols, thus influencing the amount of phenols present within the AgNPs even though the concentration of pH 10 AgNPs are lower than that of neutral pH AgNPs.



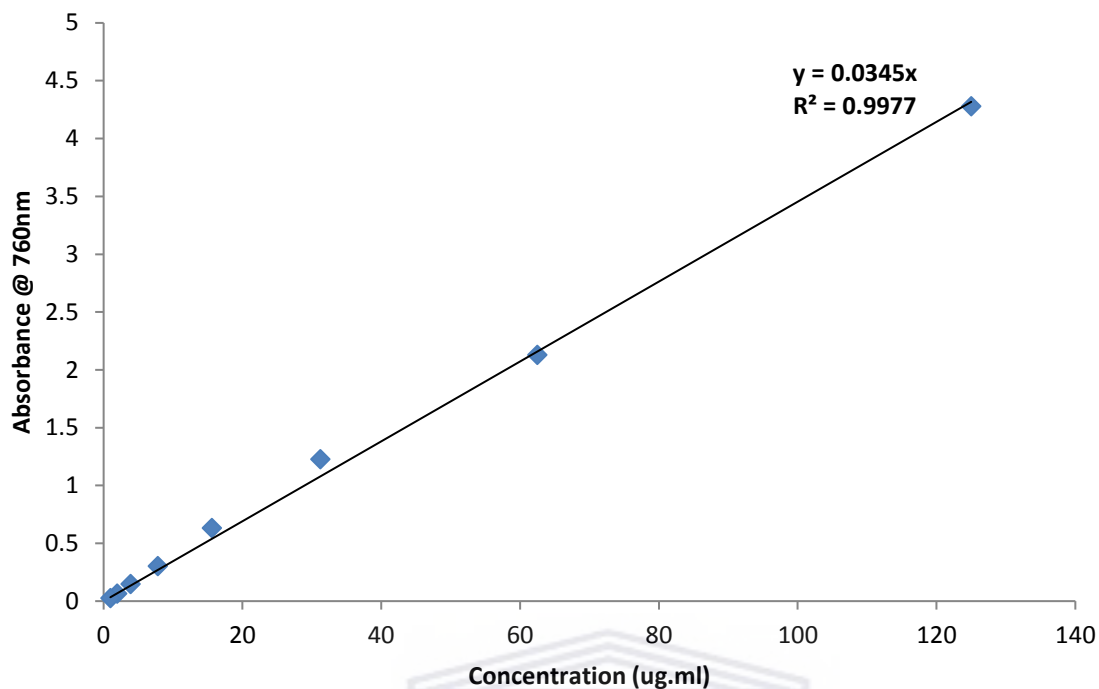


Figure 3.23: Gallic acid calibration curve for *B. frutescens* extract.

Table 3.8: Total phenolic content of various *B. frutescens* extract concentrations expressed as the amount of gallic acid per dried weight of extract.

Extract	Concentration of extract (mg/ml)	TPC (GAE $\mu\text{g.ml}/\mu\text{g}$ of extract)
Neutral pH (7.11)	50	235.19 ± 1.25
	25	26.10 ± 0.625
	12,5	2.98 ± 0.3125
	6,25	0.36 ± 0.15625
	3,125	0.043 ± 0.078125
	1,56	0.0049 ± 0.039
	0,78	0.00074 ± 0.0195
	0,39	$6.34 \times 10^{-5} \pm 0.00975$
	pH 10	50
25		21.05 ± 0.625
12,5		2.63 ± 0.3125
6,25		0.31 ± 0.15625
3,125		0.038 ± 0.078125
1,56		0.0048 ± 0.039
0,78		0.00048 ± 0.0195
0,39		$4.95 \times 10^{-5} \pm 0.00975$

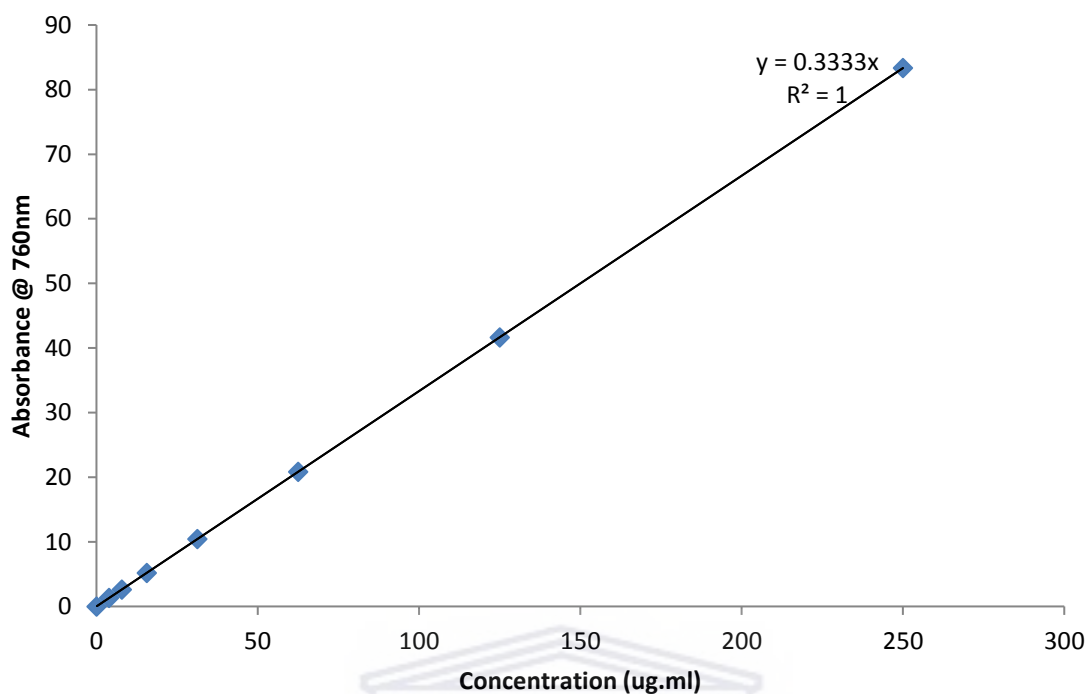


Figure 3.24: Gallic acid calibration curve for neutral pH and pH 10 AgNPs synthesized from *B. frutescens* leaf extract.

Table 3.9: Total phenolic content of neutral pH and pH 10 *B. frutescens* AgNP concentrations expressed as the amount of gallic acid per dried weight of AgNP.

Nanoparticles	Concentration of NPs (mg/ml)	TPC (GAE $\mu\text{g.ml}/\mu\text{g}$ of NPs)
Neutral pH (7.11)	0,6	70.34 ± 0.015
	0,3	6.367 ± 0.0075
	0,15	0.508 ± 0.00375
	0,075	0.0533 ± 0.0019
	0,0375	0.00853 ± 0.000938
	0,01875	0.00245 ± 0.000469
	0,009375	0.00027 ± 0.000234
	0,0046875	$6.187 \times 10^{-5} \pm 0.000117$
pH 10	0.47	243.003 ± 0.01175
	0.235	24.77 ± 0.005875
	0.1175	2.44 ± 0.0029
	0.05875	0.24 ± 0.00147
	0.029375	0.0224 ± 0.00073
	0.0146875	0.003 ± 0.00038
	0.00734375	0.00067 ± 0.00018
0.003671875	$9.53 \times 10^{-5} \pm 9.18 \times 10^{-5}$	

3.3. FTIR analysis

FTIR measurements were carried out to identify the biomolecules for reducing capping and efficient stabilization of the AgNPs synthesized using *B. frutescens* leaf gel sap extract and AgNO₃ as the preparation materials. The comparison of the FTIR spectrum results of *B. frutescens* leaf gel sap freeze-dried sample, 50 mg/ml neutral pH (7.11) and pH 10 extracts and their respective AgNPs, synthesized using the optimal conditions, are displayed in **figure 3.25.1** and **3.25.2** below.



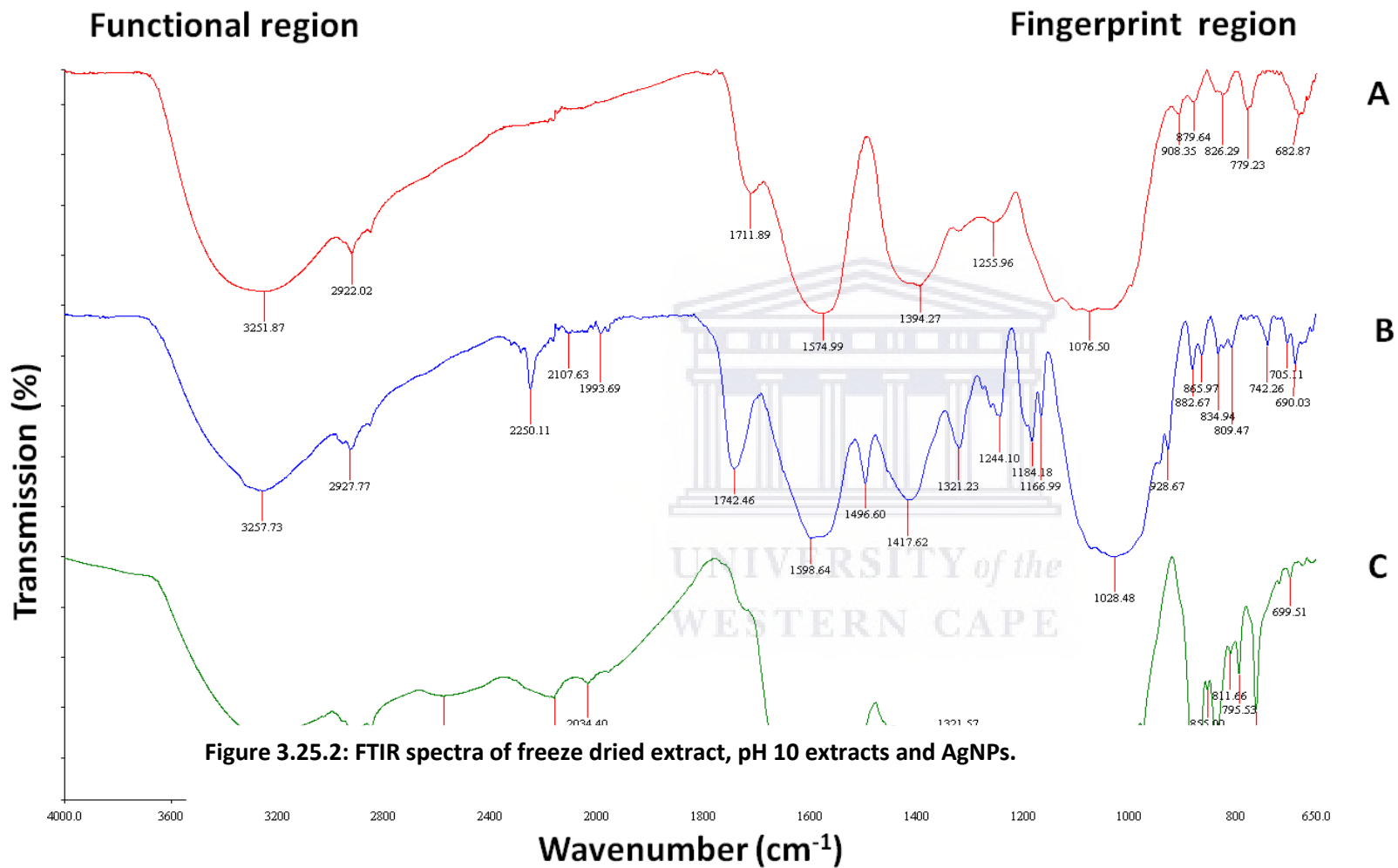


Figure 3.25.2: FTIR spectra of freeze dried extract, pH 10 extracts and AgNPs.

Figure 3.25.2: FTIR spectra of freeze dried extract (A) pH 10 extract (B) and pH 10 AgNPs (C).

The fingerprint regions of the samples are indicated between 1500 cm^{-1} - 650 cm^{-1} . The fingerprint region contains a series of absorptions which indicate the bending vibrations within each sample. The functional regions of the samples are indicated between 4000 cm^{-1} - 1500 cm^{-1} . The differences between the extracts and the AgNPs produced with the extracts gives an indication of which functional groups were modified within the process of synthesis.

From the results obtained in figure 3.25.1 and 3.25.2 it is evident that the bands at approximately 3200 cm^{-1} is fairly broad and is indicative of an O-H stretching vibration indicating that there is a phenol compound or flavonoids present across all IR spectra's. The bands around 2900 cm^{-1} are indicative of a stretching aromatic compound (N-H). The IR bands present around 2200 cm^{-1} and 2100 cm^{-1} can possibly be attributed to the presence of C-N aromatic and aliphatic amides. The IR bands that are present at approximately 1700 cm^{-1} is indicative of an aldehyde (CHO) group present within each sample. The small peaks at approximately 1000 cm^{-1} represents the presence of either an ester or ether functional group.

The troughs within the fingerprint region for the freeze-dried sample, neutral pH (7.11) extract and neutral pH (7.11) AgNPs are fairly similar in absorption wave numbers, however, the pH 10 extract and pH 10 AgNPs absorption wave numbers and spectra is different in comparison to the original extract. IR bands 2284.93 cm^{-1} , 2141.87 cm^{-1} , 2103.68 cm^{-1} , 2066.69 cm^{-1} and 1980.54 cm^{-1} are visible within the neutral pH extract which is not present within the freeze-dried sample. IR bands 2250.11 cm^{-1} , 2107.63 cm^{-1} , 1993.69 cm^{-1} are visible within the pH 10 extract which is not present within the freeze-dried sample. There are some shifts that occur within the IR spectra of the freeze-dried sample when 50 mg/ml neutral pH (7.11) and pH 10 extract are prepared. The shifts are present at the aldehyde functional group from 1711.89 cm^{-1} to 1730.17 cm^{-1} for neutral pH (7.11), and shifts from 1711.89 cm^{-1} to 1742.46 cm^{-1} for pH 10. More functional groups are added when the biological pH of the extract is adjusted to pH 10. IR bands 1321.23 cm^{-1} , 1244.10 cm^{-1} , 1184.18 cm^{-1} and 1166.99 cm^{-1} are present within pH 10 extract which is not present within the freeze-dried extract.

After neutral pH (7.11) AgNPs were formed it is evident that the O-H stretching band was significantly reduced from 3294 cm^{-1} to 3279.01 cm^{-1} , and the single peak found within the extract (2924.39 cm^{-1}) has shifted into two peaks at the N-H vibration (2917.96 cm^{-1} and 2849.89 cm^{-1}). It is clear that the C-N vibration found at 2161.13 cm^{-1} plays an integral role in the reduction of the neutral pH extract in the synthesis of AgNPs as IR bands found at 2284.93 cm^{-1} , 2141.87 cm^{-1} , 2103.68 cm^{-1} , 2066.69 cm^{-1} and 1980.54 cm^{-1} disappeared after the formation of AgNPs and formed one single IR band. The IR band at 1730.17 cm^{-1} found within the neutral pH extract is not present within the neutral pH AgNPs.

After pH 10 AgNPs were formed it is evident that the O-H stretching band was shifted from 3257.73 cm^{-1} to 3260.12 cm^{-1} , and the single peak found within the extract (2927.77 cm^{-1}) has shifted into two peaks at the N-H vibration (2917.37 cm^{-1} and 2849.56 cm^{-1}). An IR band at 2576.26 cm^{-1} which is not present within the pH 10 extract is found within the pH 10 AgNPs and is indicative of a carboxylic acid (COOH) functional group being added in the process of AgNPs synthesis. IR bands 2250.11 cm^{-1} , 2107.63 cm^{-1} and 1993.69 cm^{-1} are significantly reduced in the AgNPs to form two IR stretching bands at 2160.44 cm^{-1} and 2034.40 cm^{-1} resulting in the reduction of an alkyne (C=C) functional group. The IR band at 1742.46 cm^{-1} found within the pH 10 extract is not present within the pH 10 AgNPs. There is a shift in IR bands of the extract and AgNPs from 1598.64 cm^{-1} to 1630.44 cm^{-1} . It is evident from the IR spectra that the aldehyde functional group is removed from both AgNPs in the process of synthesis.

From the results obtained it is clear that *B. frutescens* leaf gel sap extract is an efficient source for the fabrication of neutral pH (7.11) and pH 10 AgNPs. The FTIR analysis confirms that the presence of flavonoids, amine groups, polyphenols and proteins are responsible for the reducing the AgNO_3 to form AgNPs (Kumar *et al.*, 2010), (Mittal *et al.*, 2013). The IR spectrums suggest that molecules attached with the AgNPs have free and bound amide groups and compounds that are attached with the AgNPs could potentially be polyphenols with aromatic rings and bound amide regions. There are similarities present within the extracts and AgNPs with some variation in the peak shifts positions which clearly indicate that the residual plant material is responsible for the capping agents of the AgNPs.

The shifts within the peaks around 3000 cm^{-1} to 1600 cm^{-1} and some peaks remaining unchanged are an indication that proteins are potentially binding with the AgNPs. The proteins potentially capping the metal NPs could be involved in the process of preventing agglomeration from occurring and thus stabilising the medium (Basavaraja *et al.*, 2008).



3.4. HR-TEM analysis of AgNPs

The HR-TEM analysis of neutral pH (7.11) and pH 10 AgNPs was done to determine the shape, crystalline nature, and particle size distribution.

The HR-TEM images of AgNPs produced from *B. frutescens* leaf gel sap extract show variable geometrical shapes and sizes, as illustrated in **figure 3.26 A**. Both the AgNPs synthesized triangular, truncated triangular, rod, oval, spherical and irregular shapes. This confirms the UV-Vis data obtained as described in section 2.7.1. The interparticle distance of neutral pH (7.11) AgNPs were 22.97 nm and pH 10 AgNPs were 20.294 nm. The neutral pH AgNPs triangular-, oval-, spherical and irregular-shaped NPs are 1.4 nm, 1.22, 1 and 1.36 nm in size, respectively. The pH 10 AgNPs are comprised of oval-, spherical-, irregular- and rod-shaped particles with size ranges from 1.6 to 0.9 nm. The pH 10 AgNPs consists of more circular and rod shaped particles in comparison to the neutral pH (7.11) AgNPs. The mixture of geometrical shapes is in agreement with previous reports (Chen *et al.*, 2010). This is due to the presence of different reducing phytochemicals within the extracts which produces the different AgNPs. This indicates that the interaction between the capping biomolecules and the surfaces of the AgNPs produced within this study is fairly weak, resulting in the sintering and development of various geometric shapes.

The crystalline natures of both AgNPs are presented in **figure 3.26 B**. The figure illustrates the fringes of the two AgNPs. The lattice distances were 1.16 nm for neutral pH (7.11) AgNPs, and 0.18 nm for pH 10 AgNPs. **Figure 3.26 C** depicts the selected electron diffraction (SAED) pattern, which also confirms the crystalline nature of the AgNPs. The bright rings interplanar spacing for neutral pH (7.11) AgNPs were 0.10 nm, 0.13 nm, 0.15 nm and 0.24 nm, respectively. The diameter of the each ring was 54.41 nm (**R1**), 138.22 nm (**R2**), 190.75 nm (**R3**) and 326.48 nm (**R4**), respectively. The pH 10 AgNPs bright rings interplanar spacing was 0.09 nm, 0.12 nm, 0.21 nm and 0.27 nm, respectively. The diameter of the each ring was 42.84 nm (**R1**), 69.57 nm (**R2**), 205.791 nm (**R3**) and 367.858 nm (**R4**), respectively. These values correspond with the interplanar spacing between planes of silver.

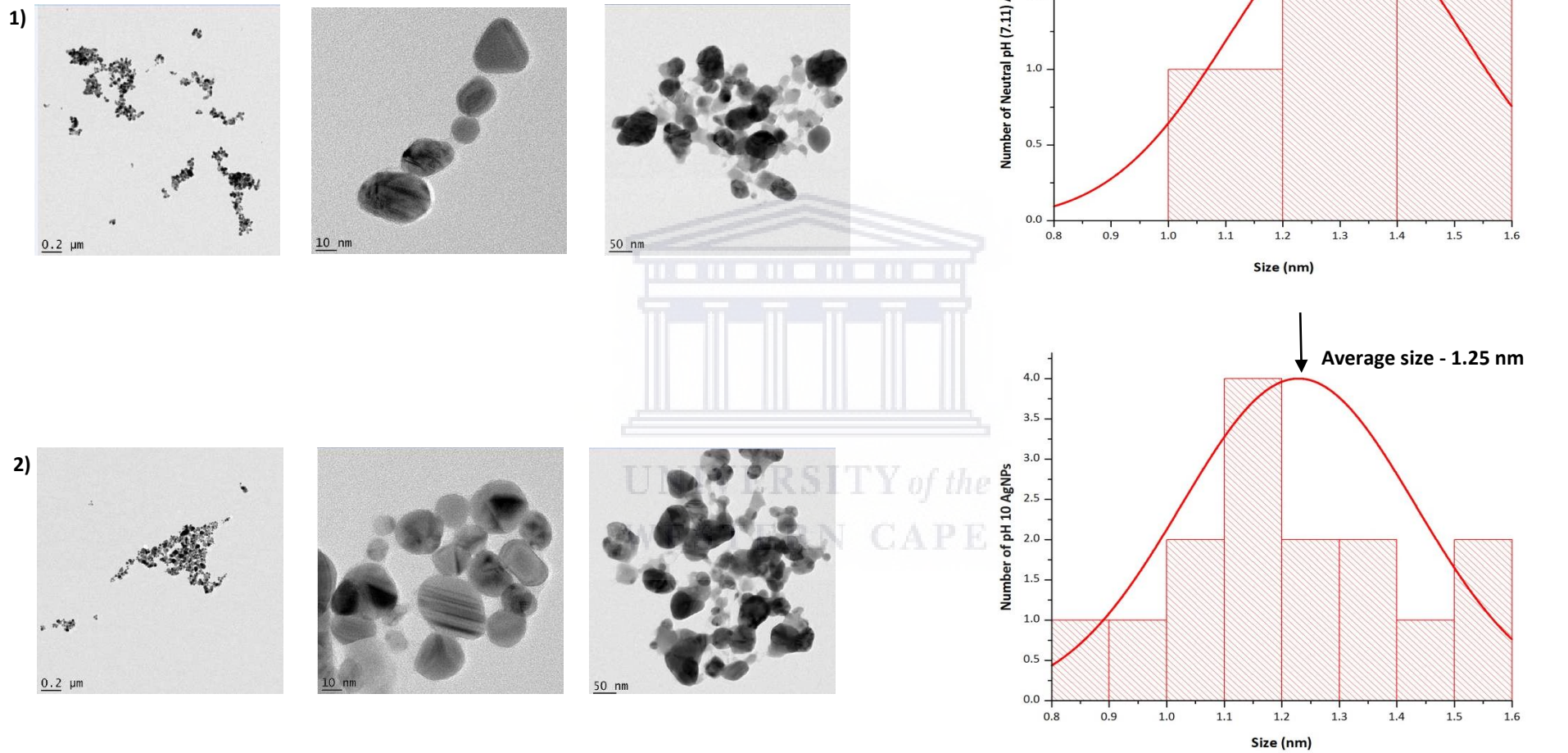


Figure 3.26 A: The morphology and average core diameter of neutral pH (7.11) and pH 10 AgNPs. – 1) Neutral pH (7.11), 2) pH 10

– The HR-TEM images at 0.2 μm , 10 nm and 50 nm resolution scales

– The number size distribution of AgNPs using Image J Software

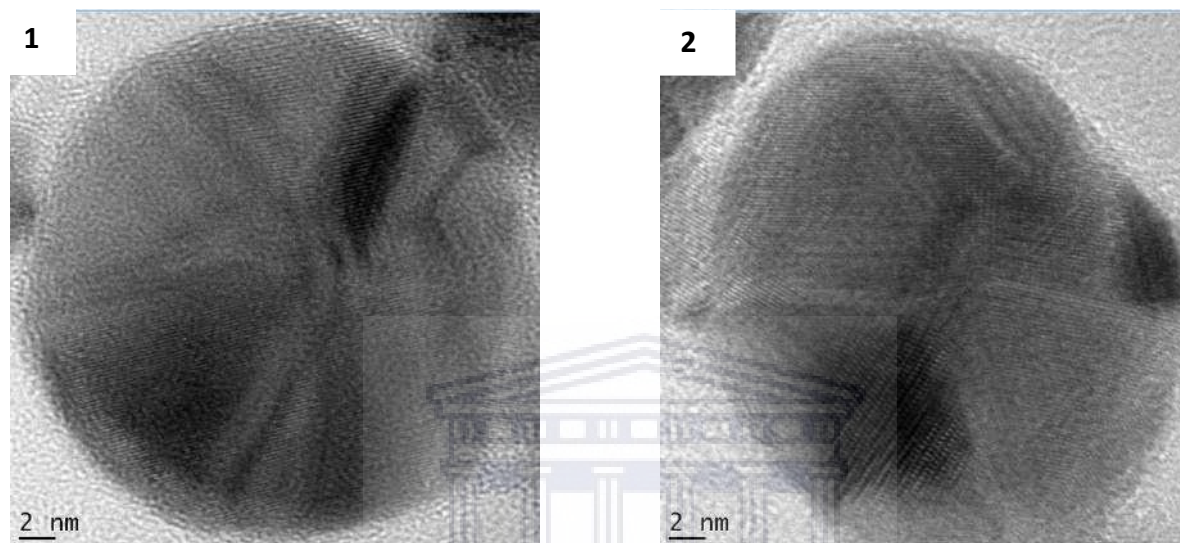


Figure 3.26 B: HR-TEM images showing the Crystalline nature lattice fringes of AgNPs – 1 Neutral pH (7.11), 2) pH 10.

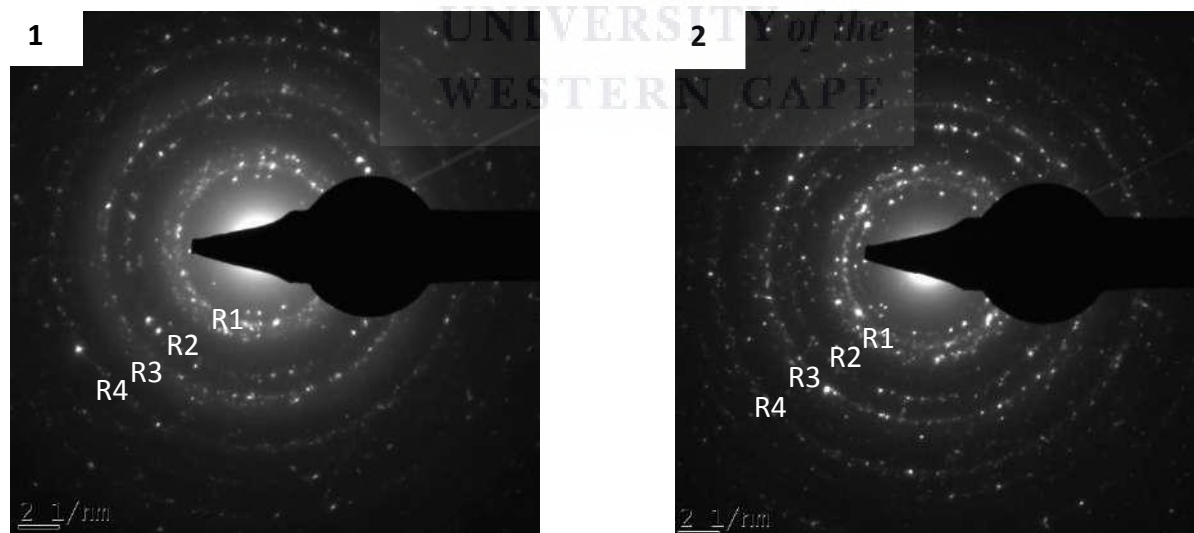


Figure 3.26 C: HR-TEM images showing the SAED pattern of AgNPs -1) Neutral pH (7.11), 2) pH 10.

3.5. Antimicrobial activity of AgNPs.

In this section, the antimicrobial activity of the synthesized nanoparticles is evaluated. Seven bacterial strains and four fungal strains were selected as depicted in table 2.1.

The dose-responses of each bacterial and fungal strain to each AgNP (neutral pH and pH 10) respectively, were compared using GraphPad Prism 6 analysis software. The results from three independent experiments average was calculated using the p-values. The mean, standard deviation of the parameters being compared was taken into account when calculating the p-values. The p-value helps to determine the significance of the results obtained in relation to the null hypothesis. The level of statistical significance is represented between values of 0 and 1. Smaller p-value of less than 0.05 (< 0.05) indicates more statistically significant results compared to larger p-values of 0.05 (> 0.05). P-value's of less than 0.05 indicate strong evidence against the null hypothesis (Ferreira and Patino, 2015). The null hypothesis is thus rejected and the alternative hypothesis is accepted. One-way ANOVA (analysis of variance) with *post hoc* Turkeys was used to determine the error variance (within-groups variance) and between-groups variance (treatment variance). ANOVA is more appropriate and less error prone than running multiple t-tests as there are more than two samples to compare within this study (Ferreira and Patino, 2015). In the statistical test, the antimicrobial effects of the AgNPs and extracts are compared to the positive control, which is ampicillin and carbendazim respectively.

Table 3.10 and **figures 3.27** and **3.28** below shows the antimicrobial effects and its statistical significance of green synthesized *B. frutescens* neutral pH and pH 10 AgNPs on 7 human pathogenic bacteria (**figure 1 and 2 in Appendix**). All bacterial strains were inhibited in a dose-dependent manner by neutral pH AgNPs with the zone of inhibition decreasing in direct proportion to the NP concentration. The negative control, MHB, had no zones of inhibition, across all the 7 bacterial strains ruling out the possibility of the growth medium playing a role in the antimicrobial activity.

From the data collated in figure 3.27 and 3.28 it is evident amongst the 7 bacterial strains that ampicillin was the most effective at inhibiting the growth of *S. pyogenes* (neutral pH: 10 ± 2.08

($p < 0.0001$), pH 10: 6 ± 0.52 ($p < 0.0001$)) and showed no inhibitory effects against *S. epidermidis*, *E. coli*, *K. pneumoniae* and *P. aeruginosa* for both neutral pH and pH 10 AgNPs. The possible reason for ampicillin displaying no inhibitory effects against these bacterial strains could be due to ampicillin being resistant to the bacterial strains or the ampicillin used had lost activity after repeated freeze-thawing. *E. coli* could potentially have an ampicillin resistant gene encoded in its genome, thus the use of ampicillin had no inhibitory effect on the growth of *E. coli*. It is possible that a higher concentration of ampicillin can be used to inhibit the bacterial strains; however, this can only be validated by performing further experiments.

For Gram- positive bacteria neutral pH AgNPs seemed to be more effective at inhibiting the growth of *S. aureus* with the largest zone of inhibition at 0.6 mg/ml ($5 \text{ mm} \pm 0.29$) ($p = 0.05$) and less effective at inhibiting the growth of *MRSA* with the largest zone of inhibition at 0.6 mg/ml ($2.5 \text{ mm} \pm 0.25$) ($p < 0.0001$). For Gram-negative bacteria neutral H AgNPs seemed to be more effective at inhibiting the growth of *P. aeruginosa* with the largest zone of inhibition at 0.6 mg/ml ($3.75 \text{ mm} \pm 0.38$) ($p < 0.0001$) and least effective at inhibiting *E. coli* with the largest zone of inhibition at 0.6 mg/ml ($3.5 \text{ mm} \pm 0.50$) ($p < 0.0001$).

From the results in figure 3.27 it is evident that ampicillin and 0.6 mg/ml neutral pH AgNPs possesses the same inhibitory effects against the growth of *MRSA* with a zone of inhibition ($2.5 \text{ mm} \pm 0.25$) ($p < 0.0001$).

For Gram- positive bacteria pH 10 AgNPs seemed to be more effective at inhibiting the growth of *S. aureus* ($4.75 \text{ mm} \pm 0.38$) ($p = 0.1272$) and *S. epidermidis* ($5 \text{ mm} \pm 0.58$) ($p < 0.0001$) with the largest zone of inhibition at 0.6 mg/ml and least effective at inhibiting the growth of *MRSA* with the largest zone of inhibition at 0.6 mg/ml ($2.5 \text{ mm} \pm 0.25$) ($p < 0.0001$). For Gram-negative bacteria pH 10 AgNPs seemed to be more effective at inhibiting *K. pneumoniae* in a dose dependent manner with the largest zone of inhibition at 0.6 mg/ml (4.75 ± 0.52) ($p < 0.0001$) and least effective at inhibiting *E. coli* with the largest zone of inhibition at 0.6 mg/ml ($4 \text{ mm} \pm 0.25$) ($p < 0.0001$).

It is evident from both figure 3.27 and 3.28 that although the concentrations of neutral pH and pH 10 AgNPs differ, they still possess the same inhibitory effects against *MRSA* with a zone of inhibition of $2.5 \text{ mm} \pm 0.25$ ($p < 0.0001$). *E.coli* and *MRSA* displayed no inhibitory effects at the lower concentrations 0.075 mg/ml and 0.0375 mg/ml of both neutral pH and pH 10 AgNPs.

The findings in this study with in classifying antibacterial activity against Gram-positive and Gram-negative microorganisms is in alignment with studies conducted by Rahman and colleagues in that Gram-positive bacteria is more susceptible to both neutral pH and pH 10 AgNPs than the Gram-negative bacteria (Rahman *et al.*, 2011). This is due to the fact that Gram-negative bacteria possess an outer membrane consisting of lipopolysaccharides which acts as a barrier for antimicrobial agents thus making it difficult for the AgNPs to penetrate the outer membrane (Delcour, 2010; Fair and Tor, 2014; Silhavy *et al.*, 2010). *P. aeruginosa* and *K. pneumoniae* is regarded as highly resistant microorganisms which is associated with community and hospital-acquired infections in immunocompromised individuals (Urizar *et al.*, 2015). However, both neutral pH and pH 10 AgNPs are able to penetrate the lipopolysaccharides outer membrane in comparison to other studies where the outer membrane is impermeable to most antibacterial compounds (Madikizela *et al.*, 2013).

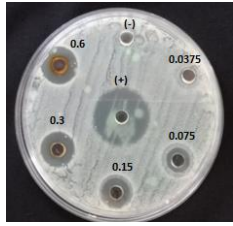
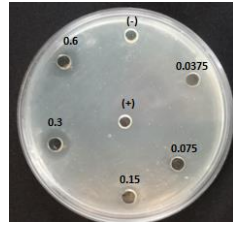
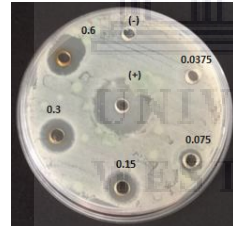
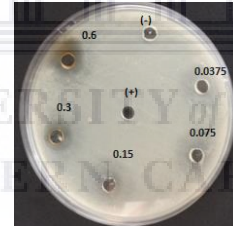
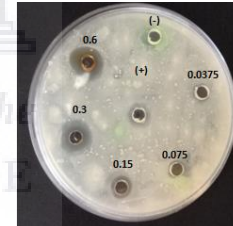
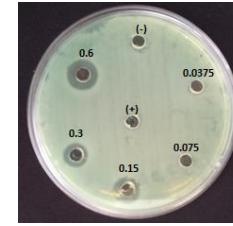
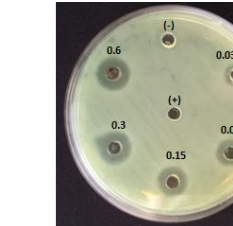
Both neutral pH and pH 10 AgNPs displayed significant antimicrobial effects against Gram-positive microorganisms *S. aureus* and *S. epidermidis*. This could be due to the fact that both bacterial strains are from the same genus and is therefore able to target a common structure or section within the organisms, hence producing almost the same concentration of inhibition of growth. This result is rather significant as Gram-positive bacteria possess a thick peptidoglycan layer to penetrate in comparison to Gram-negative bacteria (Snega *et al.*, 2015).

According to previous literature has shown that the mechanism of action of AgNPs against *E. coli* is to alter the membrane permeability and respiration (Salunke *et al.*, 2014; Manjumeena *et al.*, 2014). This is in agreement with the antibacterial activity posed by the AgNPs produced in this study. The accumulation of AgNPs on the membrane cell resulted in gaps in the integrity of the bilayer which predisposes it to a permeability increase and then bacterial cell death (Rai *et al.*, 2014)). The mechanism of action of AgNPs against *K. pneumoniae* is to alter

the membrane (Majumeena *et al.*, 2014; Naraginti *et al.*, 2014; Tamayo *et al.*, 2014). The mechanism of action of AgNPs against *P. aeruginosa* is irreversible damage to the bacteria cells by altering the membrane permeability and respiration (Biel *et al.*, 2011; Majumeena *et al.*, 2014). The mechanism of action of AgNPs against *S. aureus* is the irreversible damage to the bacterial cells. The mechanism of action of AgNPs against *S. epidermidis* is the damage of the cytoplasm's membrane and modifications of intracellular ATP levels (Shrivastava *et al.*, 2009; Jain *et al.*, 2009). Previous research further showed that the inhibitory mechanism of action of Ag⁺ ions on microorganisms is inhibition of replication, which results in the reduction of ribosomal proteins, cellular proteins and enzymes essential to adenosine triphosphate (ATP) production (Feng *et al.*, 2000). On the other hand, the Ag⁺ ions could affect the function of the enzymes/proteins bound to the membrane (Bragg and Rainnie, 1974; McDonell and Russel, 1999).



Table 3.10: The antimicrobial effects of green synthesized *B. frutescens* AgNPs against seven human pathogenic bacteria. (n=3). STDEV – standard deviation

	Zone of inhibition (mm) ± STDEV						
	<i>S. aureus</i>	<i>S. epidermidis</i>	<i>S. pyogenes</i>	<i>E. coli</i>	<i>K. pneumoniae</i>	<i>MRSA</i>	<i>P.aeruginosa</i>
	Neutral pH (7.11) AgNPs (mg/ml)						
Ampicillin (+)	9 ± 2.08	0 ± 0	10 ± 2.08	0 ± 0	0 ± 0	0 ± 0	0 ± 0
MHB growth medium (-)	0 ± 0.38	0 ± 0	0 ± 0	0 ± 0	0 ± 0	0 ± 0	0 ± 0
0.6	5 ± 0.29	3 ± 0.66	3.25 ± 43	3.5 ± 0.50	5 ± 1.42	2.5 ± 0.25	3.75 ± 0.38
0.3	4 ± 0.25	3.25 ± 0.50	4 ± 0.38	3 ± 0.50	3.75 ± 0.88	1.25 ± 0.38	3 ± 0.41
0.15	2.75 ± 0.25	1.5 ± 0.50	3 ± 0.43	0 ± 0.87	1.75 ± 0.52	1 ± 1.11	2.5 ± 0.48
0.075	2.25 ± 0.29	0.5 ± 0.29	2 ± 0.25	0 ± 0	0.5 ± 0.50	0 ± 0	2 ± 0.29
0.0375	0.5 ± 0	0 ± 0	0.5 ± 0.25	0 ± 0	0 ± 0.29	0 ± 0	1 ± 0.29
Tested Plates							

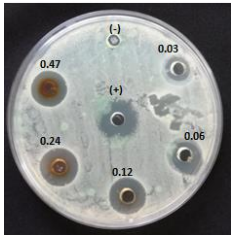
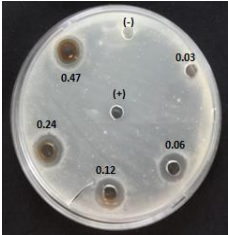
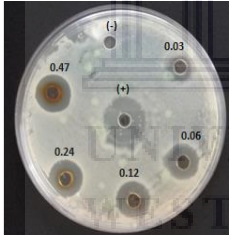
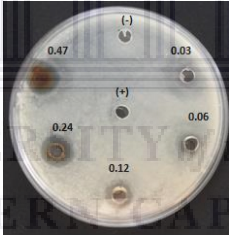
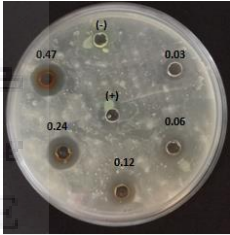
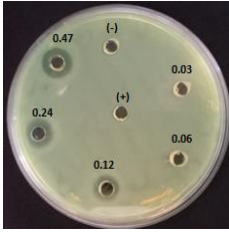
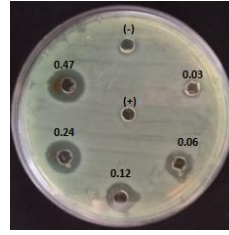
	Zone of inhibition (mm) ± STDEV						
	<i>S. aureus</i>	<i>S. epidermidis</i>	<i>S. pyogenes</i>	<i>E. coli</i>	<i>K. pneumoniae</i>	MRSA	<i>P.aeruginosa</i>
	pH 10 AgNPs (mg/ml)						
Ampicillin (+)	5.5 ± 1.04	0 ± 0	6 ± 0.52	0 ± 0	0 ± 0	0 ± 0	0 ± 0
MHB growth medium (-)	0 ± 0	0 ± 0	0 ± 0.0	0 ± 0	0 ± 0	0 ± 0	0 ± 0
0.47	4.75 ± 0.38	5 ± 0.58	4 ± 0.58	4 ± 0.25	4.75 ± 0.52	2.5 ± 0.25	4 ± 0.58
0.24	4.5 ± 0.29	3.25 ± 0.14	4 ± 0.58	3.25 ± 0.72	4 ± 0.58	1.25 ± 0.14	3.5 ± 0.25
0.12	4.25 ± 0.25	3 ± 0.25	4 ± 0.66	1.5 ± 0.87	3 ± 0.58	0.75 ± 0.14	2 ± 0.14
0.06	3 ± 0.38	3 ± 0.80	4 ± 0.87	0 ± 0	2.75 ± 0.88	0 ± 0	1.5 ± 0.29
0.03	3 ± 1.04	0 ± 0	2.5 ± 1.26	0 ± 0	1.75 ± 0.63	0 ± 0	0.5 ± 0
Tested Plates							

Figure 3.27: Comparative analysis of 0.1 mg/ml ampicillin, 0.6 mg/ml, 0.3 mg/ml, 0.15 mg/ml, 0.075 mg/ml, 0.0375 mg/ml neutral pH AgNPs to 7 human pathogenic bacteria after 24 hours of incubation at 37 °C. The data is expressed in mean \pm SD (n=3).

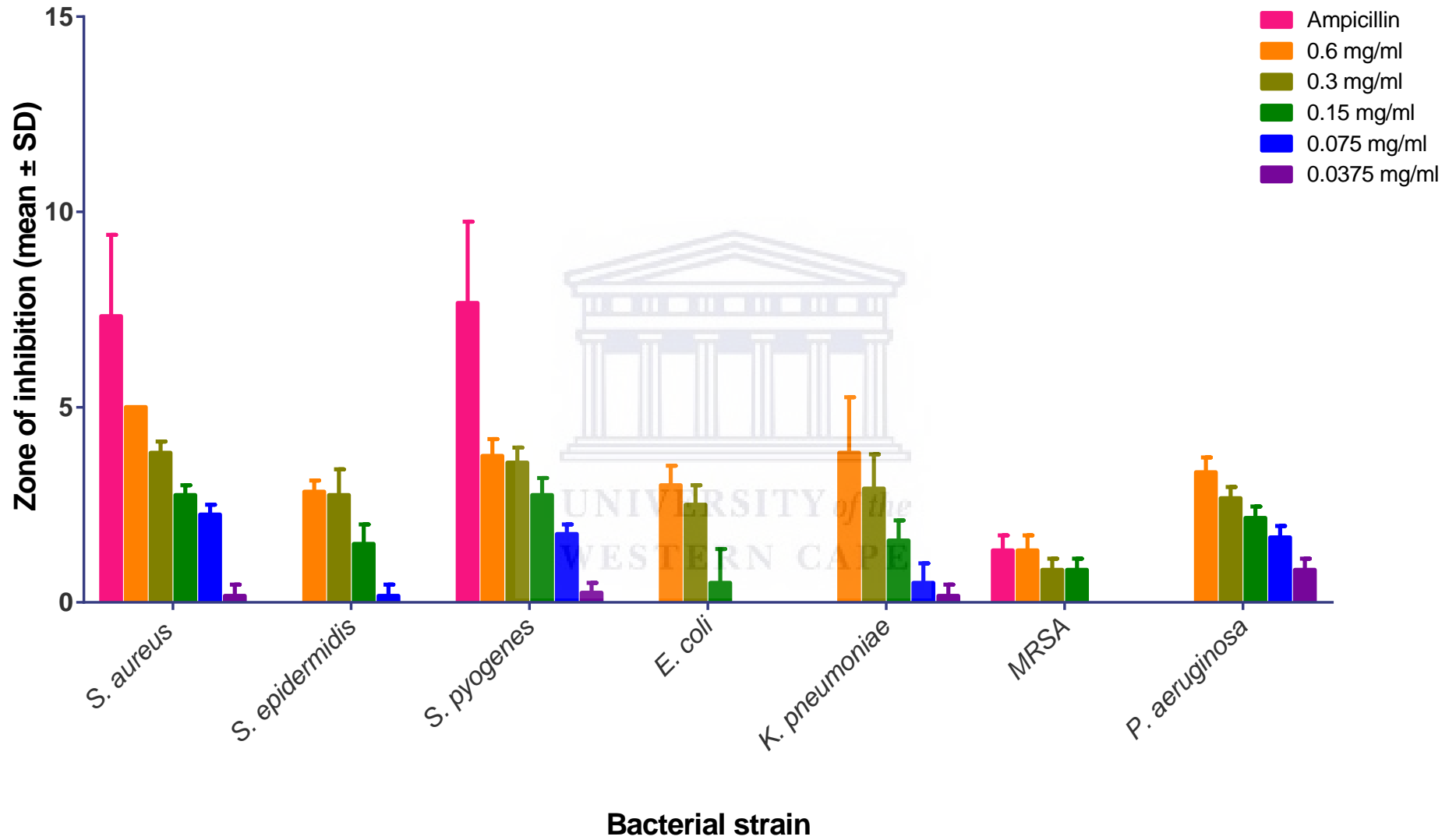


Figure 3.28: Comparative analysis of 0.1 mg/ml ampicillin, 0.47 mg/ml, 0.24 mg/ml, 0.12 mg/ml, 0.06 mg/ml, 0.03 mg/ml pH 10 AgNPs to 7 human pathogenic bacteria after 24 hours of incubation at 37 °C. The data is expressed in mean \pm SD (n=3).

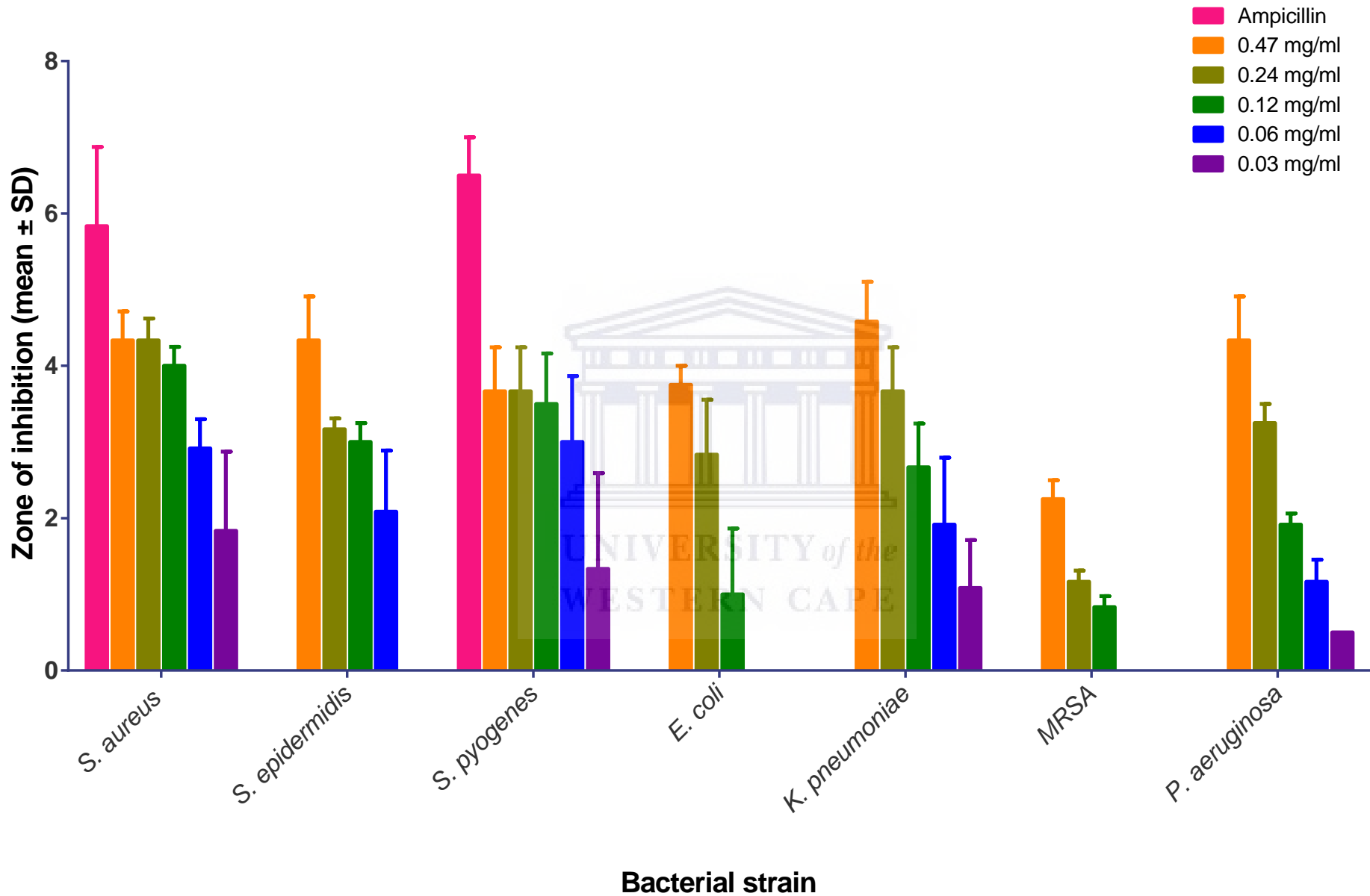


Table 3.11 and **figure 3.29** and **3.30** below shows the antifungal effects of *B. frutescens* green synthesized AgNPs against 4 *Fusarium* fungal strains (*F. culmorum*, *F. oxysporum*, *F. proliferatum*, *F. verticilloides*) (**figure 3 and 4 in Appendix**). All concentrations of neutral pH AgNPs significantly inhibited the growth of *F. culmorum* except at 0.075 mg/ml of NPs. All concentrations of pH 10 AgNPs significantly inhibited the growth of *F. culmorum* except at 0.06 mg/ml.

From the results in figure 3.29 and 3.30 it is evident that the positive control, carbendazim, displayed significant inhibitory effects across all fungal strains. Another control was included as carbendazim was made up with 99% Ethanol. From the data obtained it is evident that ethanol exhibited inhibitory effects, which is expected as ethanol is known to kill microorganisms and contaminants.

The zones of inhibition decreased in proportion to the higher concentrations of AgNPs and then increased in the lower concentrations of AgNPs for fungal strain *F. culmorum*. Neutral pH AgNPs had the largest zone of inhibition at 0.6 mg/ml (6 mm \pm 0.29) ($p < 0.0001$). pH 10 AgNPs had the largest zone of inhibition at 0.47 mg/ml (3 mm \pm 1.73) ($p < 0.0001$).

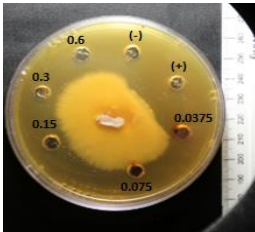
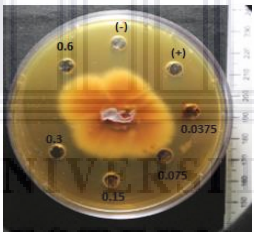
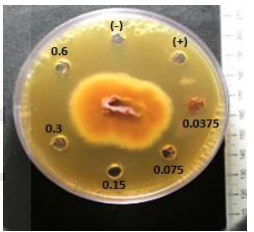
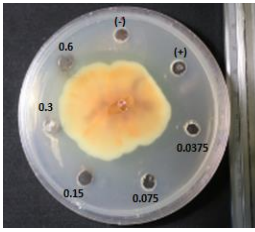
All concentrations of neutral pH AgNPs significantly inhibited the growth of *F. oxysporum* except at 0.075 mg/ml. Neutral pH AgNPs had the largest zone of inhibition at 0.15 mg/ml (4.5 mm \pm 0) ($p = 0.0363$). This observation does not make any logical sense as the inhibitory effects of the NPs should correlate with the concentration. The increase in inhibitory effects displayed from 0.66 mg/ml to 0.15 mg/ml could be attributed to the manner in which the fungus grows within the agar. It is evident that the growth pattern of the fungi is not consistent and not in a particular shape. pH 10 AgNPs had the largest zone of inhibition at 0.47 mg/ml (9.75 mm \pm 3.90) ($p = 0.2706$). Once again the observed zone of inhibition does not correlate with the concentration of the NPs.

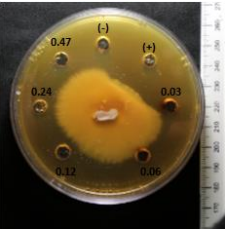
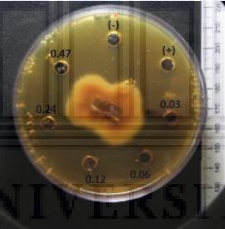
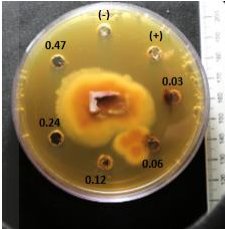
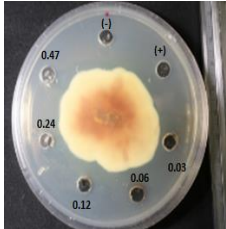
All concentrations of neutral pH AgNPs significantly inhibited the growth of *F. proliferatum* with the largest zone of inhibition at 0.15 mg/ml (8 mm \pm 2) (p = 0.6926). All concentrations of pH 10 AgNPs significantly inhibited the growth of *F. proliferatum* except at 0.06 mg/ml of NPs. Finally, the susceptibility of *F. verticilloides* against green synthesized AgNPs was also studied. All concentrations of neutral pH AgNPs significantly inhibited the growth of *F. verticilloides* with the largest zone of inhibition at 0.6 mg/ml (7 mm \pm 0.76) (p = 0.9992). All concentrations of pH 10 AgNPs significantly inhibited the growth of *F. verticilloides* with the largest zone of inhibition at 0.24 mg/ml (11.5 mm \pm 4.07) (p > 0.9999).

From the antifungal activity data it is evident that pH 10 AgNPs displayed higher inhibitory effects against *F. oxysporum* and *F. verticilloides*, whereas neutral pH AgNPs displayed higher inhibitory effects against *F. culmorum* and *F. proliferatum*. The inhibition of the fungi by the AgNPs can possibly be due to the high density at which the solution of AgNPs were able to saturate and cohere to the fungal hyphae. The results tabulated for the antifungal study is in alignment with previous published research (Park *et al.*, 2006; Kim *et al.*, 2006; Min *et al.*, 2009; and Kabir *et al.*, 2011). This finding is extremely significant as it clearly validates the antifungal nature of *B. frutescens* leaf extract synthesized AgNPs, since the water based extract mimics the plants use traditionally.

UNIVERSITY of the
WESTERN CAPE

Table 3.11: The antifungal effects of green synthesized *B. frutescens* AgNPs against four *Fusarium* fungal strains. (n=3) STDEV – standard deviation

	Zone of inhibition (mm)			
	<i>F. culmorum</i>	<i>F. oxysporum</i>	<i>F. proliferatum</i>	<i>F. verticilloides</i>
	Neutral pH (7.11) AgNPs (mg/ml)			
Carbendazim (+)	12.25 ± 0.52	9 ± 1.15	7.25 ± 0.52	7 ± 0.76
Ethanol (-)	8 ± 0.58	8.5 ± 2.60	8.25 ± 1.56	9 ± 1
0.6	6 ± 0.29	3 ± 0	7 ± 0.50	7 ± 0.58
0.3	2 ± 0.76	4 ± 0.58	4.5 ± 0.29	4.75 ± 0.95
0.15	2 ± 1.53	4.5 ± 0	8 ± 2	6.5 ± 1.89
0.075	0 ± 0	0 ± 1.44	3 ± 0.58	7 ± 2.47
0.0375	3 ± 1.04	3 ± 1.15	3 ± 1	2 ± 0.76
Test plates				

	Zone of inhibition (mm)			
	<i>F. culmorum</i>	<i>F. oxysporum</i>	<i>F. proliferatum</i>	<i>F. verticilloides</i>
	pH 10 AgNPs (mg/ml)			
Carbendazim (+)	13 ± 0.43	14.5 ± 3.18	11 ± 1	7.5 ± 1.32
Ethanol (-)	7 ± 0.58	14.25 ± 3.32	12.25 ± 0.66	7.25 ± 0.66
0.47	3 ± 1.73	9.75 ± 3.90	4.25 ± 0.52	7 ± 1
0.24	2 ± 0.87	7.75 ± 2.17	0.5 ± 1.32	11.5 ± 4.07
0.12	1.5 ± 1.32	8.5 ± 2.47	2 ± 0.87	5.25 ± 0.66
0.06	0 ± 0	5 ± 2.57	0 ± 2.83	2 ± 0.58
0.03	0.5 ± 1.32	6 ± 1.89	4 ± 1	1 ± 0.29
Test Plates				

UNIVERSITY of the
WESTERN CAPE

Figure 3.29: Comparative analysis of the antifungal effects of 0.1 g/l carbendazim, 99 % ethanol, 0.6 mg/ml, 0.3 mg/ml, 0.15 mg/ml, 0.075 mg/ml, 0.0375 mg/ml pH 10 AgNPs to 4 *Fusarium* fungal strains after 5 days of incubation at 25 °C. The data is expressed in mean \pm SD (n=3).

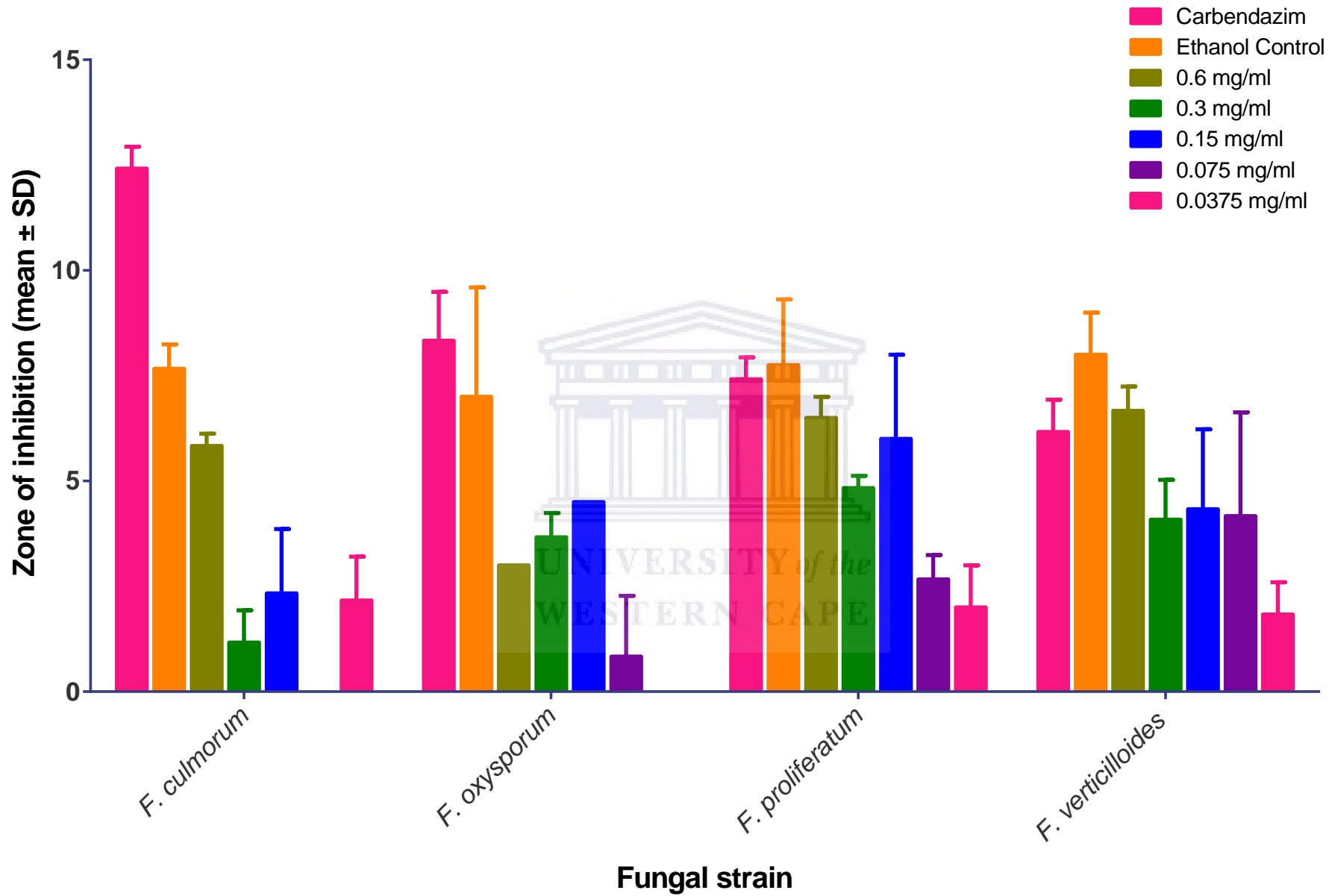
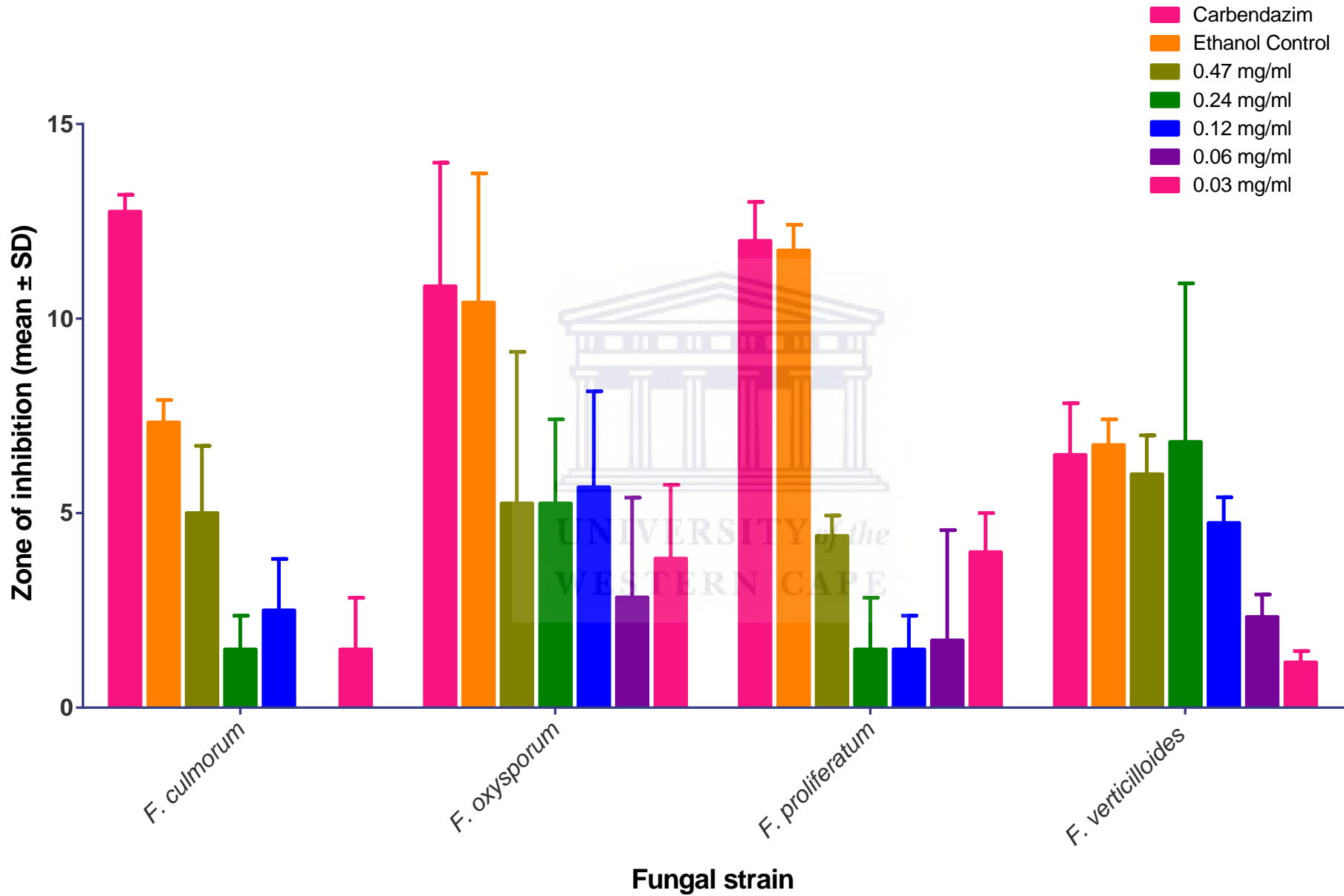


Figure 3.30: Comparative analysis of the antifungal effects of 0.1 g/l carbendazim, 99 % ethanol, 0.47 mg/ml, 0.24 mg/ml, 0.12 mg/ml, 0.06 mg/ml, 0.03 mg/ml pH 10 AgNPs to 4 *Fusarium* fungal strains after 5 days of incubation at 25 °C. The data is expressed in mean \pm SD (n=3).



Antimicrobial analysis of *B. frutescens* leaf extract

The *B. frutescens* leaf extract on its own displayed no inhibitory effects against the selected bacterial and fungal strains (**Table 1 and 2 of Appendix**). This could potentially be attributed to the chemical nature of the plant material in the presence of AgNO₃. In the presence of AgNO₃, the phytochemical activity is enhanced or certain molecules found within the plant material, known to exhibit antimicrobial effects is drastically enhanced. It is possible that a higher concentration of *B. frutescens* leaf extract can inhibit the growth of bacterial strains tested in this study. This can only be validated by conducting further experiments. This thinking is corroborated by published research (Ncube *et al.*, 2008).

Future studies using the extract on its own could possibly include using fresh *B. frutescens* leaf extract as opposed to the freeze-dried leaf extract. A previous study conducted showed that the use of fresh plant extract exhibited better antimicrobial properties than the freeze-dried extracts (Junaid *et al.*, 2006). More phytochemicals were present within the fresh plant extract whereas traces of phytochemicals were only found within the freeze-dried extract.

Deionized H₂O has been used as the extraction solvent within this study. It is also possible that antimicrobial activity can be achieved by using a different extraction solvent such as methanol or chloroform. Methanol is a polar solvent which is used to extract polar chemical compounds and chloroform is a non-polar solvent used to extract non-polar compounds (Ncube *et al.*, 2008). Water is regarded as a polar solvent. According to previous literature most antimicrobial active components that have been identified are reported to be insoluble in water (Cowan, 1999; Nang *et al.*, 2007; Yamaji *et al.*, 2005). This could potentially explain why the water based extract used within this study exhibited no antimicrobial activity on its own.

In conclusion, although pH 10 AgNPs (0.47 mg/ml) are lower in concentration compared to neutral pH AgNPs (0.6 mg/ml), they seemed to be more effective at inhibiting the various bacterial and fungal strains. This could probably be due to their smaller size in comparison to neutral pH AgNPs. It can be concluded from this study that the different bacterial strains respond differently to the AgNPs. This finding is in alignment with previous research conducted (Chwalibog *et al.*, 2010; Ncube *et al.*, 2012). The exact mechanism of action can be investigated in further studies; however one can speculate that the small core size of the AgNPs produced compared to the size of the bacterial strains enables the AgNPs to exert bacterial cell death by adhering to its cell wall (Chwalibog *et al.*, 2010). A possible mechanism for the AgNPs antibacterial activity would be that they are able to penetrate the cell wall of the bacterium and induce bacterial cell death by affecting the respiratory mechanisms and cell division process by the binding of protein thiols or phosphorus in nucleic acids (Rai *et al.*, 2009). Both AgNPs

The lack of antimicrobial activity of extracts used within this study could potentially be attributed to the bacteria adopting a mechanism to resist the free phytochemicals within the extract solution in comparison to the AgNPs which are capped with the phytochemicals (Mmola *et al.*, 2016). This study further suggests that the capping phytochemicals might influence the activity of the AgNPs because of the differential response produced by neutral pH and pH 10 AgNPs. Moreover, the higher the concentration of AgNPs the higher the antimicrobial activity against the selected bacterial and fungal strains in this study.

Chapter 4: Conclusion

The results obtained in this study have proven the hypothesis that *B. frutescens* leaf gel sap extract is capable of forming AgNPs with potent antimicrobial activities. The aim and objectives of this study were successfully achieved, since AgNPs were successfully synthesized and characterized; and their antimicrobial activity tested.

The optimum conditions for synthesis of neutral pH (7.11) AgNPs are 25 mg/ml extract, 1 mM AgNO₃ over a period of 30 minutes in direct sunlight, and for pH 10 AgNPs are 25 mg/ml extract, 2 mM AgNO₃ over a period of 45 minutes. The neutral pH AgNPs displayed a single λ_{max} absorbance peak at approximately 410 nm \pm 0.499 after synthesis which shifted to 415 nm \pm 1.178 after final centrifugation step. The hydrodynamic size shifted from 89.02 d.nm, Pdl 0.236, and ZP -18.3 mV before synthesis to 180.4 d.nm, Pdl 0.389, and ZP -22.3 mV after synthesis. The pH 10 AgNPs displayed a single λ_{max} absorbance peak at approximately 408 nm \pm 0.891 after synthesis which shifted to 415 nm \pm 1.178 after final centrifugation step. The hydrodynamic size shifted from 101.3 d.nm, Pdl 0.274, ZP -20.6 mV before synthesis to 279.7 d.nm, Pdl 0.561 and ZP -25.4 mV after synthesis.

HR-TEM analysis confirms that the AgNP suspensions within this study are comprised of an array of different shapes which include oval, spherical, triangular, irregular and even rod shaped particles. The average core diameter of each particle is between 0.9 nm and 2 nm respectively. FTIR analysis confirms that the presence of flavonoids, amine groups, polyphenols and proteins are responsible for reducing the AgNO₃ to form AgNPs. The FTIR spectra obtained showed similarities between the extracts and AgNPs with some variation in the peak shifts positions, which clearly indicate that the phytochemicals are responsible for the capping the AgNPs.

TPC analysis combined with the DLS data confirms the antimicrobial effects observed with AgNPs. The TPC analysis confirmed that an ionic charge on the pH 10 AgNPs enhanced the activity of polyphenols; thus influencing the amount of phenols present within the AgNPs, providing a greater antimicrobial effect. Neutral pH AgNPs had 49.65 \pm 0.02125 TPC content in comparison to 243.003 \pm 0.01175 for pH 10 AgNPs. The ZP decreased during the purification

process which aided in the agar well-diffusion studies as the more negative the ZP, the more potent the AgNPs were against bacterial cell walls.

The different microorganisms within this study conferred significantly different effects when the different AgNPs were applied. Although the concentration of pH 10 AgNPs are lower than that of neutral pH AgNPs, pH 10 AgNPs displayed a higher antimicrobial activity than neutral pH AgNPs. Both AgNPs displayed the highest activity against *S. aureus* and *F. oxysporum*, and the lowest activity against *E. coli* and *F. culmorum*. This can potentially be attributed to the difference in the microbial membrane structures and compositions in the cell wall of microorganisms.

4.1. Limitations of the study

Attempts were made to determine the minimum inhibitory concentrations (MIC) of the extract and the AgNPs. However, the quenching effects of the AgNPs on fluorescence and absorbance of Alamar Blue rendered this exercise unsuccessful. Although a colour change was observed from rezofurin blue to pink, the growth curve over a period of 4 hours could not be constructed. The absorbance and fluorescence of AgNPs control (AgNPs + growth media) were higher than that of the experimental sample (AgNPs + growth media + bacteria). The AgNPs stability within MHB media was monitored by measuring absorbance over time. The absorbance decreased over a period of 24 hours. A possible reason for this could be that the AgNPs are aggregating within MHB suspension, which reduced the inhibitory effects of AgNPs.

4.2. Future prospects

Future work to expand on this study must include:

- I. Development of a method to stabilize the AgNPs produced.
- II. Examination of the influence of size on the uptake of AgNPs by the respective microorganisms.
- III. A time and dose dependent antimicrobial study based on optical density measurements in order to circumvent the interference challenges posed by AgNPs.

- IV. Investigation of some mechanisms of action such as ROS production, membrane integrity disturbances, etc., in order to validate the growth inhibition activity of the AgNPs.
- V. A higher concentration of extract of more than 50 mg/ml can potentially be used to acquire antimicrobial activity for the extract alone.
- VI. The extract could be prepared with ethanol, acetate, methanol or chloroform instead of using deionized H₂O, to stabilize the phytochemicals within the solution, thus producing more potent antimicrobial activity.
- VII. Investigate the effect of AgNPs on wound lymphocyte infiltration and its effects on re-epithelialization of wounds.
- VIII. Investigate the effect the capping phytochemicals have on AgNPs antimicrobial activity.
- IX. HPLC analysis of AgNPs and *B. frutescens* extract to determine which phytochemicals are responsible for antimicrobial activity. These phytochemicals can be isolated and used for antimicrobial applications.



References

- Acar U, Kesbic O.S, Yilmaz S, Gultepe N, Turker A (2015) 'Evaluation of the effects of essential oil extracted from sweet orange peel (*Citrus sinensis*) on growth rate of tilapia (*Oreochromis mossambicus*) and possible disease resistance against *Streptococcus iniae*', *Aquaculture*, 437, pp. 282-286
- Akhtar M.S, Panwar, J, Yun Y.S ('2013) Biogenic synthesis of metallic nanoparticles by plant extracts', *ACS Sustainable Chem. Eng*, 1, pp. 591-602
- Ambiga S, Narayanan R, Durga G, Sukumar D, Madhavan S (2007) 'Evaluation of wound healing activity of flavonoids from *Ipomoea carnea Jacq.*', *Ancient Science of Life*, XXXVI (3)
- Ambiga S, Narayanan R, Gowri D, Sukumar D, Madhavan S (2007) 'Evaluation of wound healing activity of flavonoids from *Ipomoea carnea Jacq.*', *Ancient Science of Life*, 26(3), pp. 45-51
- Anderson C.W.N, Brooks R.R, Stewart R.B, Simcock R (1998) 'Harvesting a crop of gold in plants', *Nature*, pp. 553-554
- Anh-Tuan L, Thanh Huy P, Thi Tam L, Dinh Tam P (2011) 'Novel silver nanoparticles: Synthesis, properties and applications', *International Journal of Nanotechnology*, 3/4/5
- Ansari MA, Khan HM, Khan AA, Cameotra SS, Saquib Q, Musarrat J (2014) 'Gum arabic capped-silver nanoparticles inhibit biofilm formation by multi-drug resistant strains of *Pseudomonas aeruginosa*', *Journal of Basic Microbiology*, 54, pp. 688-99
- AshaRani P.V, Low Kah Mun G, Hande MP, Valiyaveetil S (2009) 'Cytotoxicity and genotoxicity of silver nanoparticles in human cells', *Department of Chemistry, Faculty of Science, National University of Singapore, Singapore 117543, Singapore 117597* [Online]. Available at: <https://www.ncbi.nlm.nih.gov/pubmed/19236062> (Accessed: 20 August 2019)
- Aslam M, Ahmad M, Riaz M, Raza S.A, Hussain S, Qureshi O.S, Maria P, Hamzah Z, Javed O (2018) 'Role of Flavonoids as Wound Healing Agent: Chapter 6' [Online]. Available at: <https://www.intechopen.com/books/phytochemicals-source-of-antioxidants-and-role-in-disease-prevention/role-of-flavonoids-as-wound-healing-agent> (Accessed: 20 August 2019)

- Azuma K, Izumi R, Osaki T, Ifuku S, Morimoto M, Saimoto H, Minami , Okamoto Y (2015) 'Chitin, chitosan, and its derivatives for wound healing: old and new materials', *Journal of functional biomaterials*, 6(1), pp. 104-142
- Baek Y.W, An Y.J (2011) 'Microbial toxicity of metal oxide nanoparticles (CuO, NiO, ZnO, and Sb2O3) to Escherichia coli, Bacillus subtilis, and Streptococcus aureus', *Science of the Total Environment*, 409, pp. 1603-1608
- Banoee M, Seif S, Nazari Z.E (2010) 'ZnO nanoparticles enhanced antibacterial activity of ciprofloxacin against *Staphylococcus aureus* and *Escherichia coli*', *Journal of Biomedical Material Res Part B: Appl Biomater*, 93, pp. 557-61
- Banoee M, Seif S, Nazari Z.E (2010) 'ZnO nanoparticles enhanced antibacterial activity of ciprofloxacin against *Staphylococcus aureus* and *Escherichia coli*', *Journal of Biomedical Material Res Part B: Application Biomaterials*, 93, pp. 557-61
- Barbosa J.A, Zoppi A, Quevedo M.A, de Melo P.N, de Medeiros A.S, Streck L (2014) 'Triethanolamine stabilization of methotrexate-b-cyclodextrin interactions in ternary complexes', *Int J Mol Sci*, 15, pp. 17077-17099
- Barnett T.C, Patel A.R, Scott J (2004) 'A novel sortase, SrC2, from *Streptococcus pyogenes* anchors a surface protein containing a QVPTGV motif to the cell wall', *J. Bacteriol*, 186, pp. 5865-75
- Basavaraja S, Balaji S.D, Lagashetty A, Rajasab A.H, Abbaraju V (2008) 'Extracellular biosynthesis of silver nanoparticles using the fungus *Fusarium semitectum*' [Online]. Available at: [https://www.researchgate.net/publication/222334237 Extracellular biosynthesis of silver nanoparticles using the fungus Fusarium semitectum/stats](https://www.researchgate.net/publication/222334237_Extracellular_biosynthesis_of_silver_nanoparticles_using_the_fungus_Fusarium_semitectum/stats) (Access: 21 August 2019)
- Basavaraja S, Balaji S.D, Lagashetty A, Rajasab A.H, Venkataraman A (2008) 'Extracellular biosynthesis of silver nanoparticles using the fungus *Fusarium semitectum*', *Mater. Res. Bull*, 43, pp. 1164-1170
- Begum F, Uddin K, Sultana S, Ferdous A.H, Begum Z.A (2008) 'Effects of methanol extract of Piper chaba stem bark on chronic inflammation in rats', *Ibrahim Med Coll J*, 2(2), pp. 37-39

- Berciano-Guerrero M.A, Montesa-Pino A, Castaneda-Penalvo G, Flores J.R (2014) 'Nanoparticles in Melanoma', [Online]. Available at: <https://www.researchgate.net/publication/264093769> *Nanoparticles in Melanoma* (Accessed 22 July 2019)
- Biel M.A, Sievert C, Usacheva M, Teichert M, Balcom J (2011) 'Antimicrobial photodynamic therapy treatment of chronic recurrent sinusitis biofilms', *Int. Forum Allergy Rhinol*, 1, pp. 329-334
- Binupriya A.R, Sathishkumar M, Yun S (2010) 'Biocrystallization of silver and gold ions by inactive cell filtrate of *Rhizopus stolonifer*', *Colloid Surfaces. B: Biointerfaces*, 79, pp. 531-534
- Boateng J and Catanzano O (2015) 'Advanced therapeutic dressings for effective wound healing- a review', *Journal of pharmaceutical sciences*, 104(11), pp. 3653-3680
- Bringmann G, Mutanyatta-Comar J, Maksimenka K, Wanjohi J.M, Heydenreoch M, Brun R, Muller W.E.G, Peter M.G, Midiwo J.O, Yenesew A (2008) 'Joziknipholones A and B: The First Dimeric Phenylanthraquinones, from the Roots of *Bulbine frutescens*', *Chem Eur. J*, 14, pp. 1420-1429
- Builders P.F, Alalor C.A, Avbunudiogba J.A, Justice I.E (2015) 'Survey on the pharmaceutical quality of herbal medicines sold in Nigeria', *Journal of Applied Pharmaceutical Science*, 5(06), pp. 097-103
- Buzea, Pacheco I, Robbie K (2007) 'Sources and toxicity', *Nanomaterials and nanoparticles Biointerphases*, 2, pp. 17-71
- Cai Y, Luo M, Corke H (2004) 'Antioxidant activity and phenolic compounds of 112 traditional Chinese medicinal plants associated with anticancer', *Life Sci*, 74, pp. 2157-2184
- Castagnola E, Caviglia I, Pistorio A, Fioredda F, Micalizzi C, Viscoli C (2014) 'Bloodstream infections and invasive mycoses in children undergoing acute leukaemia treatment: a 13-year experience at a single Italian institution', *Eur J Cancer*, 41 (10), pp. 1439-45
- Castagnola E, Cesaro S, Giacchino M, Livadiotti S, Tucci F, Zanazzo G (2006) 'Fungal infections in children with cancer: a prospective, multicenter surveillance study', *Pediatr Infect Dis J*, 25 (7), pp. 634-9

- Chakraborty M, Jain S, Rani V (2011) 'Nanotechnology: emerging tool for diagnostics and therapeutics', *Appl. Biochem. Biotechnol*, 165, pp. 1178 -1187
- Chan Y.S, Don M.M (2013) 'Optimization of process variables for the synthesis of silver nanoparticles by *Pycnoporus sanguineus* using statistical experimental design', *J. Korean Soc. Appl. Bio. Chem*, 56, pp. 11-20
- Chang D.C, Grant G.B, O'Donnell K, Wannemuehler K.A, Noble-Wang J, Rao C.Y, Jacobson L.M, Crowell C.S, Sneed R.S, Lewis F.M (2006) 'Multistate outbreak of *Fusarium* keratitis associated with use of a contact lens solution', *JAMA*, 296, pp. 953-963 [CrossRef] [PubMed]
- Chen Y.S, Hung Y.C, Liao I, Huang G.S (2009) 'Assessment of the *in vivo* toxicity of gold nanoparticles', *Nanoscale Research Letters*, 4 (8), pp. 858-864
- Choi O, Deng K.K, Kim N.J, Ross L, Surampalli R.Y, Hu Z (2008) 'The inhibitory effects of silver nanoparticles, silver ions, and silver chloride colloids on microbial growth', *Water Res*, 42, pp. 3066-74
- Choi O, Deng K.K, Kim N.J, Ross L, Surampalli R.Y, Hu Z (2008) 'The inhibitory effects of silver nanoparticles, silver ions, and silver chloride colloids on microbial growth', *Water Res*, 42, pp. 3066-74
- Christena L.R, Subramaniam S, Vidhyalakshmi M, Mahadevan V, Sivasubramanian A, Nagarajan S (2015) 'Dual role of pinostrobin- a flavonoid nutraceutical as an efflux pump inhibitor and antibiofilm agent to mitigate food borne pathogens', *RSC Adv*, 5, pp. 61881-7
- Coopoosamy R.M (2010) 'Traditional information and antibacterial activity of four *Bulbine* species (Wolf)', *African Journal of Biotechnology*, 10 (2), pp. 220-224
- Das S, Baker A.B (2016) 'Biomaterials and nanotherapeutics for enhancing skin wound healing', *Frontiers in bioengineering and biotechnology*, 4, pp. 82
- De Wet H, Ngubane S.C (2014) 'Traditional herbal remedies used by women in a rural community in northern Maputaland (South Africa) for the treatment of gynaecology and obstetrics complaints', *South African Journal of Botany*, 94, pp. 129-139
- Delcour A.H (2009) 'Outer membrane permeability and antibiotic resistance', *Biochim Biophys Acta*, 1794(5), pp. 808-816

- Dias A.M.A, Braga M.E.M, Seabra I.J, Ferreira P, Gil M.H, De Sousa H.C (2011) 'Development of natural-based wound dressings impregnated with bioactive compounds and using supercritical carbon dioxide', *International journal of pharmaceutics*, 408(1-2), pp. 9-19
- Dibrov P, Dzioba J, Gosink KK, Häse C.C (2002) 'Chemiosmotic mechanism of antimicrobial activity of Ag⁺ in *Vibrio cholerae*', *Antimicrob Agents and Chemother*, 46, pp. 2668-70
- Dibrov P, Dzioba J, Gosink KK, Häse CC (2002) 'Chemiosmotic mechanism of antimicrobial activity of Ag⁺ in *Vibrio cholerae*', *Antimicrob Agents and Chemother*, 46, pp. 2668-70
- Dubey S.P, Lahtinenb M, Sillanpaa M (2010) 'Green synthesis and characterizations of silver and gold nanoparticles using leaf extract of *Rosa rugosa*', *Colloids Surf. A Physicochem. Eng. Aspects*, 364, pp. 34-41
- Dyson A (1998) 'Discovering Indigenous Healing Plants', *National Botanical Institute, Cape Town*
- Eckhardt S, Brunetto P.S, Gagnon J, Priebe M, Giese B, Fromm K.M (2013) 'Nanobio silver: its interactions with peptides and bacteria, and its uses in medicine', *Chemical reviews*, 113(7), pp. 4708-4754
- Encycloaedia-Britannica (2009) 'Antibiotic resistance: Mechanisms antibiotic resistance' [Online]. Available at: <http://www.britannica.com/EBchecked/media/129670/Therearemultiplemechanisms-by-which-bacteria-can-develop-resistance> (Accessed: 20 July 2019)
- Eustis S, El-Sayed MA (2006) 'Why gold nanoparticles are more precious than pretty gold: Noble metal surface plasmon resonance and its enhancement of the radiative and nonradiative properties of nanocrystals of different shapes', *Chemical Society Reviews*, 35, pp. 209-217
- Fennell C.W, Lindsey K.L, McGaw L.J, Sparg S.G, Stafford G.I, Elgorashi E.E, Van Van Staden J (2004) 'Assessing African medicinal plants for efficacy and safety: pharmacological screening and toxicology', *Journal of Ethnopharmacology*, 94 (2-3), pp. 205-217

- Ferreira J, Patino M (2015) 'What does the p value really mean?', *Brazilian Journal of Pulmonology*, 41 (5), pp. 485-485
- Forest S, Forest K (2015) '*Bulbine frutescens* (Stalked bulbine)',. *Plants of Hawaii* [Online]. Available at: <http://www.starrenvironmental.com> (Accessed: 2 June 2019)
- Ghai I (2017) 'Quantifying the Flux of Charged Molecules through Bacterial Membrane Proteins', *Bremen: IRC-Library, Information Resource Center der Jacobs University Bremen*
- Ghai I, Ghai S (2017) 'Exploring bacterial outer membrane barrier to combat bad bugs', *Infect Drug Resist*, 10, pp. 261-273
- Ghosh S, Patil S, Ahire M, Kitture R, Kale S, Pardesi K (2012) 'Synthesis of silver nanoparticles using *Dioscorea bulbifera* tuber extract and evaluation of its synergistic potential in combination with antimicrobial agents', *Int. J. Nanomedicine*, 7, pp. 483-496
- Godoy P, Cano J, Gene J, Guarro J, Hofling-Lima A.L, Lopes Colombo A (2004) 'Genotyping of 44 isolates of *Fusarium solani*, the main agent of fungal keratitis in Brazil', *J. Clin. Microbiol*, 42, pp. 4494-4497
- Goordazi V, Zamani H, Bajuli L, Moradshahi A (2014) 'Evaluation of antioxidant potential and reduction capacity of some plant extracts in silver nanoparticles synthesis', *Department of Biology, Faculty of Sciences, Shiraz University, Shiraz 71454, Iran* [Online]. Available at: <https://www.ncbi.nlm.nih.gov/pmc/articles/PMC5019224/> (Accessed: 5 June 2019)
- Guarro J (2013) 'Fusariosis, a complex infection caused by a high diversity of fungal species refractory to treatment', *Eur. J. Clin. Microbiol. Infect. Dis*, 32, pp. 1491-1500
- Gurunathan S, Han J.W, Kwon D.N, Kim J.H (2014) 'Enhanced antibacterial and anti-biofilm activities of silver nanoparticles against Gram-negative and Gram-positive bacteria', *Nanoscale Res Lett*, 9, pp. 373
- Hais W, Thanh N.T.K, Aveyard J, Fernig G (2007) 'Determination of size and concentration of gold nanoparticles from UV-Vis spectra', *Anal Chem*, 79 (11), pp. 4215-4221

- Hajipour M.J, Fromm K.M, Ashkrran A, De Aberasturi D.J, De Larramendi I.R, Rojo T, Serpooshan V, Parak W.J, Mahmoudi M (2012) 'Antibacterial properties of nanoparticles', *Trends in Biotechnology*, pp. 1-13
- Hale K.A, Shaw P.J, Dalla-Pozza L, MacIntyre C.R, Isaacs D, Sorrell T.C (2010) 'Epidemiology of paediatric invasive fungal infections and a case-control study of risk factors in acute leukaemia or post stem cell transplant', *Br J Haematol*, 149 (2), pp. 263-72
- Handford C.E, Dean M, Henchion M, Spence M, Elliott C.T, Campbell K (2014) 'Implications of nanotechnology for the agri-food industry: Opportunities, benefits and risks', *Trends in Food Science & Technology*, 40(2), pp. 226-241
- Henglein A (1989) 'Small-particle research: physicochemical properties of extremely small colloidal metal and semiconductor particles', *Chemical reviews*, 89(8), pp. 1861-1873
- Hossain M.A, Rahman S.M.M (2011) 'Total phenolics, flavonoids and antioxidant activity of tropical fruit pineapple', *Food Research International, New York*, 44, pp. 672-676
- Huang J.W, Cunnigham S.D (1996) 'Lead phytoextraction: species variation in lead uptake and translocation', *New Phytol.*, 134, pp. 75-84
- Huang X, Jain K, El-Sayed I and El-sayed M (2007) 'Gold nanoparticles: interesting optical properties and recent applications in cancer diagnostics and therapy', *Nanomedicine*, 2 (5), pp. 681-693
- Hussain Z, Thu H.E, Shuid A.N, Katas H, Hussain F (2018) 'Recent advances in polymer-based wound dressings for the treatment of diabetic foot ulcer: an overview of state-of-the-art', *Current drug targets*, 19 (5), pp. 527-550
- Hutchings A, Scott A.H, Lewis G, Cunningham A (1996) 'Zulu Medicinal Plants: An Inventory', *University of Natal Press, Pietermaritzburg*
- Iravani S, Zolfaghari B (2013) 'Green synthesis of silver nanoparticles using *Pinus eldarica* bark extract', *BioMed research international*
- Jabeen H, Kemp K.C, Chandra V (2013) 'Synthesis of nano zerovalent iron nanoparticles–graphene composite for the treatment of lead contaminated water', *Journal of environmental management*, 130, pp. 429-435

- Jain J, Arora S, Rajwade J.M, Omray P, Khandelwal S, Paknikar K.M (2009) 'Silver nanoparticles in therapeutics: Development of an antimicrobial gel formulation for topical use', *Mol. Pharm*, 6, pp. 1388–1401
- Jeevanandam J, Barhoum A, Chan Y.S, Dufresne C, Danquag M.K (2018) 'Review on nanoparticles and nanostructured materials: history, sources, toxicity and regulations', *Beilstein Journal of Nanotechnology*, 9, pp. 1050-1074
- Jha A.K, Prasad K, Prasad K, Kulkarni A.R (2009) 'Plant system: nature's nanofactory', *Colloids Surf. B Biointerphases*, 73, pp. 19-223
- Joffe P (1993) 'The gardener's guide to South African plants', *Table Mountain Publishers, Cape Town*
- Kesharwani P, Jain K and Jain N.K (2014) 'Dendrimer as nanocarrier for drug delivery', *Progress in Polymer Science*, 39(2), pp. 268-307
- Kora A.J, Arunachalam J (2012) 'Green fabrication of silver nanoparticles by Gum Tragacanth (*Astragalus gummifer*): a dual functional reductant and stabilize', *J. Nanomater*, 8
- Kredic, L, Narendran V, Shobana C.S, Vagvolgyi C, Manikandan P (2015) 'Indo-Hungarian Fungal Keratitis Working Group. Filamentous fungal infections of the cornea: A global overview of epidemiology and drug sensitivity', *Mycoses*, 58, pp. 243-260
- Kumar S.A, Lo P.H, Chen S.M, (2008) 'Electrochemical selective determination of ascorbic acid at redox active polymer modified electrode derived from direct blue 71', *Biosensors and Bioelectronics*, 24(4), pp. 518-523
- Kumar V, Yadav S.C, Yadav S.K (2010) 'Syzygium cumini leaf and seed extract mediated biosynthesis of silver nanoparticles and their characterization', *J Chem Technol Biotechnol*, 85, pp. 1301–9
- Labnotesweek4 (2013) 'Modes of action for antimicrobial Agents' [Online]. Available at: <http://lifesci.rutgers.edu/skelly/spring/labnotesweek4.htm> (Accessed : 27 July 2019)
- Lara H.H, Ayala-Nunez N.V, Turrent L.C, Padilla C.R (2010) 'Bactericidal effect of silver nanoparticles against multidrug-resistant bacteria', *World Journal of Microbiology and Biotechnology*, 26, pp. 615-621

- Laxminarayan R, Matsoso P, Pant S, Brower C, Røttingen J.A, Klugman K, Davies S (2016) 'Access to effective antimicrobials: a worldwide challenge', *The Lancet*, 387(10014), pp. 168-175
- Levy S. B, and B. Marshall (2004) 'Antibacterial resistance worldwide: causes, challenges and responses', *Nat. Med*, 10(Suppl.): S122-S129
- Li S, Shen Y, Xie A, Yu X, Qiu L, Zhang L, Zhang Q (2007) 'Green synthesis of silver nanoparticles using *Capsicum annum* L. Extract', *Green Chem*, 9, pp. 852-858
- Li X, Chen S, Hu W, Shi S, Shen W, Zhang X, Wang H, (2009) 'In situ synthesis of CdS nanoparticles on bacterial cellulose nanofibers', *Carbohydrate Polymers*, 76(4), pp. 509-512
- Liow, L. H., Van Valen, L., and Stenseth, N.C (2011) 'Red Queen: from populations to taxa and communities', *Trends Ecol. Evol*, 26, pp. 349-358
- Liu Z, Wu Y, Guo Z, Liu Y, Shen Y, Zhou P, and Lu X (2014) 'Effects of Internalized Gold Nanoparticles with Respect to Cytotoxicity and Invasion Activity in Lung Cancer Cells' [Online]. Available at: <http://journals.plos.org/plosone/article?id=10.1371/journal.pone.0099175> (Accessed: 22 July 2019)
- Luoma S.N (2008) 'Silver nanotechnologies and the environment', *The project on emerging nanotechnologies report*, 15, pp. 12-13
- Manjumeena R, Duraibabu D, Sudha J, Kalaichelvan P.T (2014) 'Biogenic nanosilver incorporated reverse osmosis membrane for antibacterial and antifungal activities against selected pathogenic strains: An enhanced eco-friendly water disinfection approach', *J. Environ. Sci. Health A Toxic Hazard. Subst. Environ. Eng*, 49, pp. 1125-1133
- Marcato P.D, De Paula L.B, Melo P.S, Ferreira I.R, Almeida A.B.A, Torsoni A.S and Alves O.L (2015) 'In vivo evaluation of complex biogenic silver nanoparticle and enoxaparin in wound healing', *Journal of Nanomaterials*, 16(1), p. 91
- Mayer J (2002) 'The role of carotenoids in human health', *Nutr Clin Care*, 5 (2), pp. 56-65
- McGaw L.J, Jäger A.K, Van Staden J (2000) 'Antibacterial, anthelmintic and antiamoebic activity in South African medicinal plants', *Journal of Ethnopharmacology*, 72, pp. 247-263

- Mirunalini S and Krishnaveni M (2011) 'Coumarin: a plant derived polyphenol with wide biomedical applications', *Int J PharmTech Res*, 3(3), pp.1693-1696
- Mittal A.K, Kaler A, Banerjee U.C (2012) 'Free radical scavenging and antioxidant activity of silver nanoparticles synthesized from flower extract of *Rhododendron dauricum*', *Nano BioMed Eng*, 4, pp. 118–24
- Mollick M.M.R, Rana D, Dash S.K, Chattopadhyay S, Bhowmick B, Maity D, Mondal D, Pattanayak S, Roy S, Chakraborty M and Chattopadhyay D (2015) 'Studies on green synthesized silver nanoparticles using *Abelmoschus esculentus* (L.) pulp extract having anticancer (*in vitro*) and antimicrobial applications', *Arabian journal of chemistry*
- Morales-Cardona C.A, Valbuena-Mesa M.C, Alvarado Z, Solorzano-Amador A (2014) 'Non-dermatophyte mould onychomycosis: A clinical and epidemiological study at a dermatology referral centre in Bogota, Colombia', *Mycoses*, 57, pp. 284-293
- Morones-Ramirez J.R, Winkler J.A, Spina C.S, Collins J.J (2013) 'Silver enhances antibiotic activity against gram-negative bacteria', *Sci Transl Med*, 5, pp. 190-81
- Mu H, Tang J, Liu Q, Sun C, Wang T, Duan J, 2015. Potent antibacterial nanoparticles against biofilm and intracellular bacteria. *Scientific reports* 6: 18877–77.
- Mulvaney P (1996) 'Surface plasmon spectroscopy of nanosized metal particles', *Langmuir*, 12(3), pp.788-800
- Murray C.J, Ezzati M, Flaxman A.D, Lim S, Lozano R, Michaud C, Naghavi M, Salomon J.A, Shibuya K, Vos T and Wikler D (2012) 'GBD 2010: design, definitions, and metrics', *The Lancet*, 380(9859), pp.2063-206
- Mutanyatta-Comar J, Bezabih M, Abegaz Nb.m, Dreyer M, Brun R, Kocher N, Bringmann G (2005) 'The first 6'-O-sulfated phenylanthraquinones: isolation from *B. frutescens*, structural elucidation, enantiometric purity, and partial synthesis', *Elsevier Ltd*
- Naraginti S, Sivakumar A (2014) 'Eco-friendly synthesis of silver and gold nanoparticles with enhanced bactericidal activity and study of silver catalyzed reduction of 4-nitrophenol', *Spectrochim. Acta A Mol. Biomol. Spectrosc*, 128, pp. 357-362
- Ngiam M, Nguyen L.T, Liao S, Chan C.K and Ramakrishna S (2011) 'Biomimetic nanostructured materials - potential regulators for osteogenesis?',
- Nikaido, H (2009) 'Multidrug resistance in bacterial', *Annu Rev Biochem*, 78, pp. 119-146

- Nucci M, Anaissie E (2007) 'Fusarium infections in immunocompromised patients', *Clin. Microbiol. Rev*, 20, pp. 695-704 [CrossRef] [PubMed]
- Nucci M, Anaissie E.J, Queiroz-Telles F, Martins C.A, Trabasso P, Solza C (2003) 'Outcome predictors of 84 patients with hematologic malignancies and Fusarium infection', *Cancer*, 98 (2), pp. 315-9
- Nucci M, Garnica M, Gloria A.B, Lehugeur D.S, Dias V.C, Palma L.C (2013) 'Invasive fungal diseases in haematopoietic cell transplant recipients and in patients with acute myeloid leukaemia or myelodysplasia in Brazil', *Clin Microbiol Infect*, 19 (8), pp. 745-51
- Nucci M, Marr K.A, Vehreschild M.J, de Souza C.A, Velasco E (2014) 'Improvement in the outcome of invasive fusariosis in the last decade', *Clin Microbiol Infect*, 20, pp. 580-585
- Padwal P, Bandyopadhyaya R, Mehra S (2014) 'Polyacrylic acid-coated iron oxide nanoparticles for targeting drug resistance in mycobacteria', *Langmuir*, 30, pp. 15266-76
- Padwal P, Bandyopadhyaya R, Mehra S (2015) Biocompatible citric acid-coated iron oxide nanoparticles to enhance the activity of first-line anti-TB drugs in *Mycobacterium smegmatis*', *Journal of Chemical Technology and Biotechnology*, 90, pp. 1773-81
- Pages J.M, James C.E, Winterhalter M (2015) 'The porin and the permeating antibiotic: a selective diffusion barrier in Gram-negative bacteria', *Nat Rev Microbiol*, 6(12), pp. 893-903
- Pandey K.B, Rizvi S.I (2009) 'Plant polyphenols as dietary antioxidants in human health and disease', *Oxidative Medicine and Cellular Longevity*, 2 (5), pp. 270-278
- Pather N, Viljoen A.M and Kramer B (2011) 'A biochemical comparison of the in vivo effects of *Bulbine frutescens* and *Bulbine natalensis* on cutaneous wound healing', *Journal of ethnopharmacology*, 133(2), pp. 364-370
- Pelgrift R.Y and Friedman A.J (2013) 'Nanotechnology as a therapeutic tool to combat microbial resistance', *Advanced Drug Delivery Review*, 65, pp. 1803-1815
- Petti C.A, Polage C.R, Quinn T.C, Ronald A.R and Sande M.A (2006) 'Laboratory medicine in Africa: a barrier to effective health care,' *Clinical Infectious Diseases*, 42(3), pp.377-382

- Prathna T.C, Mathew L, Chandrasekaran N, Raichur A.M and Mukherjee A (2010) 'Biomimetic synthesis of nanoparticles: science, technology & applicability', In *Biomimetics learning from nature*. Intechopen.
- Raad I, Tarrand J, Hanna H, Albitar M, Janssen E, Boktour M (2002) 'Epidemiology, molecular mycology, and environmental sources of *Fusarium* infection in patients with cancer', *Infect Control Hosp Epidemiol*, 23 (9), pp. 532-7
- Rai M, Yadav A, Gade A (2009) 'Silver nanoparticles as a new generation of antimicrobials', *Biotechnol Adv* 27, pp. 76–83
- Rai, M, Kon K, Ingle A, Duran N, Galdiero S, Galdiero M (2014) 'Broad-spectrum bioactivities of silver nanoparticles: The emerging trends and future prospects', *Appl. Microbiol. Biotechnol*, 98, pp.1951–1961
- Rajoriya P (2017) 'Green synthesis of silver nanoparticles, their characterization and antimicrobial potential', *Department of Molecular & Cellular Engineering, Jacob Institute of Biotechnology & Bioengineering, Sam Higginbottom University of Agriculture, Technology & Sciences Allahabad, U.P (India)*.
- Roe D, Karandikar B, Bonn-Savage N, Gibbins B, Rouillet J.B (2008) 'Antimicrobial surface functionalization of plastic catheters by silver nanoparticles', *Journal of Antimicrob Chemother*, 61, pp. 869–76
- Ryu S.H, Moon S.Y, Yang Y.J, Moon S.R, Hong J.P, Choi J, Lee S.W (2009) 'Recombinant human epidermal growth factor accelerates the proliferation of irradiated human fibroblasts and keratinocytes *in vitro* and *in vivo*', *Department of Radiation Oncology, University of Ulsan College of Medicine, Asan Medical Center, Seoul, Republic of Korea*
- Salunke G.R, Ghosh S, Santosh Kumar R.J, Khade S, Vashisth P, Kale T, Chopade S, Pruthi V, Kundu G, Bellare J.R *et al* (2014) 'Rapid efficient synthesis and characterization of silver, gold, and bimetallic nanoparticles from the medicinal plant *Plumbago zeylanica* and their application in biofilm control', *Int. J. Nanomedicine*, 9, pp. 2635–2653
- Sathishkumar M, Sneha K, Kwak I.S, Mao J, Tripathy S.J, Yun Y.S (2009) 'Phyto-crystallization of palladium through reduction process using *Cinnamom zeylanicum* bark extract', *J. Hazard. Mater*, 171, pp. 400-404
- Scott J.R, Zahner D (2006) 'Assembly of pili on gram-positive bacteria: We do it differently', *Mol. Microbiol*

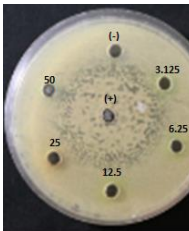
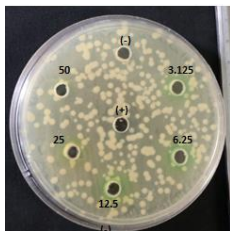
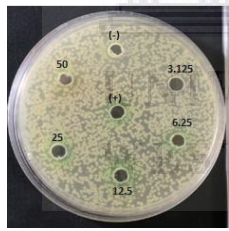
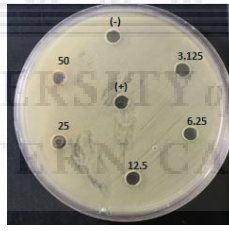
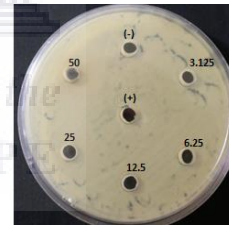
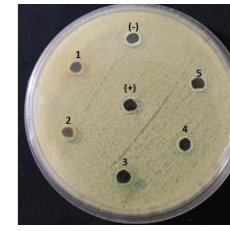
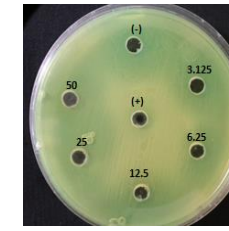
- Shankar S, Rai A, Ahmad A, Sastry, M (2004) 'Rapid synthesis of Au, Ag and bimetallic Au core-Ag shell nanoparticles using neem (*Azadirachta indica*) leaf broth', *J. Colloid. Inter. Sci.*, 275, pp. 496-502
- Shao M, Hussain Z, Thu H.E, Khan S, de Matas M, Silkstone V, Qin H.L and Bukhari S.N.A (2017) 'Emerging Trends in Therapeutic Algorithm of Chronic Wound Healers: Recent Advances in Drug Delivery Systems, Concepts-to-Clinical Application and Future Prospects', *Critical Reviews™ in Therapeutic Drug Carrier Systems*, 34(5)
- Shekhawat G.S and Arya, V (2008) 'Nanomedicines: emergence a new era in biomedical sciences', *NanoTrends*, 5, pp. 9-20
- Shrivastava S, Bera T, Singh S.K, Singh G, Ramachandrarao P, Dash D (2009) 'Characterization of antiplatelet properties of silver nanoparticles', *ACS Nano*, 3, pp. 1357–1364
- Singer A.C, Shaw H, Rhodes V, Hart A (2016) 'Review of antimicrobial resistance in the environment and its relevance to environmental regulators', *Front Microbiol*, 7, p. 1728
- Sithole, Z.N (2015) 'Synthesis of silver nanoparticles and investigating their antimicrobial effects'
- Song J.Y, Jang H.K, Kim, B.S (2008) 'Biological synthesis of bimetallic Au/Ag nanoparticles using Persimmon (*Diopyros kaki*) leaf extract', *Korean J. Chem. Eng*, 25, pp. 808-811
- Song, J.Y nand Kim, B.S (2009) 'Rapid biological synthesis of silver nanoparticles using plant leaf extracts', *Bioprocess and biosystems engineering*, 32(1), pp.79.
- Stavenger R.A, Winterhalter M (2014) 'TRANSLOCATION project: how to get good drugs into bad bugs', *Sci Transl Med*, 6(228), ed. 227
- Subramanian (2013) 'Antioxidant activity of the stem bark of *Shorea roxburghii* and its silver reducing power [Online]. Available at: <https://springerplus.springeropen.com/articles/10.1186/2193-1801-2-28> (Accessed: 25 August 2019)
- Sujitha M.V and Kannan S (2013) 'Green synthesis of gold nanoparticles using citrus fruits (*Citrus limon*, *Citrus reticulata* and *Citrus sinensis*) aqueous extract and its characterization'. *Spectrochimica Acta Part A: Molecular and Biomolecular Spectroscopy*, 102, pp. 15–23

- Takenaka M (2016) 'A case of cutaneous fusariosis of the scrotum as a complication of acute myeloid leukemia', *Med. Mycol. J*, 57, pp. 65-70
- Tamayo L.A, Zapata P.A, Vejar N.D, Azocar M.I, Gulppi M.A, Zhou X, Thompson G.E, Rabagliati F.M, Paez M.A (2014) 'Release of silver and copper nanoparticles from polyethylene nanocomposites and their penetration into *Listeria monocytogenes*', *Mater. Sci. Eng. C Mater. Biol. Appl.*, 40, pp. 24–31
- Tanaka T (2014) 'Flavonoids for allergic diseases: present evidence and future perspective', *Curr Pharm Des*, 20, pp.879-885
- Thring T.S, Weitz F.M (2006) 'Medicinal plant use in the Bredasdorp/Elim region of the Southern Overberg in the Western Cape Province of South Africa', *Journal of Ethnopharmacology*, 103 (2), pp. 261-75
- Tobwala S, Fan W, Hines C, Folk W, Ercal N (2014) 'Antioxidant potential of *Sutherlandia frutescens* and its protective effects against oxidative stress in various cell cultures', *BMC Complementary and Alternative Medicine* 2, 14, p. 271
- Tora A, Heliso T (2017) 'Assessment of the indigenous knowledge and use of traditional medicinal plants in Wolaita zone, Southern Ethiopia.', *Int J Med Plants Nat Prod*, 3(1), pp.16-22
- Van Wyk B, Gericke N (2000) 'People's Plants. A Guide to Useful Plants of Southern Africa', *Briza Publications, Pretoria*, 352
- Van Wyk B.E (2008) 'A broad review of commercially important Southern African medicinal plants', *J. Ethnopharmacol*, 119, pp. 342-355
- Van Wyk, B.E, Wink, M (2004) 'Medicinal Plants of the World', *Briza Publications, Pretoria*
- Vanaja M, Annadurai G (2013) '*Coleus aromaticus* leaf extract mediated synthesis of silver nanoparticles and its bactericidal activity', *Appl. Nanosci*, 3, pp. 217-223
- Velázquez-Velázquez JL, Santos-Flores A, Araujo-Meléndez J, Sánchez-Sánchez R, Velasquillo C, González C (2015) 'Anti-biofilm and cytotoxicity activity of impregnated dressings with silver nanoparticles', *Mater Sci and Eng: C* 49:604–11
- Vergalli J, Dumont E, Cinquin B (2017) 'Fluoroquinolone structure and translocation flux across bacterial membrane', *Sci Rep*, 7(1), pp. 9821

- Widegrow A.D, Chait L.A (2000) 'New Innovations in Scar Management', *Aesthetic Plastic Surgery*, 24, pp. 227-234
- Wiegel J, Ljungdahl L.G (1981) 'Thermoanaerobacter ethanolicus gen. nov., spec. nov., a new extreme thermophilic, anaerobic bacterium', *Arch Microbiol*, 128, pp. 343–348
- Winterhalter M, Ceccarelli M (2015) 'Physical methods to quantify small antibiotic molecules uptake into Gram-negative bacteria', *Eur J Pharm Biopharm*, 5(A), pp. 63-67
- World Health Organization (WHO) (2001) [Online]. Available at: <https://www.who.int/whr/2001/en/> (Accessed: 25 July 2019)
- World Health Organization (WHO) (2014) 'Antimicrobial resistance: Global report on surveillance', Geneva, Switzerland
- World Health Organization (WHO) (2015) Media centre. Fact sheet: Antimicrobial resistance [Online]. Available at: www.who.int/mediacentre/factsheets/fs194/en/ (Accessed: 25 July 2019)
- Yates C.C, Hebda, P. and Wells, A (2012) 'Skin wound healing and scarring: fetal wounds and regenerative restitution', *Birth Defects Research Part C: Embryo Today: Reviews*, 96(4), pp. 325-333
- Yebpella G.G, Adeyemi H.M.M, Hammuel C, Magomya A.M, Agbaji A.S, Okonkwo E.M (2011) 'Phytochemical screening and comparative study of antimicrobial activity of *Aloe vera* various extracts', *Afr. J. Microbiol. Res.*, 5, pp. 1182-1187
- Zaias N, Escovar S.X, Rebell G (2014) 'Opportunistic toenail onychomycosis. The fungal colonization of an available nail unit space by non-dermatophytes is produced by the trauma of the closed shoe by an asymmetric gait or other trauma: A plausible theory', *Journal Eur. Acad. Dermatol. Venereol*, 28, pp. 1002-1006
- Zaidi A.K, Huskins W.C, Thaver D, Bhutta Z.A, Abbas Z, Goldmann D.A (2005) 'Hospital-acquired neonatal infections in developing countries', *The Lancet*, 365(9465), pp.1175-1188
- Zhang Q, Gould L.J (2014) 'Hyperbaric oxygen reduces matrix metalloproteinases in ischemic wounds through a redox-dependent mechanism', *Journal of Investigative Dermatology*, 134(1), pp. 237-246

Appendix

Table 1: The antimicrobial effects of *B. frutescens* extract against seven human pathogenic bacteria. (n=3) STDEV – standard deviation

	Zone of inhibition (mm)						
	<i>S. aureus</i>	<i>S. epidermidis</i>	<i>S. pyogenes</i>	<i>E. coli</i>	<i>K. pneumoniae</i>	MRSA	<i>P.aeruginosa</i>
	Neutral pH (7.11) Extract (mg/ml)						
Ampicillin (+)	0 ± 0	0 ± 0	0 ± 0	0 ± 0	0 ± 0	0 ± 0	0 ± 0
MHB growth medium (-)	0 ± 0	0 ± 0	0 ± 0	0 ± 0	0 ± 0	0 ± 0	0 ± 0
50	0 ± 0	0 ± 0	0 ± 0	0 ± 0	0 ± 0	0 ± 0	0 ± 0
25	0 ± 0	0 ± 0	0 ± 0	0 ± 0	0 ± 0	0 ± 0	0 ± 0
12.5	0 ± 0	0 ± 0	0 ± 0	0 ± 0	0 ± 0	0 ± 0	0 ± 0
6.25	0 ± 0	0 ± 0	0 ± 0	0 ± 0	0 ± 0	0 ± 0	0 ± 0
3.125	0 ± 0	0 ± 0	0 ± 0	0 ± 0	0 ± 0	0 ± 0	0 ± 0
Tested Plates							

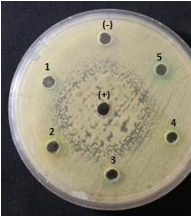
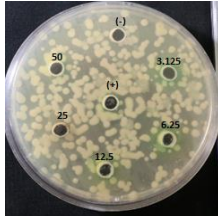
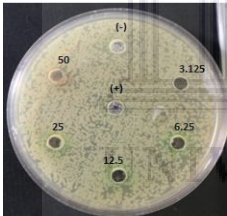
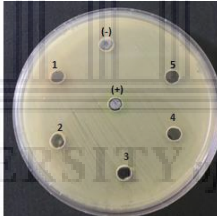
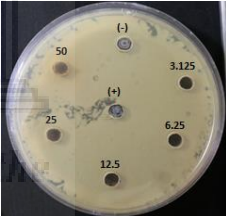
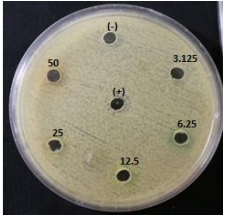
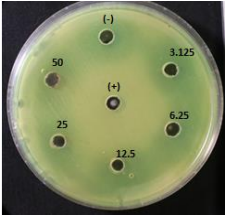
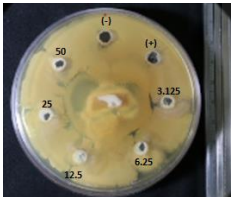
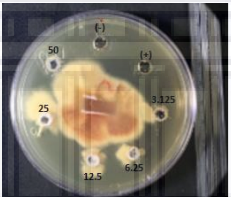
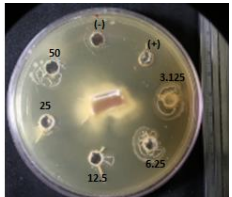
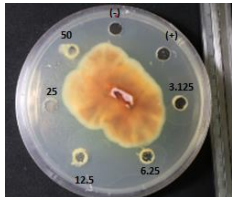
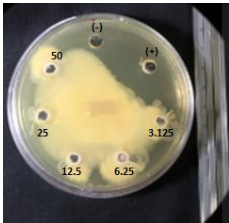
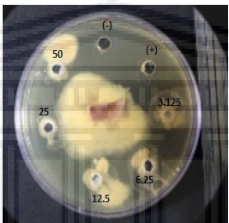
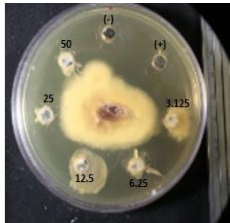
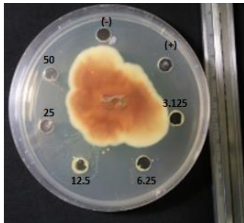
	Zone of inhibition (mm)						
	<i>S. aureus</i>	<i>S. epidermidis</i>	<i>S. pyogenes</i>	<i>E. coli</i>	<i>K. pneumoniae</i>	MRSA	<i>P. aeruginosa</i>
pH 10 AgNPs (mg/ml)							
Ampicillin (+)	0 ± 0	0 ± 0	0 ± 0	0 ± 0	0 ± 0	0 ± 0	0 ± 0
MHB growth medium (-)	0 ± 0	0 ± 0	0 ± 0	0 ± 0	0 ± 0	0 ± 0	0 ± 0
50	0 ± 0	0 ± 0	0 ± 0	0 ± 0	0 ± 0	0 ± 0	0 ± 0
25	0 ± 0	0 ± 0	0 ± 0	0 ± 0	0 ± 0	0 ± 0	0 ± 0
12.5	0 ± 0	0 ± 0	0 ± 0	0 ± 0	0 ± 0	0 ± 0	0 ± 0
6.25	0 ± 0	0 ± 0	0 ± 0	0 ± 0	0 ± 0	0 ± 0	0 ± 0
3.125	0 ± 0	0 ± 0	0 ± 0	0 ± 0	0 ± 0	0 ± 0	0 ± 0
Tested Plates							

Table 2: The antifungal effects of *B. frutescens* extracts against four *Fusarium* fungal strains. (n=3) STDEV – standard deviation

	Zone of inhibition (mm)			
	<i>F. culmorum</i>	<i>F. oxysporum</i>	<i>F. proliferatum</i>	<i>F. verticilloides</i>
	Neutral pH (7.11) Extract (mg/ml)			
Carbendazim (+)	0 ± 0	12 ± 0.21	8.75 ± 0.1	8.25 ± 0.64
Ethanol (-)	0 ± 0	10 ± 0.32	6.25 ± 0.3	4.25 ± 0.35
50	0 ± 0	0 ± 0	0 ± 0	0 ± 0
25	0 ± 0	0 ± 0	0 ± 0	0 ± 0
12.5	0 ± 0	0 ± 0	0 ± 0	0 ± 0
6.25	0 ± 0	0 ± 0	0 ± 0	0 ± 0
3.125	0 ± 0	0 ± 0	0 ± 0	0 ± 0
Test plates				

UNIVERSITY of the
WESTERN CAPE

	Zone of inhibition (mm)			
	<i>F. culmorum</i>	<i>F. oxysporum</i>	<i>F. proliferatum</i>	<i>F. verticilloides</i>
	pH 10 Extract (mg/ml)			
Carbendazim (+)	11 ± 0.22	9 ± 0.1	12 ± 0.87	6.25 ± 0.55
Ethanol (-)	3 ± 0.11	11 ± 0.34	10 ± 0.12	2 ± 0.57
50	0 ± 0	0 ± 0	0 ± 0	0 ± 0
25	0 ± 0	0 ± 0	0 ± 0	0 ± 0
12.5	0 ± 0	0 ± 0	0 ± 0	0 ± 0
6.25	0 ± 0	0 ± 0	0 ± 0	0 ± 0
3.125	0 ± 0	0 ± 0	0 ± 0	0 ± 0
Test Plates				

UNIVERSITY of the
WESTERN CAPE

Figure 1: Comparison of the antibacterial effects of 0.6 mg/ml, 0.3 mg/ml, 0.15 mg/ml, 0.075 mg/ml, 0.0375 mg/ml neutral pH AgNPs to 0.1 mg/ml ampicillin after 24 hours of incubation at 37°C. The data is expressed in mean ± SD (n=3). Statistical significance is indicated by * (p-value <0.05), ** (p-value <0.01), * (p-value <0.001) and **** (p-value <0.0001). Letters a, b, c, d, e and f denote the similarity or difference within the NP concentrations.**

Mean ± SD

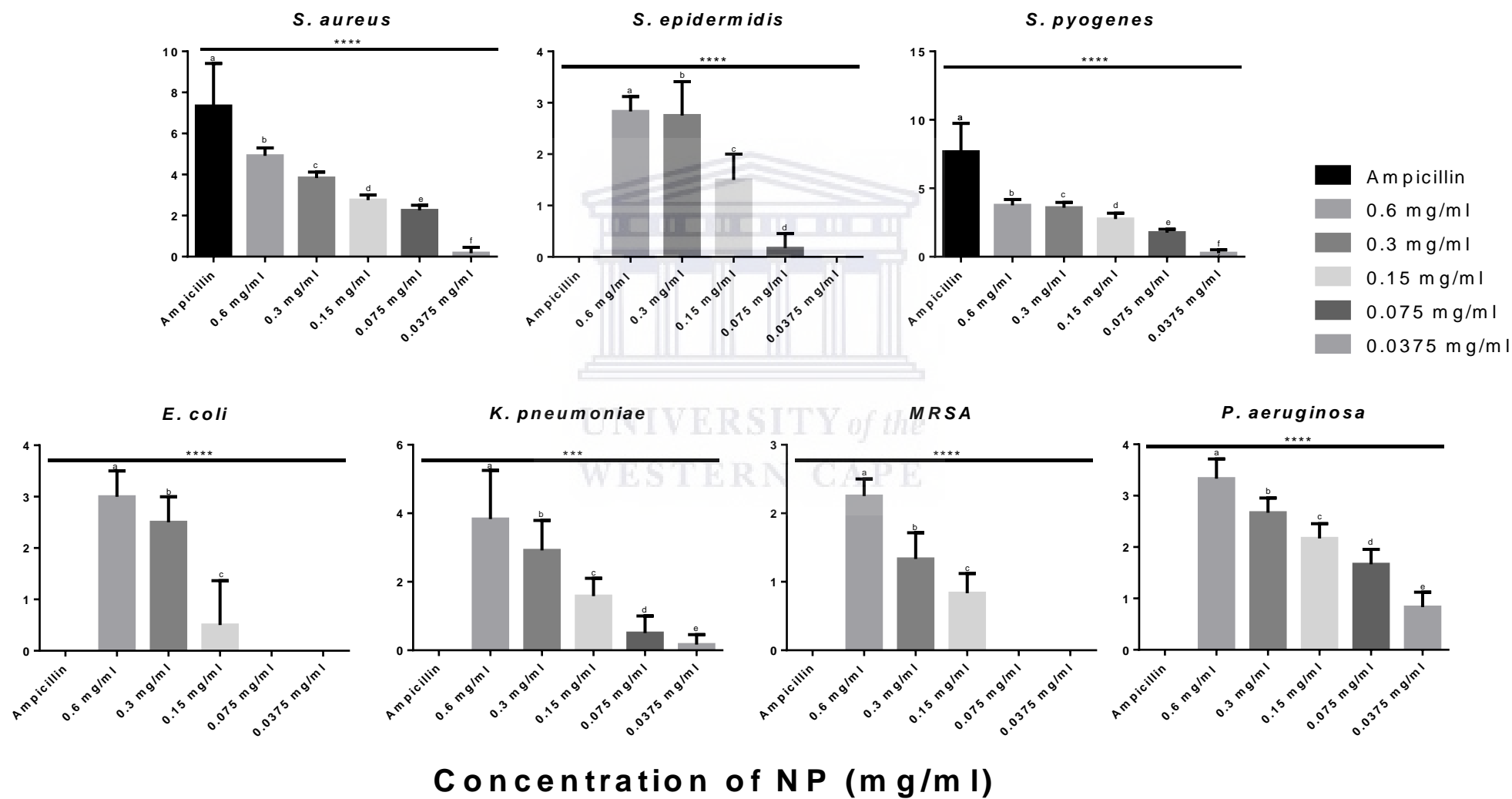


Figure 2: Comparison of the antibacterial effects of 0.47 mg/ml, 0.26 mg/ml, 0.12 mg/ml, 0.06 mg/ml, 0.03 mg/ml pH 10 AgNPs to 0.1 mg/ml ampicillin after 24 hours of incubation at 37°C. The data is expressed in mean \pm SD (n=3). Statistical significance is indicated by * (p-value <0.05), ** (p-value <0.01), * (p-value <0.001) and **** (p-value <0.0001). Letters a, b, c, d, e and f denote the similarity or difference within the NP concentrations.**

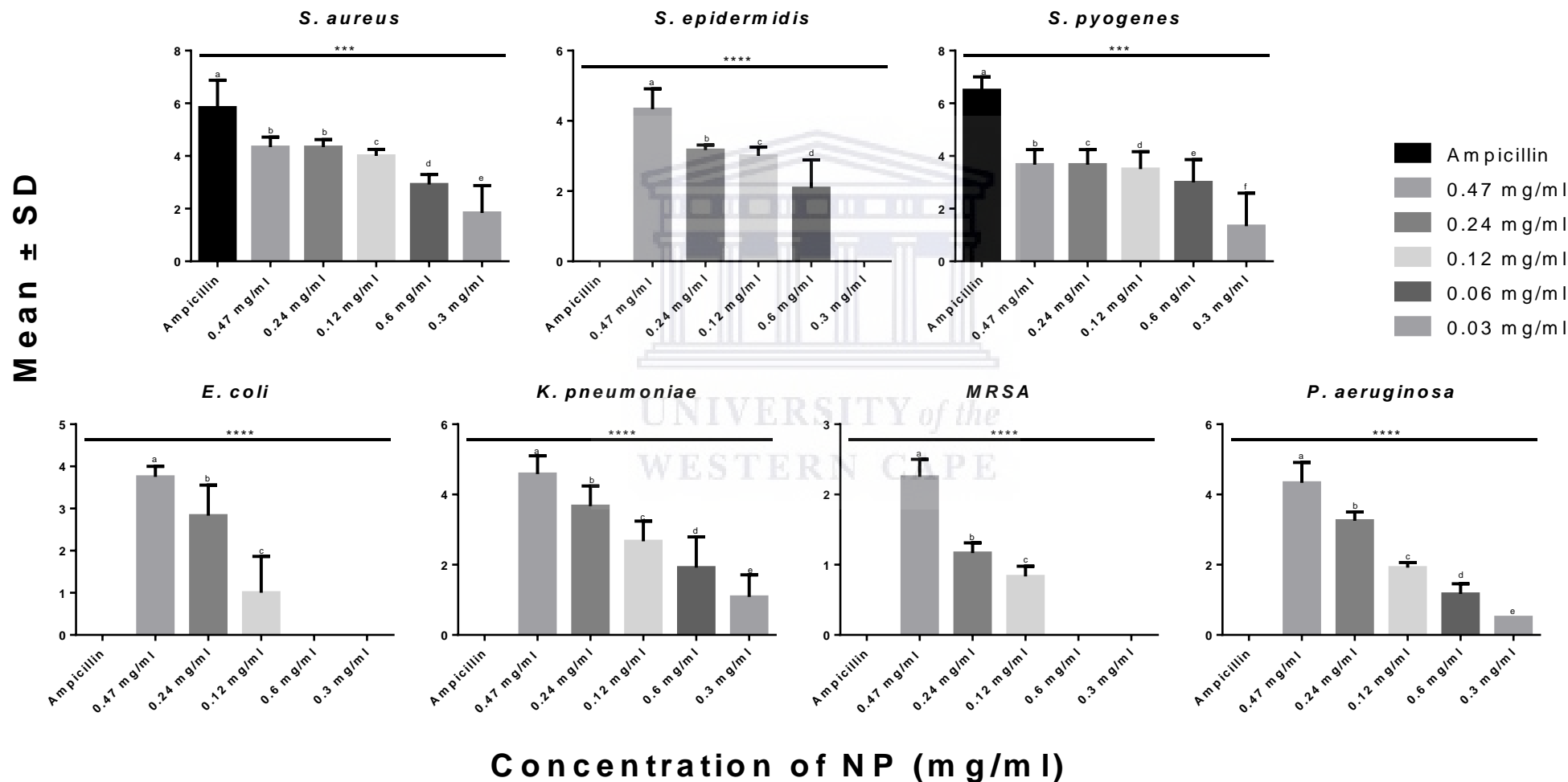


Figure 3: Comparison of the antifungal effects of 0.47 mg/ml, 0.26 mg/ml, 0.12 mg/ml, 0.06 mg/ml, 0.03 mg/ml neutral pH AgNPs to 0.1 g/l carbendazim and ethanol after 5 days of incubation at 25°C. The data is expressed in mean \pm SD (n=3). Statistical significance is indicated by * (p-value <0.05), ** (p-value <0.01), *** (p-value <0.001) and **** (p-value <0.0001). Letters a, b, c, d, e, f and g denote the similarity or difference within the NP concentrations.

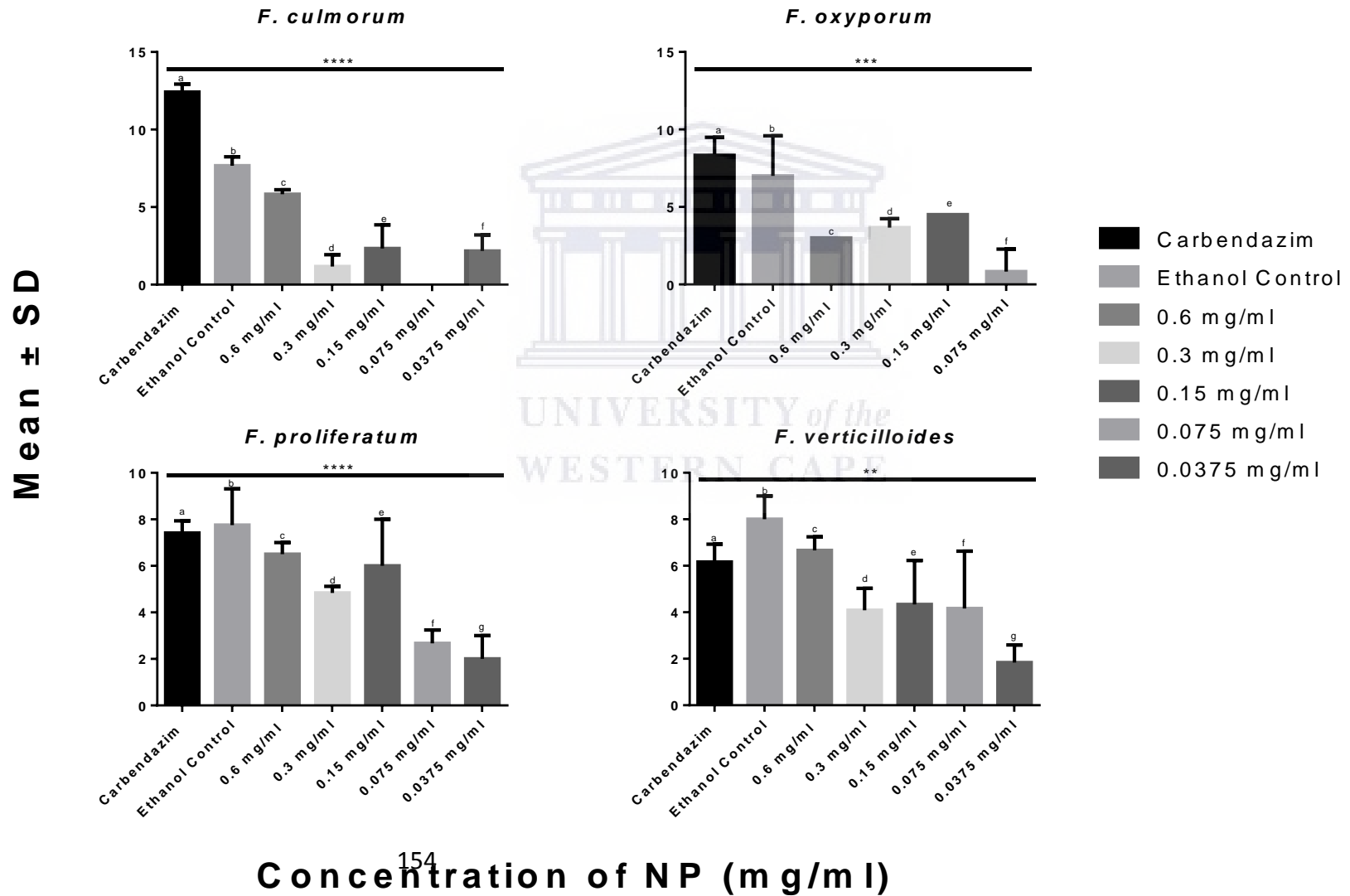
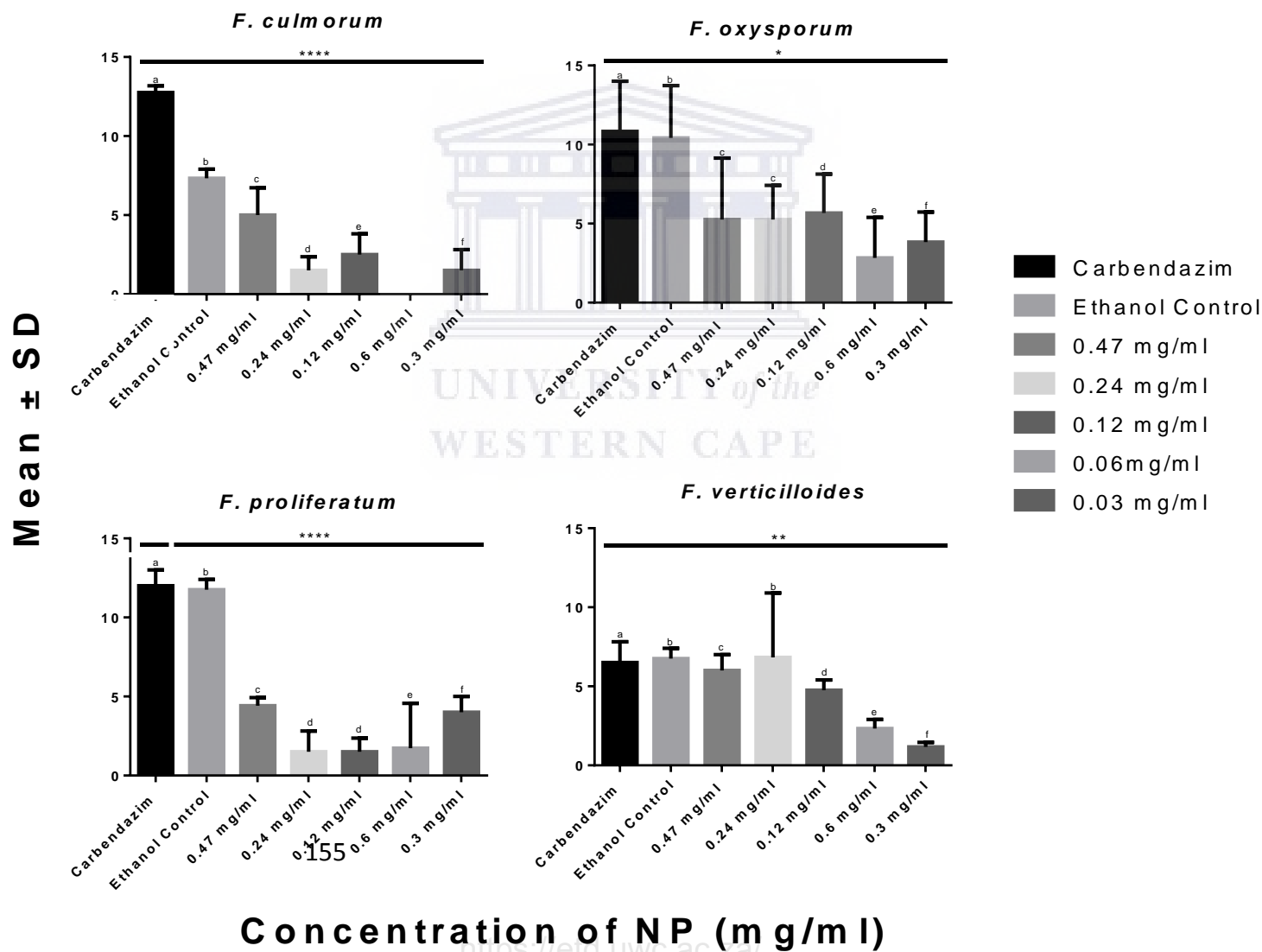


Figure 4: Comparison of the antifungal effects of 0.47 mg/ml, 0.24 mg/ml, 0.12 mg/ml, 0.06 mg/ml, 0.03 mg/ml pH 10 AgNPs to 0.1 g/l carbendazim and ethanol after 5 days of incubation at 25°C. The data is expressed in mean \pm SD (n=3). Statistical significance is indicated by * (p-value <0.05), ** (p-value <0.01), *** (p-value <0.001) and **** (p-value <0.0001). Letters a, b, c, d, e, f and g denote the similarity or difference within the NP concentrations.





UNIVERSITY *of the*
WESTERN CAPE